(19) Europäisches Patentamt
European Patent Office
Office européen des brevets

(11) EP 1 299 711 B1

(12) **EUROPEAN PATENT SPECIFICATION**

(45) Date of publication and mention of the grant of the patent:
24.05.2006 Bulletin 2006/21

(21) Application number: **01951277.1**

(22) Date of filing: **10.07.2001**

(51) Int Cl.:
G01N 21/47 *(2006.01)*

(86) International application number:
PCT/CA2001/000992

(87) International publication number:
WO 2002/004929 (17.01.2002 Gazette 2002/03)

(54) **METHOD AND APPARATUS FOR HIGH RESOLUTION COHERENT OPTICAL IMAGING**

VERFAHREN UND VORRICHTUNG ZUR HOCHAUFLÖSENDEN KOHÄRENTEN OPTISCHEN ABBILDUNG

TECHNIQUE ET APPAREIL RELATIFS A UNE IMAGERIE OPTIQUE COHERENTE A HAUTE RESOLUTION

(84) Designated Contracting States:
DE FR GB

(30) Priority: **10.07.2000 US 217090 P**

(43) Date of publication of application:
09.04.2003 Bulletin 2003/15

(73) Proprietor: **University Health Network**
Toronto,
Ontario M5G 2M9 (CA)

(72) Inventors:
- **YANG, Victor, Xiao, Dong**
  Richmond Hill,
  Ontario L4B 4J8 (CA)
- **VITKIN, I., Alex**
  Toronto, Ontario M6P 1E5 (CA)
- **WONGKEESONG, Louie**
  Rochester, MN 55901 (US)
- **KATZ, Sharon**
  Toronto, Ontario M4M 2X2 (CA)
- **GORDON, Margaret, Leslie**
  Toronto, Ontario M4P 2N4 (CA)
- **WILSON, Brian, C.**
  Toronto, Ontario M6R 2Y6 (CA)
- **MOK, Alvin, Ho, Kwan**
  Richmond Hill, Ontario L4B 3C5 (CA)

(74) Representative: **Harrison Goddard Foote**
Belgrave Hall,
Belgrave Street
Leeds, LS2 8DD (GB)

(56) References cited:
EP-A- 0 470 942

- **TEARNEY G J ET AL: "IN VIVO ENDOSCOPIC OPTICAL BIOPSY WITH OPTICAL COHERENCE TOMOGRAPHY" SCIENCE, AMERICAN ASSOCIATION FOR THE ADVANCEMENT OF SCIENCE,, US, vol. 276, no. 5321, 27 June 1997 (1997-06-27), pages 2037-2039, XP001041246 ISSN: 0036-8075**
- **SCHMITT J M ET AL: "An optical coherence microscope with enhanced resolving power in thick tissue" OPTICS COMMUNICATIONS, NORTH-HOLLAND PUBLISHING CO. AMSTERDAM, NL, vol. 142, no. 4-6, 15 October 1997 (1997-10-15), pages 203-207, XP004093980 ISSN: 0030-4018**
- **C.H. SCHMITZ ET AL.: "A fast versatile instrument for dynamic optical tomography" OPTICAL SOCIETY OF AMERICA, [Online] - 1999 pages 1-3, XP002193130 Retrieved from the Internet: < URL:http://138.5.51.241/index/Publication /SchmitzOSA00.pdf> [retrieved on 2002-03-14]**

EP 1 299 711 B1

Description

FIELD OF THE INVENTION

[0001] This invention relates to both a method and an apparatus for high-resolution optical imaging. More particularly, this invention is concerned with providing high-resolution imaging suitable for incorporation into an endoscope.

BACKGROUND OF THE INVENTION

[0002] Modern medical imaging techniques have important applications in health care. Modalities such as X-ray computed tomography (CT), magnetic resonance imaging (MRI) and ultrasound imaging are the main tomographic techniques available in most modern medical centers. Visible-light endoscopy is another major imaging modality which is used extensively in procedures like bronchoscopy or colonoscopy. Each of these techniques employs different physical principles and measures different properties of the biological tissue under study with different resolution. Further, they can commonly be performed *in-vivo*. A third type of imaging, optical microscopy, is still utilized widely in clinical medicine. However, optical microscopy is currently limited to detailed examination of excised or resected specimens and is not used *in-vivo.* In many circumstances, the superior contrast and resolution afforded by optical microscopy is such that physical biopsy followed by optical microscopic histology is considered the gold standard for diagnosis.

[0003] Combinations of these techniques, such as using a low-resolution tomographic modality along with high-resolution imaging, biopsies or interventional procedures are constantly being studied and evaluated. Evaluation of these techniques is based on technological feasibility, clinical benefit and cost.

[0004] Optical Coherence Tomography (OCT) is a relatively new imaging technique based on the low-coherence property of electromagnetic radiation that enables high-resolution depth profilometry in a turbid, highly scattering media such as biological tissue. Its use in biomedical imaging is currently being investigated in several research and industrial laboratories. The main advantage of OCT lies in its ability to localize the depth of reflection from a sub-surface site in tissue. This localization is essentially determined by the coherence properties of the light source used and can be as low as 2 to 20 μm for selected near-IR sources (e.g. lasers or amplified spontaneous emission devices). This gives a measure of the depth resolution attainable with OCT. Independently of the coherence characteristics, the lateral resolution is determined by the beam cross-section at the depth of imaging and by the lateral spacing of the acquired data. Typical values for lateral spacing in the literature are in the 5 to 30 μm range. The price to be paid for this remarkable cross-sectional imaging ability in intact turbid tissue is the limited imaging depth since, due to multiple scattering and absorption, both coherence and penetration of light are degraded resulting in OCT imaging depths of approximately 2 to 3 mm.

[0005] Most current implementations of OCT are based on Michelson interferometry with a 50/50 beam splitter directing the incident coherent light beam into a reference path containing a mirror (i.e. a reference arm) and a sample path containing the interrogated sample (i.e. a sample arm). Both free-space optic and fiber-optic implementations of this scheme are currently used. Reflected beams from the mirror in the reference arm and from the tissue in the sample arm are recombined in the same splitter and half of the resultant light energy impinges on a detector. Incoherent superposition of the two light fluxes typically occurs except when the optical path lengths of the two beams are matched to within the coherence length of the source. Within this limited distance, the coherent superposition of the two light fluxes yields an interference pattern with a fringe magnitude that is proportional to the reflectivity of the tissue at that particular depth. Depth profiling of the sample is then achieved by scanning the reference arm length or more correctly by scanning the optical path length of the reference arm by using a time delay in the reference arm (this is equivalent to lengthening the reference arm). Various detection methods to measure and quantify these faint amplitude modulations amidst large background diffuse reflectance have been developed having a dynamic range of approximately 70 to 110 dB. Furthermore, lateral translation of the beam and axial motion of the reference mirror enables one to construct a two-dimensional reflectivity picture over a desired field of view. Means of improving the final image quality, such as performing image processing through de-convolution, have also been investigated.

[0006] The foregoing is a brief description of conventional reflectivity OCT imaging. Other variations include, for example, flow (Doppler) imaging and polarization imaging (albeit at the expense of additional complexity of the OCT optics and/or signal processing techniques). Images from these additional techniques are usually obtained in conjunction with images from conventional OCT so some image overlay or fusion is possible. Upon further technological development and/or clinical implementation, may add sufficient information content to increase the clinical utility of OCT in medicine.

[0007] However, many OCT designs and approaches that have been successfully implemented in tabletop research systems are not directly suitable for *in-vivo* imaging such as in gastroenterologic or bronchoscopic endoscopy. Instead, they may be more suitable for dermatological, ophthalmologic and dental applications. In contrast, *in-vivo* OCT imaging must address the issues of speed, resolution, contrast, penetration and instrument size. Images must be obtained sufficiently quickly to negate the effects of patient motion while still achieving suitable axial and lateral resolution, and maintaining an instrument size which is small enough to be endoscopically useful. Powerful near-IR sources, fast means

of altering the reference arm length and custom-designed distal optical devices have been successfully developed to overcome the difficult challenges posed by *in-vivo* endoscopy.

[0008] The latest OCT technology employs a single-mode optical fiber with distal side-viewing optics introduced into the accessory channel of a conventional white-light endoscope. To build-up an image, the viewing direction of the OCT fiber is either linearly scanned to and fro over an approximate 2 mm distance, or is rotated via a flexible guide-wire or interlocking gear mechanism at several revolutions per second. Simultaneous with this translation or rotation, the reference arm length outside the endoscope is rapidly varied via an optical phase delay to generate depth scans (i.e. A-scans). Currently, these OCT systems operate at frame rates up to conventional video rates but more typically at 4 to 8 frames per second, with a frame presenting a fully circumferential view to a depth of 2 to 3 mm. The resultant resolution values are approximately 5 to 25 μm in the depth (axial) direction and approximately 20 to 40 μm in the lateral direction. As well, the lateral resolution generally degrades with an increase in distance from the fiber tip of the OCT device due to geometric divergence. These OCT systems have a dynamic range which is somewhat lower than that of corresponding ex-vivo systems due to increased noise levels and faster imaging speeds.

[0009] Based on the latest OCT technology, it is questionable whether coherent *in-vivo* OCT systems are adequate for successful clinical imaging. The images are certainly useful, but substantial improvement is required if the elusive goal of "optical biopsy" is to be realized. For example axial and lateral resolution can be improved. While the improvement in the former usually involves the use of better low-coherence sources (i.e. CW and pulsed sources), the issue of sub-optimal and depth-varying lateral resolution is more difficult to address. In *ex-vivo* systems, with its relaxed constraints of speed and physical size, lateral resolution is improved by focusing the beam to a few microns with a high-NA (numerical aperture) objective lens. In contrast to conventional OCT scanning, the imaging can now be performed in the lateral *(en face)* direction with a pre-selected depth with small oscillations in path length difference, followed by a small depth increment as necessary. The high-NA objective lens is often coupled to tissue via a refractive-index matching liquid. The general approach of using OCT with a high-NA distal optic lens is known as Optical Coherence Microscopy (OCM). However, the improved lateral resolution at the beam waist location comes at the expense of lateral blurring at other depths because the highly focused beam has a very shallow depth of field. Thus, the lens-to-surface distance must be varied to focus to different depths. In addition, a dynamic tracking scheme is needed to keep the location of the coherence gate (within which coherent interference between the optical beams from the sample arm and the reference arm is possible) and the beam waist at the same depth. These techniques for lateral resolution improvement have not been attempted during *in-vivo* endoscopy because of size and speed requirements.

SUMMARY OF THE INVENTION

[0010] The present invention is useful in combination with an endoscopic optical coherence tomography (OCT) device with microscopic resolution which will hereinafter be referred to as an endomicroscope. After reviewing possible clinical applications of the endomicroscope, the following parameters and features were identified since it is difficult to achieve these parameters and features simultaneously with current *in vivo* OCT systems.

1. High Resolution

[0011] In order to achieve cellular and sub-cellular resolution, an endomicroscope should preferably resolve features smaller than 5 μm both in the axial and lateral directions. In contrast to most existing *in vivo* OCT systems, the lateral resolution must not degrade substantially with the depth of the tissue being imaged due to geometric divergence.

2. Large field of view

[0012] An appropriate field of view of the endomicroscope is approximately 2 x 2 mm in the axial and lateral directions of the optical axis. This field of view is considered to be adequate for clinical applications. In order to achieve a 5 μm resolution in both the axial and lateral directions throughout the entire image, more than 800 A-scans (i.e. depth scans) have to be performed for each frame. The resultant image will contain more than 640,000 pixels. This is several orders of magnitude higher than existing *in vivo* OCT systems.

3. Small size of endoscope tip

[0013] Most of the existing *in vivo* OCT systems are designed around the constraints of the instrument channel of existing endoscopes. As a result, the outer diameter of these systems is restricted to approximately 2 to 3 mm which limits the numerical aperture of the imaging system. This makes it difficult to obtain high lateral resolution under *in vivo* conditions. These constraints may be technically unnecessary and limit one from fully exploiting the benefit of OCT/OCM in the clinical applications under consideration. Accordingly, a larger outer diameter, such as 3 mm or more, for example,

may be used for the endoscope as well as a length of less than 20 mm for the rigid tip.

4. High imaging speed

[0014] Since the endomicroscope will be used to image a large area at high resolution under *in vivo* conditions, motion artifacts must be considered because of tissue motion due to physiological motion. These motion artifacts should be eliminated to ensure good image quality. Accordingly, the endomicroscope should preferably be able to acquire a single frame image within 12.6 ms given a typical physiological motion speed of 5 mm/s. This results in 63,000 A-scans per second. This imaging speed is more than one order of magnitude higher than that of current *in vivo* OCT systems.

5. Integration with currently available endoscopic imaging procedures

[0015] In order to improve clinical usefulness, conventional white light imaging should preferably be integrated into the endomicroscope. In addition, instrument channels should be preferably designed so that an excisional biopsy could be performed under the guidance of the endomicroscope. As well, instrument channels for water and air delivery may be preferably made available.

[0016] The advanced requirements for an endomicroscope outlined above are not compatible with existing OCT/OCM designs. For instance, if an outer diameter of 6 mm is allowed for the endomicroscope and a distal optical design is used based on a single rotating fiber as described by Tearney, G.J., Brezinski, M.E., Bouma, B.E., Boppart, S.A., Pitris, C., Southern, J.F., and Fujimoto, J.G. ("In vivo Endoscopic Optical Biopsy with Optical Coherence Tomography", Science, **276:** 2037-2039, 27 June 1997), then although the 5 μm lateral resolution can be achieved at a single specific depth within the tissue in any one scan, such lateral resolution will degrade due to beam divergence at other depths. In addition, since a high NA system will be required to produce the requisite small beam waist size, the coherence gate and the focal point will not stay together in depth over a substantial (e.g. 2 mm) distance unless some dynamic compensation is implemented as described by Schmitt, J.M., Lee, S.L., and Yung, K.M ("An Optical Coherence Microscope with Enhanced Resolving Power in Thick Tissue", Optics Communications, **142:** 203-207, 1997). Therefore, in order to achieve some of the aforementioned requirements of the endomicroscope, dynamic focusing (changing the probe/tissue distance) and dynamic compensation (changing the path length difference) must be used. However, these focusing and compensation techniques complicate the practical realization of the device and may make it more difficult to satisfy the high imaging speed requirement. If one tries to first satisfy the imaging speed, as described by Rollins, A.M., Kulkarni, M.D., Yazdanfar, S., Ung-arunyawee, R., and Izatt, J.A. ("In vivo Video Rate Optical Coherence Tomography", Optics Express, **Vol. 3 No. 6**: 219-229, 14 September 1998), then image resolution, particularly lateral resolution, is degraded to an extent that the clinical utility of the device is compromised.

[0017] The present invention can be used for an endomicroscope with multiple fibers (i.e. channels) employing OCT to allow for different parts of the image to be scanned in parallel, instead of in series as is currently implemented in existing *in vivo* or *ex vivo* OCT/OCM systems. Using multiple parallel channels focused to different depths in the tissue, with each channel collecting high-resolution OCT data only across a very small axial range allows for a series of tight focal points to be achieved throughout the entire field of view without dynamic focusing or dynamic compensation. This greatly simplifies the design of the device which may now use mostly fixed optical components, and may facilitate high-speed operation. In addition, the intrinsically miniature dimension of the fiber optic based OCT technique makes the multichannel concept possible to implement in a flexible endoscopic device while the proximal part of the endoscope, which is outside of the patient, allows room for sources, detectors, and other equipment.

[0018] Zahirudeen (EP 0 470 942) teaches a method and apparatus for detecting focusing errors using chromatic aberration. In particular, the reference teaches using an objective lens having chromatic aberration to focus beams on a surface of an optical disc. When the surface of the disc is positioned midway between the focal points of the two beams, the beams have equal intensity. The light intensity of the two spots is detected so that focusing errors can be determined based on the difference between the detected intensities.

[0019] In accordance with a first aspect of the present invention, there is provided an apparatus for optical examination of a sample, the apparatus comprising:

an optical source means for providing a plurality of separate optical radiation sources;
a first optical path extending from the optical source means;
a focusing means in the first optical path for focusing optical radiation from the optical radiation sources into a plurality of respective focal points located on a surface within the first optical path to provide substantially continuous coverage of a selected portion of the first optical path, whereby, in use, a sample can be located at least partially within said selected portion, thereby permitting simultaneous scanning of a plurality of points within the sample; characterised in that:

the optical source means comprises optical coupling means having one of a plurality of optical fibers and a plurality of optical waveguide wafers, wherein ends of the plurality of optical fibers or the plurality of optical waveguide wafers are stepped relative to one another along the first optical path and wherein optical radiation from each optical fiber or each optical waveguide wafer is focused to a different focal point on the surface of the first optical path.

[0020] In accordance with a second aspect of the present invention, there is provided a method for optical examination of a sample, the method comprising:

(a) providing radiation from a plurality of separate optical radiation sources, along a first optical path;
(b) providing focusing means in the first optical path;
(c) focusing the optical radiation from the optical sources into a plurality of respective focal points along a surface within the first optical path to provide substantially continuous coverage of a selected portion of the first optical path; and
(d) providing a sample located at least partially within the first optical path; and,
(e) simultaneously scanning a plurality of points within the sample;

characterised in that the method further comprises:

providing an optical coupling means for the plurality of separate optical radiation sources wherein the optical coupling means have one of a plurality of optical fibers and a plurality of optical waveguide wafers, wherein the method further comprises stepping the ends of the plurality of optical fibers or the plurality of optical waveguide wafers relative to one another in a common plane along the first optical path for focusing optical radiation from each optical fiber or each optical waveguide wafer through a common lens to a different focal point on the surface of the first optical path.

[0021] It is to be appreciated that a sample, for use with the present invention, may comprise any biological tissue or other suitable material.

[0022] Further objects and advantages of the invention will appear from the following description, taken together with the accompanying drawings.

BRIEF DESCRIPTION OF THE DRAWINGS

[0023] For a better understanding of the present invention and to demonstrate how it may be carried into effect, reference will now be made, by way of example, to the accompanying drawings which show a preferred embodiment of the present invention and in which:

Figure 1a is a top view of the tip of an apparatus in accordance with the present invention showing optical paths and ignoring the refraction effects of an air-tissue interface;
Figure 1b is a side view of the tip of an apparatus in accordance with the present invention showing optical paths and ignoring the refraction effects of an air-tissue interface;
Figure 1c is an end view of the tip of an apparatus in accordance with the present invention showing optical paths and ignoring the refraction effects of an air-tissue interface;
Figure 1d is an alternate embodiment of the tip of the apparatus of Figure 1a showing optical paths and ignoring the refraction effects of an air-tissue interface;
Figure 2a shows the fiber bundle tip of Figure 1;
Figure 2b is a top view of an enlarged section of the fiber bundle tip;
Figure 2c is an end view of an enlarged section of the fiber bundle tip;
Figure 3a illustrates the focal points of three of the imaging fibers of the fiber bundle tip of Figure 1;
Figure 3b is a magnified view of the focal points of Figure 3a showing details of the focal points at different depths;
Figure 4a is a schematic indicating different directions for directing the optical beams from the fiber bundle tip of Figure 1;
Figures 4b and 4c are top and end views of optical beams in directions A and C of Figure 4a;
Figures 4d and 4e are top and side views of optical beams directed in directions B and D of Figure 4a;
Figure 4f shows a perspective view of the optical beams in the directions B and D;
Figure 5a is a beam spot diagram of a 5 channel fiber bundle tip showing electric field strength distribution near multiple focal zones;
Figure 5b is a beam spot diagram of 5 central channels of a 15 channel fiber bundle tip showing electric field strength distribution near multiple focal zones;

Figure 5c is a graph of beam spot diameter versus focal zone distance for the fiber bundle tip of Figure 5a;
Figure 5d is a graph of beam spot diameter versus focal zone distance for the fiber bundle tip of Figure 5b;
Figure 6 is a schematic layout of an apparatus using the present invention;
Figures 7a is a top view of an optical delay generator used in the apparatus using the present invention;
Figure 7b is a front view of a scanning mirror used in the optical delay generator of Figure 7a.
Figure 8a is an end view of the mirror and the focal points from three of the imaging fibers of the fiber bundle tip of Figure 1a;
Figure 8b shows a combined A-scan and a two-dimensional brightness-mode (B-mode) scan path for light radiated from a single imaging fiber according to an embodiment;
Figure 9 is a diagram illustrating mismatch between the coherence gate and the focal point due to the air-tissue interface for light radiating from a single imaging fiber;
Figure 10 is a diagram illustrating flexible triggering of the apparatus using an embodiment of the present invention to accommodate the mismatch shown in Figure 9;
Figure 11a is a schematic diagram of a Prior Art single channel Optical Coherence Tomography device;
Figure 11b is a schematic diagram of a two channel Optical Coherence Tomography device;
Figure 11c is a schematic diagram of an optical network that could be used to construct an N-channel Optical Coherence Tomography device;
Figure 12a is a schematic diagram of a single channel Optical Coherence Tomography device with an optical circulator;
Figure 12b is a schematic diagram of a two channel Optical Coherence Tomography device employing optical circulators;
Figure 12c is a schematic diagram of an optical network that could be used to construct an N channel Optical Coherence Tomography device employing an optical circulator;
Figure 13a is a schematic of an experimental setup used to investigate cross-talk between optical channels sharing components;
Figure 13b is an experimental result from experimentation on the setup of Figure 13a;
Figure 13c is another experimental result from experimentation on the setup of Figure 13a;
Figure 14 is an end view of a GI endoscopic coherent optical microscope using an embodiment of the present invention;
Figure 15 is a cutaway side view of the GI endoscopic coherent optical microscope of Figure 14 showing a biopsy channel;
Figure 16 is a simulated image of a human colon epithelium that is expected to be obtained with the apparatus using the present invention;
Figure 17a has two panels which each show a microscopy image of sweat ducts in the human skin; and,
Figure 17b has three panels which each show an *in vivo* OCT image of sweat ducts in the human skin.

DETAILED DESCRIPTION OF THE INVENTION

[0024] In the following description, various specific dimensions and other parameters are mentioned such as the wavelength used by the imaging source and the physical dimensions of the optical components used in the apparatus. It is to be appreciated that this is for exemplary purposes only and does not limit this invention. Specific parameters, dimensions and the like may be chosen depending on an intended application of the invention.

[0025] Figure 1, shows an apparatus comprising an endoscopic coherent optical microscope having multiple single mode fibers **10,** a fiber bundle tip **12,** a focusing lens **14** and a mirror **16.** The multiple single mode fibers **10** and the focusing lens **14** are stationary while the mirror **16** is rotatable. Accordingly, the mirror **16** is mounted for rotation in known manner. Details of the rotating mechanism for the mirror **16** are not described further and can be conventional. Multiple single mode fibers **10** (of which there may be approximately 50 fibers) form an array at the fiber bundle tip **12.** This array is cleaved and arranged in a "staircase" pattern as shown in Figure 2. Radiated light from the fiber bundle tip **12** is focused by the focusing lens **14** and reflected by the mirror **16.** The focusing lens **14** may have a diameter of 5 mm (i.e. ϕ = 5 mm) and a focal length of 5 mm (i.e. f = 5 mm). The mirror **16** may have a diameter of 5 mm and a front face that is cleaved at 45°. A magnified image of the focal points of the fiber bundle tip **12** is shown in Figure 3.

[0026] Figure 1a shows three beams **21, 22** and **23** from three exemplary fibers arbitrarily chosen from the multiple single mode fibers **10.** Due to the staggered or staircase nature of the multiple single mode fibers **10** (see Figure 2), each of the beams **21, 22** and **23** originates from a different point and consequently is brought into focus, by the focusing lens **14,** at a different point **21a, 22a** and **23a** on a surface **18** when the mirror **16** is not used. It will be appreciated that a similar effect is achieved for all of the multiple single mode fibers **10** of the fiber bundle tip **12** to produce beams focused to different points on the surface **18.** As indicated at **24** (and as shown in Figure 3), if the multiple single mode fibers **10** comprise 50 optical fibers, each being focused within a short range of approximately 40 microns and having their ends

staggered to space the focal points apart by 40 microns (as measured along axis **20** of the focusing lens **14),** a total range or depth of 2 mm is covered. The axis **20** for the focusing lens **14** is part of a first optical path.

[0027] With the mirror **16** present, the optical beams **21, 22** and **23** are focused as shown in Figures 1b and 1 c. Thus, three focal points **21b, 22b** and **23b** are spaced apart in a vertical or depth direction along axis **26** which forms an extension of the first optical path. As the view of Figure 1c shows, the three focal points **21b, 22b** and **23b** are also spaced apart in the circumferential direction (i.e. they are spaced apart laterally) relative to the motion of the mirror **16.** The three focal points **21b, 22b** and **23b** fall on a surface **27** to facilitate imaging of a selected portion of the first optical path. The surface **27** may be a complex surface or a planar surface. If multiple single mode fibers **10** comprises 50 individual fibers, then the focal points of all the individual fibers from the fiber bundle tip **12** would be spaced apart correspondingly.. Alternatively, the reflected focal points **21b, 22b** and **23b** do not necessarily have to be perpendicular to the axis 20 but may be at a large angle to the axis **20.**

[0028] Rotation of the mirror **16** results in motion of the surface **27.** This enables a two-dimensional B-scan image **30** to be obtained, as shown in Figure 1 c, covering a scan area **28** which has a square shape with preferable dimensions of 2 mm x 2 mm. The B-scan image **30** indicates an exemplary view that may be obtained for the scan area **28.**

[0029] Redesigning the multiple single mode fibers **10,** for example, by changing the diameter of the core and cladding of the multiple single mode fibers **10,** results in variations on the surface **27.** Furthermore, optical wave guide wafers may also be used in the place of the multiple single mode fibers **10.**

[0030] In an alternative embodiment, the mirror **16** may be replaced by a mirror **16'** that moves linearly in combination with the focusing lens **14** and the fiber bundle tip **12** as shown in Figure 1d. The linear translation may preferably incorporate a reciprocal motion. In terms of mechanics, the fiber bundle tip **12,** depicted in Figure 1a, utilizes a radial scanning motion. The radial scanning motion is well suited for scanning organs having larger diameters, such as the esophagus or the large intestine. However, due to the complex driving mechanism needed for radial scanning, the diameter of the fiber bundle tip **12** will not allow for endomicroscopy in organs having small inner diameters such as blood vessels. Therefore, the alternative embodiment shown in Figure 1d may be used which comprises a similar fiber bundle tip **12'** that is adapted to perform linear translational scanning instead of radial scanning.

[0031] As shown in Figure 1d, the main differences between the two methods of scanning are that the mirror **16'** will not be rotating and the entire fiber bundle tip **12'** needs to be translated along its horizontal axis in preferably a reciprocal motion over a range of 4 mm for example. Mechanically, the linear translational scanning motion is less complicated than the radial scanning motion. In addition, linear translational scanning is better suited for endomicroscopy in organs having a small inner diameter such as blood vessels. However, for some larger organs, such as the large intestine, linear translational scanning is not as well suited due to positioning difficulties.

[0032] In a further alternative embodiment, both of the scanning motions may be combined to produce an endomicroscopy device having helical scanning. The helical scanning motion would comprise the rotational movement of the mirror **16** in combination with the linear translation of the mirror **16,** the focusing lens **14** and the fiber bundle tip **16.** Such an endomicroscopy device may be more suitable for imaging certain types of organs such as the human large intestine. The helical scanning endomicroscopy device may be implemented by linearly translating the apparatus shown in Figure 1a.

[0033] In yet another alternative embodiment, the fiber bundle tip **12** may be altered to employ a Micromachined Electro-Mechanical System (MEMS) driving mechanism. Since the aforementioned embodiments require some form of motion for the mirror **16,** all embodiments require mechanical driving mechanisms. Accordingly, a motor is situated outside of the endoscope and a mechanical drive-train mechanism or wire is placed along the entire length of the endoscope. However, the multi-channel fiber optical design is not restricted to such mechanical driving means. In fact, due to the extremely small spatial resolutions realizable by the multi-channel system, adverse effects, such as vibration induced polarization dependence, from the mechanical drive means, may limit the full potential of the present invention if a mechanical drive means is utilized. Therefore, a MEMS electrical driving mechanism may be employed where electrically-driven, micro-mechanical optical devices are used to facilitate the scanning. This implementation may potentially circumvent the adverse effects that may be caused by a mechanical driving mechanism since the MEMS implementation reduces vibrations along the axis of the device except in the vicinity of the object which is being translated such as the mirror 16. The MEMS implementation may also offer advantages in terms of miniaturization and performance.

[0034] In a further alternative embodiment, the fiber bundle tip may not require the mirror **16.** The combination of the fiber bundle tip **12** and the focusing lens **14** may be pivotally attached. Accordingly, through a pivoting motion, the combination of the fiber bundle tip **12** and the focusing lens **14** may be adapted to direct a plurality of focusing points along portions of a plurality of surfaces extending into the sample to construct the B-scan image **30** of the scan area **28.**

[0035] In yet another embodiment, the mirror **16** may be a surface of a prism. The rest of the apparatus would follow as previously described and shown in Figures 1a to 1d.

[0036] It should further be understood that the optical path can be straight, bent or curved. Furthermore, the optical path may be a 3 dimensional path having a length, width and height. Depending on the scanning motion (i.e. radial, linear or helical), the orientation of the surface, upon which the focal points reside, may also vary. Furthermore, the

optical path may comprise optical radiation from one optical radiation source or a plurality of optical radiation sources (i.e. a plurality of light sources or a plurality of fibers each transmitting optical radiation).

[0037] Referring now to Figures 2b and 2c, a magnified view of the fiber bundle tip **12** comprising the multiple single mode fibers **10** is shown. Each of the multiple single mode fibers **10** comprises a cladding **10a** around a core **10b** having diameters of, for example, 40 μm and 5 μm respectively. The ends of the multiple single mode fibers **10** may be stepped by 40 μm so that the focal points of the optical radiation through each of these fibers are spaced apart. However, a step spacing other than 40 μm may also be used.

[0038] Referring now to Figure 3, A-scans for each of the multiple single mode fibers **10,** in the fiber bundle tip **12**, are acquired over approximately the entire 2 mm imaging depth, but retained only over a short axial range of approximately 40 μm near the focal point of each fiber where the beam diameter is close to a minimum (indicated at **34)** and does not vary substantially with axial position. This range of 40 μm, in this exemplary design, is indicated at **31.** The A-scans are performed simultaneously by each of the multiple single mode fibers **10** within the fiber bundle tip **12.** Effectively, the multiple A-scans cover the entire depth of 2 mm in the sample tissue at different radial directions, but for each of the multiple single mode fibers **10,** only sections of the respective A-scan in a corresponding 40 μm depth-of-focus **31** are used to build up the image. As shown in the focal zone **31,** each of the beams **21b, 22b** and **23b** show a distinct "hourglass" shape for the focal points 38, 37 and 36, in known manner. For each of the beams **21b, 22b** and **23b,** the far field beam spread is indicated by lines **32** and the near field beam spread is indicated by lines **34.**

[0039] The purpose of rotating the mirror **16** is to create radial (i.e. lateral) scans in a direction that is perpendicular to the A-scan direction to create a B-scan image, i.e. the scan area **28** of Figure 1. The resultant radial scan pattern of the focal points of the individual fibers from the multiple single mode fibers **10** is illustrated in Figure 4. It is worth noting that a continuous scan surface is only present when the cleaved face of the mirror **16** is faced substantially in the direction of locations "A" and "C", where B-scan images should be taken. At other locations on the radial scan pattern, a "dead space" between the individual A-scans is too large to allow for sufficient sampling of the tissue. Therefore, the present invention comprises a sector-scan imaging device, to scan a sector substantially in the "A" or "C" locations, with a sector angle of about 20°, within which a 2 mm by 2 mm image is obtained. In this example, with the given geometry, a larger sector angle will produce "dead spaces" which are too large to form a suitable cross-sectional image.

[0040] Figures 4b and 4c show beam focal points **36, 37** and **38** from both a top view and an end view respectively. As shown, and corresponding to earlier figures, the individual focal points **36, 37** and **38** are spaced apart in the radial plane perpendicular to the axis **20.** As Figure 4c shows, in an end view along the axis **26,** the focal points **36, 37** and **38** are spaced apart in terms of depth but overlap to create a continuous scanning surface or scan area **28.**

[0041] If, the cleaved face of the mirror **16** is faced substantially in the direction of the locations indicated at "B" and "D", in Figure 4a, which is perpendicular to the scanning surface or scan area **28,** then the patterns shown in Figure 4d (a top view of the pattern) and Figure 4e (a side view of the pattern) are obtained. Here, the focal points are indicated at **40, 41** and **42.** As shown in Figure 4d, the focal points **40, 41** and **42** are each in an individual plane **40', 41'** and **42'** which are spaced apart corresponding to the spacing of the fibers in the fiber bundle tip **12.** The planes **40', 41'** and **42'** are perpendicular to the axis **20.** In Figures 4b to 4e, arrows **44** indicate the direction of the radial scan.

[0042] For the linearly translated system shown in Figure 1d, there are no "dead spaces" and thus linear translation can produce images suitable images approximately 2 mm by 2 mm in size.

[0043] In the exemplary design of the endomicroscopic system, the maximal speed of tissue motion, due to physiological motion, was chosen as 5 mm/s for *in vivo* imaging. A near diffraction-limited focusing lens (i.e. a lens which approximates an ideal lens by providing very small focal points) was chosen as the focusing lens **14.** The near diffraction-limited focusing lens was supplied by Melles Griot Inc. In addition, each single mode fiber, from the plurality of single mode fibers **10,** had a core diameter of 5 microns (i.e. $\varnothing_c \approx 5$ μm) and was operated at a wavelength of 0.86 μm. Furthermore, the design incorporates an approximate core index of $n_c = 1.447$ and a difference in the refractive index between the core and the cladding of $\Delta n = 0.005$. Using these values, the NA of the fiber is then given by:

$$NA \approx n_c(2\Delta n)^{1/2} = 0.145 \qquad (1)$$

and the acceptance angle, θ_a, of the fiber is given by:

$$\theta_a = \sin^{-1}(NA) = 8.32° = 0.145 \text{ rad} \qquad (2)$$

[0044] The design further incorporates the concept of an ideal lens which is used to focus optical radiation, from the plurality of single mode fibers **10,** at a magnification of 1 to 1 and that the far field beam divergence angle is similar to

θ_{a1}. Then, for light beam radiation with a center wavelength λ_o, the beam diameter at the focal point is given by:

$$\varnothing_f = 2w_o = 2\,\frac{\lambda_0}{\pi\theta_a} = 3.95\mu m \approx \varnothing_c \qquad (3)$$

The spot diameter $\varnothing_f$ is approximately equal to the core diameter ($\varnothing_c$=5μm) which results in efficient optical coupling. The depth of focus is $2\frac{\pi w_0^{\,2}}{\lambda_0} = 27.2$ mm and the beam diameter at the ends of the focal zones for focal points **36, 37** and **38** is given by:

$$\varnothing_f' = 2\sqrt{2}\,w_0 = 5.59\ mm \qquad (4)$$

Since the $\varnothing_f$ and $\varnothing_{f'}$ parameters are defined in terms of amplitudes, within 40 μm of the focal point in the axial direction, the beam diameter based on light intensity (i.e. the square of the light amplitude) may actually be smaller than 5 μm.

[0045] The above calculation is based on ideal optics operating on the principle optical axis. Using an off-the-shelf lens system with ∅=5 mm, f = 5 mm, and a working distance of 8.2 mm, it has been found that the off-axis angle required to cover a 2 by 2 mm image is about 5° using commercial ray-tracing software. At approximately an 80% fill factor of the focusing lens **14,** the ray-tracing results show the on-axis RMS focal point to be 5.3 μm in radius, and the 5° off-axis RMS focal point to be 10.3 μm in radius. A custom designed lens system should have better performance.

[0046] As illustrated in Figure 1, the working distance of the entire optical system, i.e. the distance from the focusing lens **14** to the focal point of the apparatus is determined by the focal length of the lens system, the diameter of the focusing lens **14** and the gap between the focusing lens **14** and the mirror **16.** Using the off-the-shelf lens system discussed above, the working distance is about 2.35 mm. The distance from the center of the image to the rotational axis of the mirror **16** is about 5.47 mm. To obtain a 2 mm scan in the radial direction, the sector scanning angle should be approximately ±10.4°, or about 20° in total, as determined by the geometry of the optical system.

[0047] Currently existing *in vivo* OCT systems perform radial scans at 4 to 8 revolutions per second (RPS) to yield a biologically acceptable 4 to 8 frames per second. For the design of the present embodiment, 4.4 RPS is chosen as the rotational speed. The rotational speed depends on the repetition rate of the A-scans and the number of A-scans required to obtain a 5 μm lateral resolution. Therefore, the imaging speed of the apparatus of the present invention is 4.4 frames/s while other imaging speeds may be chosen based on different end-user applications. The imaging time for each individual frame is 12.6 ms, as determined by the rotation speed and the sector scanning angle. Therefore, for a given frame, the system is acquiring signals for 12.6 ms and the time between frames is about 215 ms during which data processing is performed. These parameters are dependent on the performance of the optical delay generator (which is described later) that is used in the system.

[0048] While the above calculations were made based on a light source operating at a light wavelength of 860 nm and custom made single mode fibers, implementation using a light source operating at other wavelengths, such as 1300 nm, and off-the-shelf fiber may also be possible. Figure 5a shows a beam spot diagram for a 5 channel fiber bundle tip operating at a wavelength of 1300 nm and using off-the-shelf fibers (Corning SMF-28). The fiber bundle tip has a fiber step size of 125 μm. The light beams from these fibers, focused by a lens having a 5 mm diameter and a 4.5 mm focal length, cover a focal zone of approximately 0.65 mm. The resulting lateral imaging resolution is approximately 10 μm. Figure 5b shows a beam spot diagram for a 15 channel fiber bundle tip operating at a wavelength of 890 nm and using custom designed fibers having a core diameter of 5 μm and a cladding diameter of 40 μm. This fiber bundle tip has a fiber step size of 40 μm. The beams spots of only the central 5 channels are shown. The resulting lateral imaging resolution is approximately 5 μm over a focal zone of approximately 0.65 mm.

[0049] Figure 5c shows beam spot diameter versus distance along the focal zone for the 5 channel fiber bundle tip of Figure 5a. Figure 5c shows that the beam spot diameter is consistently less than 15 μm over the entire 0.65 mm focal zone. Figure 5d shows beam spot diameter versus distance along the focal zone for the 15 channel fiber bundle tip of Figure 5b. Figure 5d shows that the beam spot diameter is approximately 5 μm over the entire 0.65 mm focal zone.

[0050] Referring now to Figure 6, the overall general layout of the basic optical elements of the apparatus of the present invention comprises a plurality of optical sources **50,** a plurality of tree couplers **52,** a plurality of 3 dB couplers **54,** a fiber bundle tip **56,** a plurality of detectors **58,** a plurality of demodulators **60** and an optical delay generator **64.** The plurality of optical sources **50,** which may be lasers, are connected to the plurality of tree couplers **52.** More than

one laser may be needed to ensure that adequate optical radiation is provided to each of the fibers (i.e. channels) in the tip **56.** Each tree coupler **52** couples a respective optical source **50** to a subset of the plurality of 3 dB couplers **54.** The plurality of 3 dB couplers **54** are connected to the fiber bundle tip **56** for onward transmission of approximately half of the light radiation from the plurality of optical sources **50.** The fiber bundle tip **56** includes fiber bundle tip **12** and the other optical elements of Figure 1 (i.e. the focusing lens **14** and the mirror **16).** The other half of the radiation from the plurality of optical sources **50** is reflected back to detectors **58** which in turn are connected through the demodulators **60** to a computer **62** which functions to process the sampled data to generate the B-scan image **30.** The optical delay generator **64** is used by the 3 dB couplers **54** to provide a delayed reflected signal to the detectors **58.** The sample being investigated by the tip 56 is indicated at **65.**

[0051] In the layout shown in Figure 6, 1 dB or 10 dB optical couplers and the like may be used in place of the 3 dB couplers **54.** Furthermore, the intensity of the optical radiation transmitted to each of the 3 dB couplers **54,** and consequently each fiber, by the tree couplers **52** need not be the same and in fact is chosen depending on whether the 3 dB coupler provides optical radiation to a fiber (i.e. channel) that facilitates a deep or shallow scan into the tissue. High intensity optical radiation is needed to scan deeply into the tissue. Accordingly, tree couplers **52** and 3 dB couplers **54** that feed optical radiation to fibers that scan deeply into the tissue are adapted to provide larger amounts of optical radiation.

[0052] Figures 7a and 7b show the optical delay generator **64** in greater detail. The optical delay generator **64,** similar to those in existing *in vivo* OCT systems, is used to perform the A-scans using the coherence envelope of each individual fiber. The optical delay generator **64** comprises a grating **66,** a lens **67,** a scanning mirror **68** and a mirror **69.** Rapid depth scanning can be achieved with the optical delay generator **64** by dispersing quasi-monochromatic light from the multiple single mode fibers **10** in the fiber bundle tip **12** onto the diffraction grating **66** and focusing the dispersed light onto the oscillating mirror **69.** This has the effect of applying a linear ramp in the frequency or Fourier domain as described by G. J. Tearney, B.E. Bouma and J. G. Fujimoto ("High-speed phase and group delay scanning with a grating based phase control line" Nature Medicine 4(7), 861-865 (1998)). With recombination of the reflected wavelengths at the diffraction grating **66,** a real space-time delay is created. The angle of the scanning mirror **68** is rapidly oscillated through several degrees of rotation creating a rapidly varying time delay in the reference arm which allows for fast, repeated depth scanning of a sample.

[0053] The optical radiation **70** from one fiber from the multiple single mode fibers **10** is shown in Figure 7a. The optical radiation **70** is dispersed into spectral components represented by spectral components **71, 72** and **73** by the grating **66.** Spectral component **71** represents the lowest wavelength in the optical radiation **70;** spectral component **73** represents the highest wavelength in the optical radiation **70;** and spectral component **72** represents the center wavelength in the optical radiation **70.** These spectral components of the optical radiation **70** are vertically aligned in the optical delay generator **64.** In a similar fashion, optical radiation from other fibers from the multiple single mode fibers **10** are dispersed and vertically aligned, with a vertical spacing between the dispersed optical radiation from the different fibers. The offset of the center wavelength of the dispersed optical radiation from the pivot axis of the scanning mirror **68,** for a given fiber, is represented by X_d which facilitates phase modulation of the dispersed optical radiation from each of the multiple single mode fibers **10.** Alternatively, if X_d were zero then a phase modulator would be needed, for each of the single mode fibers **10,** to phase modulate the optical radiation from each of the single mode fibers **10.** This has the advantage of allowing for a reduction in size of the scanning mirror **68** which in turn allows for a higher frame rate to be used. Furthermore, the phase modulator is electrically controlled which allows for very stable signals are generated

[0054] Referring now to Figure 7b, the multiple single mode fibers **10** are aligned in the fiber bundle tip **12,** such that dispersed optical radiation from each of the multiple single mode fibers **10** is vertically aligned on the scanning mirror **68** as rows **75, 76, 77** and **78.** Alternatively, other ordered arrangements may also be used for the spectral components of the optical radiation from each fiber from the multiple single mode fibers **10** such as columns.

[0055] As illustrated in Figure 6, a single optical delay generator may be used to introduce delay in multiple fibers. The limiting factor in determining the number of channels that may be coupled to a single optical delay generator is the physical size of the scanning mirror which is in turn limited by the resonance frequency of the optical delay generator. Commercially available resonance optical scanners can operate up to 16 kHz. Accordingly, a size of 4 mm by 5 mm may be used for the scanning mirror **68.** Since the fiber bundle array is about 2 mm in size, it is possible to fit the entire array onto one optical delay generator. Therefore, for the embodiment of the present invention, a single optical delay generator is used having an optical scanner operating at f_r = 16 kHz with an optical scan angle α of $\pm$ 2°. The embodiment also incorporates a grating pitch of p = 3.33 μm, a center wavelength of λ_0 = 0.86 μm and a focal length of f_l = 21 mm. Accordingly, the free space group path length difference Δl_g is given by (from Rollins et al. 1998):

$$\Delta l_g = 4\alpha(f_l \frac{\lambda_0}{p} - x_d) = 0.618 \text{ mm} \qquad (5)$$

which is also 1.24 mm peak to peak. In equation 5, X_d = 1 mm is the displacement between the λ_0 spectral line and the pivoting axis on the resonance mirror. The peak A-scan speed is given by:

$$V_{Amax} = 2\pi\Delta l_g f_r = 62.1 \text{ m/s} \quad (6)$$

and the A-scan speed varies according to equation 7.

$$V_A = V_{Amax}\cos(2\pi f_r t) \quad (7)$$

Choosing a source with a coherence length l_c of 5 μm and a Gaussian emission spectrum, the equivalent emission bandwidth is given by:

$$\Delta\lambda = \beta\frac{\lambda_0^{\,2}}{l_c} = 98 \text{ nm} \quad (8)$$

where b = 0.66 for a Gaussian envelope.

[0056] The size of the resonant mirror is determined next. For an optical delay generator with a grating having a first order diffraction, the diffraction angle is given by:

$$\theta(\lambda) = \sin^{-1}(\lambda/p) \quad (9)$$

The spread of the spectrum from (λ_0-Δλ/2) to (λ_0 +Δλ/2) at the Fourier plane of the lens is given by:

$$\Delta x \approx 2f_l\left[\theta\left(\lambda_0 + \Delta\lambda/2\right) - \theta\left(\lambda_0 - \Delta\lambda/2\right)\right] = 1.3 \text{ mm} \quad (10)$$

[0057] Since the mirror width is 4 mm, one can fit the spectrum on one side of the resonant mirror with the displacement x_d having a value of approximately 1 mm. This is illustrated in Figures 7a and 7b. The carrier frequency of an individual channel of the system is given by (Rollins et al. 1998) :

$$f_c = (4x_d\alpha 2\pi f_r/\lambda_0)\cos(2\pi f_r t) \quad (11)$$

which is 16.3 MHz at the maximum.

[0058] The bandwidth of the interferogram (i.e. the interference fringe pattern) is given by:

$$\Delta f = \frac{\Delta\lambda}{\lambda_0^{\,2}} 4\pi\alpha f_r 2\left(f_l\lambda_0/p - x_d\right)\cos(2\pi f_r t) \quad (12)$$

which is 8.4 MHz at the maximum.

[0059] Since $f_c(t) > \Delta f(t)$, proper demodulation can be performed by conventional rectifying and low-pass filtering, although a sharp frequency cut-off is needed. It is preferable to set up the individual channels of the system such that D_A= 40 μm (the depth of the A-scan performed by a single channel) coincides with the maximum carrier frequency, so that the variation in carrier frequency over D_A is minimized. The carrier frequency varies sinusoidally in time given by:

$$\Delta f_c = f_c\{1 - \cos[\sin^{-1}(D_A/\Delta l_g)]\} = 34 \text{ kHz} \qquad (13)$$

which is about 0.2% of f_c.

[0060] At other locations, the signal can still be properly demodulated, but the variation in carrier frequency will be larger. The demodulators **60** may incorporate an analog high-speed rectifier and a 10-pole low-pass filter to demodulate the signal. Effectively, the signal is frequency down-shifted such that the signal is centered at DC and has a bandwidth of Δf. The demodulated envelope signal is then digitized at an appropriate sampling rate. Current existing data acquisition (DAQ) cards operate at 30 MegaSamples per second (MS/s) with an SNR of about 60 dB. Choosing a Gaussian shape for the interferogram spectrum with Δf = 8.4 MHz, the 60 dB point is at about 14.5 MHz. Accordingly, the Nyquist rate for digitizing such a signal is approximately 29 MS/s. Therefore, current existing DAQ cards will be able to digitize the envelope signal without aliasing.

[0061] Given a sampling rate of 30 MS/s for digitizing the envelope signal at the maximum carrier frequency, the spatial sampling interval in the axial direction is: $\Delta_{axial} = V_{Amax}/S$ = 2.07 μm. As shown in Figure 8, a scan path **80** is indicated showing A-scans alternately going up and down through the sample. Sampling points are indicated at **82.** The axial spacing of 2.07 μm is indicated at **84.** The spatial sampling interval in the lateral direction is determined by the lateral or B-scan velocity and the resonant frequency of the optical scanner in the optical delay generator **64.** At the center of the image, where the radial distance r is 5.47 mm from the rotational axis of the mirror, the radial sampling interval is given by:

$$\Delta_{radial} = V_{radial}/2f_r = 2\pi\Omega r/2f_r = 4.73 \text{ μm} \qquad (14)$$

This interval is indicated at **86** in Figure 8. For the fiber scanning the shallowest depth, the spatial lateral sampling interval is 3.86 μm and for the deepest channel it is 5.59 μm. Therefore, the pixel size at the center of the image is 2.07 by 4.73 μm in the axial and lateral direction respectively. The lateral pixel size varies across the depth of the image from 3.86 to 5.59 μm. By varying the rotational speed of the mirror **16,** the lateral sampling interval can be changed, at the expense of frame rate. If a higher resonance frequency optical scanner is used, the sampling interval may also be reduced.

[0062] For a pulsed optical source (e.g. a 15 to 20 fs pulsed laser emitting light with a wavelength of 860 nm), the coherence length will be approximately 4.5 to 6 μm. Since the spatial sampling interval in the axial direction is about 2 μm, which is smaller than half of the coherence length, the image is reasonably sampled in the axial direction. Using a near diffraction-limited focusing lens as the focusing lens **14,** the beam spot size should be about 5 μm. Since the spatial sampling interval in the lateral direction varies from 3.86 to 5.59 μm, the image is slightly under sampled, given that the beam waist size is about 5 μm. However, the spatial sampling interval is not equivalent to the final image resolution, which is also influenced by local contrast and noise levels. Local contrast is the difference in reflectivity between two points in the sample that show up as adjacent pixels in the image. If the two points have similar reflectivity, i.e. low local contrast, it will be difficult to resolve these points.

[0063] Imaging speed should be fast enough to reduce motion blurring. Given that the target speed (i.e. tissue motion) is typically 5 mm/sec, then within a frame time (an elapsed time of 12.6 ms), the target can move up to 63 μm in a particular direction which is much larger than the designed 5 μm resolution. In the present embodiment, the A-scan is performed simultaneously in all channels such that one line of the image is formed within 0.6 μs which is the time required to scan the coherence gate through a 40 μm distance. The time between two consecutive A-scans is about 16 μs, which is determined by the rotational speed of the mirror **16** of the system and the number of A-scans per image. Thus, the resultant image should be crisp since the motion during 16 μs is 0.08 μm which is much less than the resolution. Accordingly, there should be no motion blurring in the image but a motion artifact may still exist. The resultant motion artifact may be a geometric deformation of the features being imaged that may be as large as 63 μm depending on the size of the feature and the target velocity. This motion artifact is due to the effect that the air-tissue interface has on the optical radiation from the plurality of optical sources **50.**

[0064] As illustrated in Figure 9, the focal point of an individual fiber of the apparatus, inside the tissue being imaged, can vary depending on the distance do of the location of the focal point in the tissue, whether the tissue surface had a refractive index of 1, and the actual refractive index of the tissue (which is typically approximately 1.4). Accordingly, the actual focal point is at a distance d_f below the tissue surface given by:

$$d_f = d_0 \frac{\tan\theta_1}{\tan\theta_2} = d_0 \frac{\tan\theta_a}{\tan\left[\sin^{-1}\left(\frac{n_1}{n_2}\sin\theta_a\right)\right]} \qquad (15)$$

where θ_1 is assumed to be equal to θ_a, the acceptance angle of the individual fibers and θ_2 will be determined by the refractive index $n_1 = 1$ (i.e. air) outside the tissue and $n_2 = 1.4$ inside the tissue.

[0065] The coherence gate location varies according to:

$$d_c = \frac{n_1}{n_2} d_0 \qquad (16)$$

Accordingly, due to the fact that optical radiation travels more slowly in a medium with a larger refractive index there is an optical path mismatch between the focal point and the coherence gate of an optical beam which is matched in a medium with $n_1 = 1$ (i.e., with no tissue present). This mismatch is:

$$\Delta d = n_2(d_f - d_c) = \frac{n_2 d_0 \tan\theta_a}{\tan\left[\sin^{-1}\left(\frac{\sin\theta_a}{n_2}\right)\right]} - d_0 \qquad (17)$$

A tissue refractive index of $n_2 = 1.4$ yields $\Delta d = 0.97\, d_o$. This mismatch problem is common for all high-NA OCM systems and many existing high-NA OCM systems use some form of dynamic compensation, i.e., changing the reference path length dynamically to compensate for $\triangle d$, however, such dynamic compensation is difficult with a high imaging speed. Accordingly, one aspect of the embodiment of the present invention is to use 'flexible triggering' of the detected interferogram signal.

[0066] As shown above, the free space group path length difference is $2\Delta l_g = 1.24$ mm peak to peak, which is much larger than the useful A-scan range of only 40 μm. This leaves room for dealing with the mismatch since one then can trigger to obtain the interferogram only when the coherence gate is passing through the focal point.

[0067] As shown in Figure 9, the working distance for each fiber channel, d_w, varies with n_2, which is approximately constant Therefore, if one knows where the tissue surface is, d_0 can be determined and in turn Δd can be determined.

[0068] Referring to Figure 10, showing a perspective view of a tissue surface and an arbitrary axial line **90,** channel 1, which is designated to scan the surface of the tissue, is the first to pass through the axial line **90,** in the scan area **28.** The focal points of channels 1 and 2 are indicated at **91** and **92** in a schematic representation **94** of the optical radiation from the multiple single mode fibers **10** (i.e. channels) passing through the axial line **90.** The focal point of the last channel, i.e. channel 50 in this example, is indicated at **95** and is designated to scan the deepest layer of the tissue in the image. The overall profile of the representation **94** defines a flexible trigger zone, within which the coherence gate and the focal length can be matched. One of the 50 channels, i.e. channel "v", will experience a large and distinctive specular reflection since the air-tissue interface approximates a mirror and reflects incident light. Underneath the tissue surface, the tissue acts as a turbid media which scatters and absorbs incident optical radiation. Thus, channel "v" will determine d_0 for this particular axial line **90** since all of the channels before channel "v" will return a signal that is at noise level. Accordingly, the "flexible triggering" method comprises comparing the detected reflected optical radiation for adjacent channels to locate the tissue surface by identifying the channel in which there is a large increase in reflectance compared to its 'neighboring' channels. This information is then passed on to each of the subsequent channels and the trigger point for each channel is set accordingly to reduce mismatch between the focal point and the coherence gate.

[0069] As an example, if channel "v" is channel 13 then the apparatus is calibrated such that channels 1 to 12 are set to scan free space above the tissue surface, channel 13 to scan the tissue surface, and subsequent channels are set to scan deeper tissue, with no mismatch between the focal point and the coherence gate of the optical beam of each channel. During imaging, a tolerance of $\Delta d_o = \pm$ 0.5 mm of the location of the tissue surface can be allowed as indicated at **96** in Figure 10. This tolerance is related to the A-scan performance and the frequency response of the envelope detector as will now be explained.

[0070] Given $\Delta d_o = 0.5$ mm, the mismatch that needs to be compensated for is given by:

$$\Delta d' = 0.693 \times 0.5 = 0.347 \text{ mm} \qquad (18)$$

This means that instead of triggering the interferogram signal at the maximum carrier frequency, the actual carrier frequency needs to be:

$$f_c' = f_{cmax} \cos(\sin^{-1}(\Delta d'/\Delta l_g)) = 13.5 \text{ MHz} \qquad (19)$$

which is about 83% of the maximum carrier frequency with the interferogram signal bandwidth changing accordingly. Although the envelope detector's frequency response can be tuned dynamically, it is simpler and faster for the envelope detector to have a fixed response but it was designed for a 17% tolerance of the cut-off frequencies. In this way, the entire flexible triggering scheme contains only fixed components and all of the compensation is performed electronically to satisfy the high imaging speed requirement.

[0071] The optical components shown in Figure 6 can be chosen as follows. Based on Boppart, S.A., Bouma, B.E., Pitris, C., Southern, J.F., Brezinski, M.E., and Fujimoto, J.G. (*In vivo Cellular Optical Coherence Tomography Imaging,* Nature Medicine, **Vol. 4 No.7**:861-865, July 1998), an SNR of greater than 100 dB can be achieved in a non-endoscopic OCT system using 2 mW of incident power on the tissue to allow for imaging to a depth of approximately 2 to 3 mm. The optical source used was a Kerr-lens mode-locked solid-state Cr^{4+}: forsterite laser operating at a 1280 nm center wavelength with a coherence length of 5.1 μm. However, the embodiment of the present invention is not limited to this type or any other particular type of source, such as a broadband superluminescent diode. For instance, another possibility is a white-light emission Cr:LiSAF optical source with a bandwidth of approximately 100 nm centered at 860 nm which will provide a coherence length of approximately 4.5 to 6 μm. This diode-pumped, solid-state, mode-locked laser should operate with a pulse-repetition rate of about 100 MHz and an average power of 30 mW when operated at 860 nm. The pulse energy variation should be less than 1%. Several (e.g., 2 or 4) of these lasers as indicated at **50** in Figure 6 are needed to provide the total power requirement of the 50 channels. The channels scanning the deeper portion of the tissue will need about approximately 1 to 2 mW of incident power per channel and the channels scanning the shallower portion will need less. The tree couplers **52** can be configured to split the source power to match these requirements. Since the maximum carrier frequency is 16.3 MHz, each interference fringe will contain at least 6 laser pulses. Therefore the fringe pattern should be adequately sampled.

[0072] For each channel, a separate photo receiver or detector **58** may be used to detect the interference fringes. The maximum detector bandwidth is 125 MHz, although in the apparatus of the present invention, a detector bandwidth of 30.8 MHz may be sufficient, as determined by the carrier frequency and the bandwidth of the interferogram.

[0073] An alternate embodiment of the present invention involves the concept of sharing optical components to reduce device complexity and cost. Referring to Figure 11a, a typical single channel interferometer **150** with balanced detection in which the AC component of the interferogram is separated from the DC component of the interferogram and only the AC component is amplified is shown. The single channel interferometer **150** comprises an IR broadband light source **L,** a visible wavelength guide light **G,** a balanced detector **BD**, a polarization controller **PC,** a phase modulator ϕ**MOD** and an optical delay generator **ODG** which are connected through a network of optical fibers and 3 dB couplers **140, 142** and **144.** The "x" denotes a dead end in the fiber network. The visible wavelength guide light **G** may be a green laser which indicates the direction in which the single channel interferometer **150** is pointing (i.e. it indicates what will be imaged). The single channel interferometer **150** is connected to a sample **S.**

[0074] The design of Figure 11a can be extended to construct a two channel interferometer **160** as shown in Figure 11b. The subscripts denote the components that are in the two channels. A component without subscripts indicates that the component is used in both channels. The two channel interferometer **160** comprises a laser **L'**, a visible wavelength guide laser **G',** a 2 to 1 tree coupler **TC1,** polarization controllers $\mathbf{PC_1}$, $\mathbf{PC_2}$ and phase modulator ϕ**MOD',** variable delay elements $\mathbf{VD_1}$ and $\mathbf{VD_2}$, an optical delay generator **ODG',** detectors $\mathbf{BD_1}$ and $\mathbf{BD_2}$ and 3 dB couplers **162, 164, 166, 168, 170** and **172.** The variable delay elements $\mathbf{VD_1}$ and $\mathbf{VD_2}$ are introduced to adjust the coherence gate positions for each channel. The two channels are coupled to samples $\mathbf{S_1}$ and $\mathbf{S_2}$ which may be two points at different locations in a tissue sample. The light source **L'** is shared between the two channels in this case, with the optical power in channel 1 being twice that in channel 2. Therefore, channel 1 should be used to scan a deeper region of tissue than channel 2. The 1 to 2 tree coupler **TC1** is used so that both channels can share the same reference arm (comprising the phase modulator ϕ**MOD'** and the optical delay generator **ODG').** The ability to share the same reference arm allows one phase modulator to be used to phase modulate the optical radiation from the multiple single mode fibers **10** (i.e. all the channels). Note that the two channels are combined into one fiber by the tree coupler **TC1** and then fed to the same phase modulator ϕ**MOD'.** Accordingly, cost and complexity of the two channel interferometer **160** is reduced.

[0075] Based on Figure 11b, it is conceivable that a general optical network can be used to construct an N channel OCT system such as optical network **180** shown in Figure 11c. The optical network **180** comprises an optical network for an n^{th} channel **182** and a reference arm **184** that is shared by all n channels. The optical network for the n^{th} channel **182** comprises a detector $\mathbf{BD_n}$, 3 dB couplers **194, 196** and **198** and a sample arm comprising a polarization controller $\mathbf{PC_n}$ and a variable delay element $\mathbf{VD_n}$ connected to a sample $\mathbf{S_n}$. The optical network for the n^{th} channel **182** receives optical source radiation **186** from the $n\text{-}1^{th}$ channel and transmits optical source radiation **188** to the $n+1^{th}$ channel via 3 dB coupler **194.** The optical network for the n^{th} channel **182** receives guide light power **190** from the $n\text{-}1^{th}$ channel and sends guide light power **192** to the $n+1^{th}$ channel via 3 dB coupler **196.** In this embodiment, a light source (not shown) may be shared between each of the N channels with a power distribution that follows a geometric series or another suitable power partition scheme. The reference arm **184,** comprising an N to 1 tree coupler **TCn,** a phase modulator ϕ**MOD"** and an optical delay generator **ODG",** is shared between each of the N channels.

[0076] Each of the schematics shown in Figures 11a, 11b and 11c, suffer from the fact that a portion of the optical radiation of the interference pattern, from the interference between the reflected optical radiation from the sample and reference arms, which is sent from the 3 dB coupler connected to the detector is lost. In this case 50% of the optical radiation of the interference pattern is lost since a 3 dB coupler is used. For instance in Figure 11a, only 50% of the optical radiation of the interference pattern is sent from 3 dB couplers **140** and **142** to the detector **BD.** This makes it more difficult to detect the interference pattern especially for interference patterns with low intensities. To address this, a non-reciprocal optical device, such as an optical circulator may be used to send, to a detector, the portion of the optical radiation that would have been lost if only a 3 dB coupler were used.

[0077] Referring to Figures 12a, 12b and 12c, alternate embodiments of a single channel OCT device **200,** a two channel OCT device **210** and an optical network for an N channel OCT device **220** are shown comprising optical circulators. In Figures 12a, 12b and 12c, the optical circulators **C,** $\mathbf{C_1}$, $\mathbf{C_2}$ and $\mathbf{C_n}$ are used to salvage and direct the optical radiation of the interference pattern to the detectors **BD,** $\mathbf{BD_1}$, $\mathbf{BD_2}$ and $\mathbf{BD_n}$ respectively to provide a larger intensity interference signal for detection. The rest of the components in these embodiments are similar to those in the of the single channel OCT device **150,** the two channel OCT device **160** and the optical network for the N channel OCT device **180** shown in Figures 11a to 11c. The concept of using optical circulators to salvage optical radiation and provide the salvaged optical radiation to a detector may also be applied to the apparatus of Figure 6 in which optical circulators could be placed between the 3 dB couplers and the detectors.

[0078] The schematic shown in Figure 11c and 12c leads to an elegant design, however, parallel interferometers that share components (i.e. a phase modulator) may produce prohibitive amounts of channel cross talk which may consequently lead to image degradation. However, with fiber length mismatching between channels, cross talk may be effectively handled. Electronic cross-talk can be handled using standard shielding and grounding techniques. The following describes the optical cross-talk.

[0079] Referring now to Figure 13a, a two channel OCT system **230** was assembled to investigate channel cross talk. The two channel OCT system **230** comprises a laser $\mathbf{L_E}$, detectors $\mathbf{D_1}$ and $\mathbf{D_2}$, beam splitters $\mathbf{BS_1}$ and $\mathbf{BS_2}$, a 1 to 2 tree coupler $\mathbf{TC_E}$, a phase modulator $\mathbf{PM_E}$, an optical delay generator $\mathbf{ODG_E}$, beam collimators $\mathbf{BC_1}$ and $\mathbf{BC_2}$ and two mirrors $\mathbf{S_1}$ and $\mathbf{S_2}$ which simulate samples. In the two channel OCT system **230,** the desired imaging signals come from the channel 1 and channel 2 optical paths. The desired imaging signal for channel 1 occurs when light from the optical pathway:

$$\mathbf{L_E \rightarrow BS_1 \rightarrow S_1 \rightarrow BS_1 \rightarrow D_1} \qquad (20)$$

interferes coherently with light from the optical pathway:

$$\mathbf{L_E \rightarrow BS_1 \rightarrow ODG_E \rightarrow BS_1 \rightarrow D_1} \qquad (21)$$

and is detected by the detector $\mathbf{D_1}$. The desired imaging signal for channel 2 occurs when light from the optical pathway:

$$\mathbf{L_E \rightarrow BS_2 \rightarrow S_2 \rightarrow BS_2 \rightarrow D_2} \qquad (22)$$

interferes coherently with light from the optical pathway:

$$\mathbf{L_E \rightarrow BS_2 \rightarrow ODG_E \rightarrow BS_2 \rightarrow D_2} \qquad (23)$$

and is detected by the detector D_2. Furthermore, OCT imaging in the two channels occurs only when the optical distance $BS_1 \rightarrow S_1$ is equal to the optical distance $BS_1 \rightarrow ODG_E$ and when the optical distance $BS_2 \rightarrow S_2$ is equal to the optical distance $BS_2 \rightarrow ODG_E$. Otherwise, image degradation could occur from constructive interference of light reflected from two (or more) different paths that are not the desired imaging paths stated above.

[0080] Based on the optical network shown in Figure 13a, there may be two major classes of potential cross talk. The primary source of cross talk may be coherent light that is reflected (from a mirror or the sample) from one channel's beam splitter into the other channel's beam splitter and detector. Such cross talk would have intensities equal to the imaging signal intensities and could potentially cause significant image degradation. Reflection from one channel to the other could occur at the optical delay generator ODG_E or at the samples S_1 or S_2. Therefore, light from the optical pathway:

$$L_E \rightarrow BS_1 \rightarrow S_1 \rightarrow BS_1 \rightarrow D_1 \quad (20)$$

may interfere with light from the optical pathway:

$$L_E \rightarrow BS_2 \rightarrow ODG_E \rightarrow BS_1 \rightarrow D_1 \quad (24)$$

Alternatively, light from the optical pathway:

$$L_E \rightarrow BS_2 \rightarrow S_2 \rightarrow BS_2 \rightarrow D_2 \quad (22)$$

may interfere with light from the optical pathway:

$$L_E \rightarrow BS_1 \rightarrow ODG_E \rightarrow BS_2 \rightarrow D_2 \quad (25)$$

[0081] Sample arms 1 and 2 would not normally be separated as they are in Figure 13a because the sample arms would be aimed at different points (i.e. different depths) on a tissue sample. When the sample arms are not separate, reflection could occur from channel 1 into channel 2 and vice-versa. In such a case, light from the optical pathway:

$$L_E \rightarrow BS_2 \rightarrow S_2 \rightarrow BS_1 \rightarrow D_1 \quad (26)$$

may interfere with light from the optical pathway:

$$L_E \rightarrow BS_1 \rightarrow ODG_E \rightarrow BS_1 \rightarrow D_1 \quad (21)$$

Alternatively, light from the optical pathway:

$$L_E \rightarrow BS_1 \rightarrow S_1 \rightarrow BS_2 \rightarrow D_2 \quad (27)$$

may interfere with light from the optical pathway:

$$L_E \rightarrow BS_2 \rightarrow ODG_E \rightarrow BS_2 \rightarrow D_2 \quad (23)$$

[0082] It should be recalled that reflection may also occur at undesirable locations such as beam splitters and connector insertion points. Conceivably, such reflections may contribute to image noise if the light from these pathways produced

interference fringes having a significant intensity. However, this kind of noise may be secondary to the channel cross talk previously described because of its lower intensity.

[0083] Analysis of the system revealed that the worst-case scenario for interference of such back-reflections involves one reflection from a connector. For example, light from the following optical path:

$$L_E \rightarrow BS_1 \rightarrow S_1 \rightarrow BS_1 \rightarrow D_1 \qquad (20)$$

may interfere with light from the optical pathway:

$$L_E \rightarrow BS_2 \rightarrow ODG_E \rightarrow PM_E \rightarrow ODG_E \rightarrow BS_1 \rightarrow D_1 \qquad (28)$$

[0084] There are four possible outcomes for the interference of light from any two pathways and the outcome depends on path length difference. Firstly, if the path lengths are identical, then the intensity of the interference fringes at the detector will be greater than the true signal intensity based solely on the sample reflectivity. This sort of image noise would not be detectable as noise and would alter the measured sample intensity throughout the image. Fortunately, the probability of the path lengths matching exactly is remote. A second possibility is that the path lengths could match to within the coherence length of the light source. This situation would result in an increase in the width of the interference fringe envelope and consequently degradation in axial resolution. This situation is unlikely, but it may be detected by measuring the full-width-half-maximum of the mirror surface depth profile. A third possibility involves the path lengths differing by a distance greater than the coherence length of the source L_E and less than the scanning depth of the optical delay generator ODG_E. This situation may manifest as two separate coherence envelopes within one depth sweep by the optical delay generator ODG_E. The final and most likely possibility is that the path lengths differ by more than the scanning depth of the optical delay generator ODG_E and no noise or extraneous interference fringes will be detected by the system.

[0085] The primary type of channel cross talk should be unlikely because of fiber optic manufacturing. Optical path lengths $BS_1 \rightarrow ODG_E$ and $BS_2 \rightarrow ODG_E$ are essentially predetermined by the lengths of the fiber pigtails coming from beam splitters BS_1 and BS_2. Optical path lengths $BS_1 \rightarrow S_1$ and $BS_2 \rightarrow S_2$ are deliberately matched to the predetermined corresponding reference arm lengths. Typically manufactured fiber lengths differed by several tens of millimeters which is at least one order of magnitude greater than the scanning depth of the optical delay generator ODG_E. Therefore, this type of cross talk should not be a problem in a dual channel system.

[0086] In the case of insertion point reflections, if the optical distance $PM_E \rightarrow ODG_E$ matched the path length difference between optical paths $BS_1 \rightarrow S_1$ and $BS_2 \rightarrow ODG_E$, then interference fringes and image degradation may occur. Again, this sort of secondary noise should be unlikely because the fiber lengths are about 300 mm while the optical delay generator ODG_E scans through only a couple of millimeters. Furthermore, the intensity of such interference fringes would be lost in the system noise. Secondly, the equipment used has a maximum 0.6 dB insertion loss (in other words a maximum of reflection of 0.6 dB) and therefore such a signal is below the detection limits used in the setup of Figure 13a.

[0087] To demonstrate that two channels can use the same fiber and optical components, the OCT system **230** was evaluated. The sample arm mirrors S_1 and S_2 were placed such that the sample arm optical path length and the optical delay generator ODG_E reference arm optical path length matched for each channel and a set of interference fringes were seen at each of the detectors D_1 and D_2. The sample arms for samples S_1 and S_2 were kept separate for alignment purposes and to eliminate the possibility of light from channel 1 reflecting into the fiber containing channel 2 and vice-versa. Although an optical delay generator could be used to produce both phase modulation and group delay (Tearney et al. 1997), with the setup shown in Figure 13a, the optical delay generator ODG_E was used for group delay (i.e. depth scanning) while the phase modulator PM_E in the reference arm was used to produce phase delay.

[0088] In the experimental setup of Figure 13a, the light source L_E comprised a 1310 nm, 9 mW. light source (model BBS1310) made by AFC Technologies Inc. The central wavelength of the light source L_E was 1310 nm with a measured spectral spread of $\pm$ 40 nm. The measured coherence length of the light source L_E was 10 μm. The detectors D_1 and D_2 were 155 Mbps Perkin Elmer InGaAs photodiode receivers with a detection band centered at 1310 nm having a bandwidth greater than or equal to 100 nm. The phase modulator PM_E was a JDS Uniphase 43 MHz phase modulator. The beam splitters BS_1 and BS_2 were made by MetroTek. OZ Optics manufactured the beam collimators BC_1 and BC_2. Alternate suitable components may be used from these or other suppliers.

[0089] The optical delay generator ODG_E dispersed the collimated light using a 150 line/mm diffraction grating blazed for 1310 nm which was made by CVI Spectral Products. A Melles Griot glass doublet lens with a 30 mm diameter and 100 mm focal length was used to focus light onto the oscillating mirror. EOPC (Electro-Optical Products Corporation)

manufactured the resonant scanner that operated at 8 kHz and scanned through a ± 1° mechanical or a ± 2° optical angle. This angular setting corresponded to a depth scan of about 1 mm in the sample arms for the samples $\mathbf{S_1}$ and $\mathbf{S_2}$. Scanning depth is an important consideration in terms of mismatching the optical lengths of the two channels. For instance, if the optical path lengths differ by more than 1 mm then cross talk between the two channels should be minimal and proper shielding and grounding techniques should address electronic cross-talk as well.

[0090] Figures 13b and 13c show results from experiments conducted on the setup shown in Figure 13a. Figure 13b shows the oscilloscope trace from the detectors $\mathbf{D_1}$ and $\mathbf{D_2}$ in channel 1 and channel 2. Figure 13b shows that the interference fringes occur at different points in the cycle of the optical delay generator $\mathbf{ODG_E}$ which reflects the slightly different positioning of the two channels within the cycle of the optical delay generator $\mathbf{ODG_E}$, i.e. the sample arm mirrors $\mathbf{S_1}$ and $\mathbf{S_2}$ were deliberately offset by a small amount to simulate imaging at different depths. Figure 13b shows that there is a strong imaging signal in each of the channels and no evidence of any cross talk. The arrows **232** and **234** indicate reflection from two different sample points which could correspond to two different points in a tissue sample. Furthermore, the full-width-half-maximum of the envelope of each detected pulse corresponded to the coherence length of the light source $\mathbf{L_E}$ which indicates that the light signal in each channel originated from the light source $\mathbf{L_E}$. Figure 13c shows the experimental results when one of the sample points was moved relative to the other sample point. In this case, cross-talk was also not observed.

[0091] In another embodiment of the invention, the fiber optic network, previously disclosed herein, is incorporated into an endoscope so that the multi-channel OCT methodology may be used clinically. Due to the size of the fiber bundle tip **12** of the apparatus, the fiber bundle tip **12** will not fit into the working channel of a conventional diagnostic endoscope (although it may be incorporated into the larger-diameter therapeutic endoscopes). Therefore, an alternate design approach was taken. Instead of designing the fiber bundle tip **12** to accommodate the working channel of a conventional diagnostic endoscope, all of the functionality of a conventional diagnostic endoscope was designed around the fiber bundle tip **12**. As shown in Figure 14, one embodiment of a GI endoscope **300** (corresponding to the tip **56** of Figure 6) incorporating the endomicroscope of the present invention is approximately 11 mm in diameter. This is slightly larger than the conventional diagnostic endoscope which is 8 - 9 mm in diameter. The GI endoscope **300** has the endomicroscopy capability disclosed above in addition to conventional forward-viewing white light imaging. Therefore, a user of the GI endoscope **300** should be able to obtain a 2 by 2 mm cross-sectional image as illustrated in Figure 16.

[0092] The GI endoscope **300** includes a 2.7 mm diameter suction/biopsy channel **302**. The end of the suction/biopsy channel **302** is bent so as to present an opening **304** directed towards the tissue area of interest **306**. The axis of the suction/biopsy channel **302** may be on the order of 6.7 mm from the center of the tissue area of interest **306**. Two channels **308** and **310** are provided for white light illumination and a channel 312 is provided for white light endoscope forward viewing. Each of the channels **308**, **310** and **312** may have a diameter of 2.7 mm. A small channel **314** is also provided for an air or water nozzle.

[0093] In accordance with an embodiment of the present invention, a side-viewing Endoscopic Coherent Optical Microscope (ECOM) **316** is provided in the GI endoscope **300**. The side-viewing ECOM **316** includes a drive mechanism **318** for rotating the mirror **16** (not shown in Figures 14 and 15). As mentioned previously, radial, translational or helical scanning may be employed. Furthermore, as previously mentioned, a MEMS drive mechanism may be used instead of a mechanical drive mechanism. The side-viewing ECOM **316** is configured to scan through the tissue area of interest **306** having the depth set by the boundaries **320** and the angular extent set by the boundaries **322**. Additionally an optical window **324** may be provided for the side-viewing ECOM **316** (see Figure 15).

[0094] The forward-viewing white light channel **312** is updated at a rate of 30 frames/sec. The cross-sectional images obtained by the side-viewing ECOM **316** are updated at 4.4 frames/sec. All imaging channels are displayed simultaneously. The images that may be generated by the GI endoscope **300** are illustrated in Figures 16 and 17. Figure 16 shows a simulated image of a human colon epithelium incorporating the expected spatial resolution which may achievable with the side-viewing ECOM **316**. Figures 17a and 17b are a comparison of microscopy imaging versus *in vivo* OCT imaging. Figure 17a has two panels which each show a microscopy image of sweat ducts in the human skin. Figure 17b has three panels which each show an *in vivo* OCT image of sweat ducts in the human skin. The *in vivo* OCT images were generated with a light source operating at a wavelength of 1300 nm.

[0095] Typical maneuvers or use of the GI endoscope **300** by an endoscopist will incorporate the following steps:

a) Following the steps of a general endoscopy procedure, the GI endoscope **300** is inserted under the guidance of the conventional forward-viewing white light channel **312.** This maneuver should be no different from that of currently available GI endoscopes.

b) When the endoscopist needs to make microscopic examinations, he/she first pushes the GI endoscope **300** into contact with the wall of the lumen as shown in Figure 13. The optics are designed such that when the GI endoscope **300** is in contact with the tissue, the correct working distance of the entire optical system is obtained. Although the GI endoscope **300** is in contact with the wall, the part of the tissue under microscopic examination is not, as illustrated in Figure 15. Therefore, the surface features of the tissue are not distorted by contact pressure. However, this does

not imply that the GI endoscope **300** can only be operated in a contact mode. In fact, the GI endoscope **300** may be operated in a non-contact mode, as long as images are formed, which is dictated by whether the previously described dynamic triggering algorithm has found an air-tissue interface. If the air-tissue interface lies within the working distance of the system then the interface should be specific and easily detected since the interface produces clear peaks in the detected light pattern as previously described in the 'flexible triggering' method.

c) If the endoscopist needs to examine a region adjacent to the area imaged in step (b), then the endoscopist can torque the GI endoscope **300** and rotate the field of view to a new location.

[0096] The best techniques currently in use for visualization of the gastrointestinal (GI) tract include endoscopic ultrasonography (EUS) and magnification endoscopy (ME). The resolution of high-frequency EUS, approximately 70 to 100 mm, is insufficient for the identification of many conditions that perturb tissue microstructure, most notably subtle pathologic changes arising within the superficial layers of the GI tract (mucosa and submucosa). ME, with a magnification of up to 170X, provides excellent images of fine superficial mucosal patterns but subsurface structures and lesion staging cannot be determined. Accordingly, tissue biopsy and histology currently remain the standard of care for detecting microscopic diseases involving the GI tract.

[0097] The side-viewing ECOM **316** disclosed herein may achieve real-time, 2 mm deep cross-sectional images of the GI wall at a resolution of 5 μm in both axial and transverse (lateral) dimensions. For reference, gastrointestinal epithelial cells average 7 to 10 μm in size which increases further as dysplastic or neoplastic transformation ensues. In the GI tract, a depth of view at 2 mm is nevertheless sufficient to detect mucosally-based diseases as well as any neoplastic invasion into the underlying submucosa, which is of important for prognostic and therapeutic purposes. The image resolution of the side-viewing ECOM **316** may correspond to observing an *unstained* histology slide under a 100X (total magnification) microscope. Accordingly, many important entities such as dysplasia (cellular neoplastic alterations) or neoplastic violation of structures such as the lamina propria or muscularis mucosae may be discernible with the side-viewing ECOM **316.**

[0098] The present invention may allow for *in-situ* diagnosis of diverse *microscopic* mucosal pathologies and lesion staging. In essence, this "optical biopsy" technique may replace, or at the very least, guide the standard biopsy and histology method. This may translate into reducing unnecessary biopsy samples and tissue processing, decreasing patient risk and increasing sampling rate and diagnostic yield thus providing immediate diagnostic feedback both to the physician and the patient and targeting biopsies (which in itself may become a therapeutic maneuver in some cases). Pre-neoplastic GI conditions such as Barrett's esophagus, chronic ulcerative colitis, early flat adenomas, or foci of aberrant colonic crypts, to name a few, may be applicable to the side-viewing ECOM **316.** Currently, detection and surveillance of neoplastic progression within these conditions are suboptimal due to their microscopic nature.

[0099] Secondly, the side-viewing ECOM **316** may serve as a functional imaging system permitting monitoring of neoplastic and non-neoplastic tissue alterations over time. For instance, the recovery of the structure of small intestinal villi and reduction in inflammatory cells may be monitored by the side-viewing ECOM **316** in diverse malabsorptive disorders of the gut such as gluten-sensitive enteropathy, tropical sprue and intestinal infestation. The natural history of many mucosal diseases at the microscopic level may also be assessed in a minimally invasive manner. The ability to monitor structural cellular changes that are occurring *in vivo* with time may provide important physiologic information on cellular function and insight into cellular pathologic transformation.

[0100] Thirdly, the side-viewing ECOM **316** may be used in the monitoring of tissue post therapy. *In vivo* microscopic evaluation of surgical resection margins or treatment margins during post-therapeutic surveillance of cancer resection or assessment of the adequacy of photodynamic therapy of mucosal preneoplastic conditions are only some examples.

[0101] Applications in other medical specialties may also be possible. It should be understood by those skilled in this art that the multichannel OCT apparatus disclosed herein may have application in a large number of medical specialties such as dermatology, hematology, oncology (medical and radiation), ophthalmology, urology, surgery, respirology and gastroenterology.

[0102] The multichannel OCT system disclosed herein may be altered to further improve system performance. For instance a modification that may be made would be to employ coded transmission for the optical radiation which is radiated from the optical sources. This technique may increase the image resolution by increasing the SNR of the optical radiation of the interference pattern obtained in channels which suffer from poor SNR.

[0103] It should be understood that various modifications can be made to the preferred embodiments described and illustrated herein, without departing from the present invention, the scope of which is defined in the appended claims. For instance, in each of the schematics, herein disclosed, other optical couplers may also be used in place of the 3 dB couplers.

Claims

1. An apparatus for optical examination of a sample (S,65), the apparatus comprising:

   an optical source means for providing a plurality of separate optical radiation sources;
   a first optical path (20) extending from the optical source means;
   a focusing means (14) in the first optical path (20) for focusing optical radiation from the optical radiation sources into a plurality of respective focal points (21a,21b,22a,22b,23a,23b) located on a surface (18) within the first optical path (20) to provide substantially continuous coverage of a selected portion of the first optical path (20), whereby, in use, a sample (S,65) can be located at least partially within said selected portion, thereby permitting simultaneous scanning of a plurality of points within the sample (S,65); **characterised in that**:

   the optical source means comprises optical coupling means having one of a plurality of optical fibers (10) or a plurality of optical waveguide wafers, wherein ends of the plurality of optical fibers (10) or the plurality of optical waveguide wafers are stepped relative to one another along the first optical path (20) and wherein optical radiation from each optical fiber (10) or each optical waveguide wafer is focused to a different focal point (21a,21b,22a,22b,23a,23b) on the surface (18) of the first optical path (20).

2. An apparatus as claimed in claim 1, wherein the optical source means further comprises a primary optical source and wherein the optical coupling means connects the primary optical source to the optical radiation sources.

3. An apparatus as claimed in claim 1, wherein the optical source means further comprises a plurality of optical sources (50), and wherein the optical coupling means connects the plurality of optical sources (50) to the optical radiation sources and further includes a plurality of optical couplers (54) adapted to adjust the intensity of the optical radiation provided by each of the plurality of optical fibers (10) or each of the plurality of optical waveguide wafers for facilitating deep or shallow scanning.

4. An apparatus as claimed in claim 1, 2 or 3, which includes a rotatable mirror (16) in the first optical path (20), for deflecting radiation from the optical radiation sources to permit rotational movement of the surface (18).

5. An apparatus as claimed in claim 1, 2 or 3, which includes a mirror (16) in the first optical path (20) and wherein the optical source means, the focusing means (14) and the mirror (16), in combination, may be linearly translated to permit linear movement of the surface (18).

6. An apparatus as claimed in claim 1, 2 or 3, which includes a rotatable mirror (16) in the first optical path (20) and wherein the optical source means, the focusing means (14) and the rotatable mirror (16), in combination, may be linearly translated to permit helical movement of the surface (18).

7. An apparatus as claimed in claim 4, 5 or 6, wherein the surface (18) is a complex surface.

8. An apparatus as claimed in claims 4, 5 or 6, wherein the mirror (16) is a surface of a prism.

9. An apparatus as claimed in claims 4 or 6, including a micromachined electro-mechanical system coupled to the mirror (16) for rotating the mirror (16).

10. An apparatus as claimed in claim 5 or 6, including a micromachined electro-mechanical system for linearly translating the optical source means, the focusing means (14) and the mirror (16).

11. An apparatus as claimed in claim 2 or 4, which further includes a plurality of optical couplers (54) between the primary optical source (50) and the optical fibers (10), an optical delay generator (64) coupled to the optical couplers (54) and detector means (58) coupled to the optical couplers (54), wherein the optical couplers (54) transmit a portion of the radiation from the primary optical source (50) along the first optical path (20) and a portion of the radiation from the primary optical source (50) to the optical delay generator (64), the optical delay generator (64) providing a second optical path, wherein an interference effect occurs between radiation returned along the first (20) and second optical paths to the optical couplers (54) and the optical couplers (54) transmit the radiation returned along the first (20) and second optical paths to the detector means (58).

12. An apparatus as claimed in claim 11, which includes a plurality of primary optical sources (50) and a plurality of tree

couplers (52), each tree coupler (52) being associated with one primary optical source (50) and coupling said one primary optical source (50) to at least one of the optical couplers (54).

13. An apparatus as claimed in claim 12, which includes a plurality of optical circulators, placed between the optical couplers (54) and the detectors (58) for providing salvaged optical radiation to the detectors (58).

14. An apparatus as claimed in claim 11, wherein a plurality of optical fibers couple the optical couplers (54) to the optical delay generator (64), the optical delay generator (64) having a grating and a scanning mirror, the scanning mirror having an axis, wherein the grating separates optical radiation from each optical fiber into spectral components linearly oriented on the scanning mirror, wherein the midpoint of said spectral components is offset from the axis of the scanning mirror by a distance x_d to phase modulate said spectral components.

15. An apparatus as claimed in claim 11, which includes a first plurality of optical fibers for coupling each optical coupler (54) to a phase modulator and a second plurality of optical fibers for coupling each phase modulator to the optical delay generator (64), the optical delay generator (64) having a grating and a scanning mirror, the scanning mirror having an axis, wherein for each optical fiber, the phase modulator phase modulates the optical radiation and said grating separates said phase modulated optical radiation into spectral components which are linearly oriented on said scanning mirror, the midpoint of said spectral components being centered on the axis of said scanning mirror and wherein the spectral components from each optical fiber is spaced apart from the spectral components of the optical radiation from the other optical fibers.

16. An apparatus as claimed in claim 11, which includes a plurality of optical fibers coupling each optical coupler (54) to a tree coupler (52) for combining optical radiation from each of the optical fibers into a first optical fiber, said first optical fiber connected to a phase modulator for phase modulating said combined optical radiation and including a second optical fiber for coupling said phase modulator and said optical delay generator (64).

17. An apparatus as claimed in claims 4, 5 or 6, wherein the apparatus is configured as an endoscope for internal examination of a body, wherein the first optical path (20), the focusing means (14) and the mirror (16) are provided in the endoscope, and wherein the endoscope includes at least one of: at least one channel for white light illumination; a channel for white light endoscope forward viewing; a channel for one of an air nozzle and a water nozzle; and a suction/biopsy channel.

18. An apparatus as claimed in claim 17, wherein the endoscope is adapted to perform radial, translational or helical scanning.

19. An apparatus as claimed in claim 18, wherein the endoscope further includes a micromachined electro-mechanical system as a drive mechanism.

20. A method for optical examination of a sample (S,65), the method comprising:

(a) providing radiation from a plurality of separate optical radiation sources, along a first optical path (20);
(b) providing focusing means (14) in the first optical path (20);
(c) focusing the optical radiation from the optical sources into a plurality of respective focal points (21a,21b,22a, 22b,23a,23b) along a surface (18) within the first optical path (20) to provide substantially continuous coverage of a selected portion of the first optical path (20); and
(d) providing a sample (S,65) located at least partially within the first optical path (20); and,
(e) simultaneously scanning a plurality of points within the sample (S,65);

characterised in that the method further comprises:

providing an optical coupling means for the plurality of separate optical radiation sources wherein the optical coupling means have one of a plurality of optical fibers (10) or a plurality of optical waveguide wafers, wherein the method further comprises stepping the ends of the plurality of optical fibers (10) or the plurality of optical waveguide wafers relative to one another in a common plane along the first optical path (20) for focusing optical radiation from each optical fiber (10) or each optical waveguide wafer through a common lens (14) to a different focal point (21a,21b,22a,22b,23a,23b) on the surface (18) of the first optical path (20).

21. A method as claimed in claim 20, which includes providing radiation from a primary optical source and transmitting

the radiation along the plurality of optical fibers (10) or the plurality of optical waveguide wafers to the plurality of separate optical radiation sources.

22. A method as claimed in claim 20, wherein the method further includes providing a plurality of optical sources (50), connecting the plurality of optical sources (50) to the optical radiation sources and using a plurality of optical couplers (54) to adjust the intensity of the optical radiation provided by each of the plurality of optical fibers (10) or each of the plurality of optical waveguide wafers for facilitating deep or shallow scanning.

23. A method as claimed in any one of claims 20 to 22, which includes:

(a) providing a rotatable mirror (16) in the first optical path (20);
(b) deflecting the first optical path (20);
(c) causing the plurality of focal points (21a,21b,22a,22b,23a,23b) to be located on a surface (18);
(d) performing an axial scan;
(e) rotating the mirror (16) to move the surface (18); and,
(f) repeating step (d) at least two times and performing step (e) between each repetition.

24. A method as claimed in any one of claims 20 to 22, which includes:

(a) providing a mirror (16) in the first optical path (20);
(b) deflecting the first optical path (20);
(c) causing the plurality of focal points (21a,21b,22a,22b,23a,23b) to be located on a surface (18);
(d) performing an axial scan;
(e) linearly translating, in combination, the focusing means (14), the plurality of optical radiation sources and the mirror (16) to move the surface (18); and,
(f) repeating step (d) at least two times and performing step (e) between each repetition.

25. A method as claimed in any one of claims 20 to 22, which includes:

(a) providing a mirror (16) in the first optical path (18);
(b) deflecting the first optical path (20);
(c) causing the plurality of focal points (21a,21b,22a,22b,23a,23b) to be located on a surface (18);
(d) performing an axial scan;
(e) simultaneously rotating the mirror (16) and linearly translating, in combination, the focusing means (14), the plurality of optical radiation sources and the mirror (16) to move the surface (18); and,
(f) repeating step (d) at least two times and performing step (e) between each repetition.

26. A method as claimed in claim 23, 24 or 25, which includes providing a surface of a prism as the mirror (16).

27. A method as claimed in any one of claims 23, 24 or 25 depending from claim 21, which includes supplying radiation from the primary optical source (50) through a plurality of couplers (54) to the optical fibers (10), providing an optical delay generator (64) connected to the optical couplers (54) and providing a second optical path, permitting radiation to be transmitted back along the first (20) and second optical paths to the couplers (54), for forming interference, and transmitting radiation received from the first (20) and second optical paths at the optical couplers (54) to detection means (58) for detection of the interference pattern.

28. A method as claimed in claim 27, which includes providing a plurality of primary optical sources (50) and, for each primary optical source (50), a respective tree coupler (52), and coupling each primary optical source (50) through said respective tree coupler (52) to each of the optical couplers (54).

29. A method as claimed in claim 27, which includes providing optical circulator means between the optical couplers (54) and the detection means (58) for providing salvaged optical radiation to the detection means (58).

30. A method as claimed in claim 28, wherein the primary optical sources (50), the tree couplers (52) and the optical couplers (54) are configured as an endoscope adapted for examining an internal cavity of the body, including at least one of: at least one channel for white light illumination, a white light endoscope forward viewing channel, a suction/biopsy channel and a channel for one of an air nozzle and a water nozzle.

31. A method as claimed in claims 25, 26 or 27, wherein there is a change in refractive index between a medium containing the optical radiation sources and the sample (S,65) and for each focal point, a distance mismatch due to the change in refractive index between the coherence gate of each optical radiation source and the focal point in the sample (S,65) is obtained according to the steps of:

(a) scanning optical radiation from the plurality of optical radiation sources in said first optical path (20) such that the focal points (21a,21b,22a,22b,23a,23b) of the optical radiation sources are aligned along a path extending from the medium containing the optical radiation sources into the sample (S,65);
(b) detecting the reflected optical radiation for each focal point (21a,21b,22a,22b,23a,23b); and,
(c) locating the focal point (21a,21b,22a,22b,23a,23b) for which there is a large change in reflected optical radiation compared to neighboring focal points (21a,21b,22a,22b,23a,23b),

whereby, the focal point (21a,21b,22a,22b,23a,23b) located in step (c) indicates the location of the interface between the sample (S,65) and the medium containing the optical radiation sources.

32. A method as claimed in claim 31, wherein the method further comprises repeating steps (a) to (c) for each axial scan to obtain proper spatial resolution for the selected scan zone.

Patentansprüche

1. Vorrichtung zur optischen Prüfung einer Probe (S, 65), wobei die Vorrichtung Folgendes aufweist:

ein optisches Quellenmittel zum Bereitstellen einer Mehrzahl von getrennten optischen Strahlenquellen;
einen ersten optischen Weg (20), der sich von dem optischen Quellenmittel aus erstreckt;
ein Fokussiermittel (14) in dem ersten optischen Weg (20) zur Fokussierung der optischen Strahlung von der optischen Strahlenquelle auf eine Mehrzahl von betreffenden Brennpunkten (21a, 21b, 22a, 22b, 23a, 23b), die sich auf einer Oberfläche (18) innerhalb des ersten optischen Weges (20) befinden, um eine im Wesentlichen kontinuierliche Abdeckung eines ausgewählten Bereiches des ersten optischen Weges (20) zu erhalten, wodurch während der Benutzung eine Probe (S, 65) wenigstens teilweise innerhalb des ausgewählten Bereiches angeordnet sein kann, wodurch ein gleichzeitiges Scannen einer Mehrzahl von Punkten innerhalb der Probe (S, 65) erlaubt wird,

dadurch gekennzeichnet, dass
das optische Quellenmittel ein optisches Kopplungsmittel aufweist, das eine Mehrzahl von Lichtleitfasern (10) oder eine Mehrzahl von optischen Wellenleiter-Wafern aufweist, wobei Enden der Mehrzahl von Lichtleitfasern (10) oder der Mehrzahl von optischen Wellenleitern-Wafern relativ zueinander entlang des ersten optischen Weges abgestuft sind, und wobei die optische Strahlung von jeder Lichtleitfaser (10) oder jedem optischen Wellenleiter-Wafer auf einen anderen Brennpunkt (21a, 21b, 22a, 22b, 23a, 23b) auf der Oberfläche (18) des ersten optischen Weges fokussiert wird.

2. Vorrichtung nach Anspruch 1, bei der das optische Quellenmittel ferner eine primäre optische Quelle aufweist, und wobei das optische Kopplungsmittel die primäre optische Quelle mit den optischen Strahlenquellen verbindet.

3. Vorrichtung nach Anspruch 1, bei der das optische Quellenmittel ferner eine Mehrzahl von optischen Quellen (50) aufweist, und wobei das optische Kopplungsmittel die Mehrzahl von optischen Quellen (50) mit den optischen Strahlenquellen verbindet und ferner eine Mehrzahl von optischen Kopplern (54) aufweist, die dazu geeignet sind, die Intensität der optischen Strahler einzustellen, die von jeder der Mehrzahl der Lichtleitfasern (10) oder von jedem der Mehrzahl von optischen Wellenleiter-Wafern bereitgestellt wird, um ein tiefes oder ein flaches Scannen zu erleichtern.

4. Vorrichtung nach Anspruch 1, 2 oder 3, die einen drehbaren Spiegel (16) in dem ersten optischen Weg (20) aufweist, um Strahlung von den optischen Strahlenquellen abzulenken, um eine Drehbewegung der Oberfläche (18) zu erlauben.

5. Vorrichtung nach Anspruch 1, 2, oder 3, die einen Spiegel (16) in dem ersten optischen Weg (20) aufweist, und wobei das optische Quellenmittel, das Fokussiermittel (14) und der Spiegel (16) in Kombination linear angetrieben sein können, um eine lineare Bewegung der Oberfläche (18) zu erlauben.

6. Vorrichtung nach Anspruch 1, 2 oder 3, die einen drehbaren Spiegel (16) in dem ersten optischen Weg (20) aufweist, und wobei das optische Quellenmittel, das Fokussiermittel (14) und der drehbare Spiegel (16) in Kombination linear angetrieben werden können, um eine Schraubenbewegung der Oberfläche (18) zu erlauben.

7. Vorrichtung nach Anspruch 4, 5 oder 6, bei der die Oberfläche (18) eine komplexe Oberfläche ist.

8. Vorrichtung nach Anspruch 4, 5 oder 6, bei der der Spiegel (16) eine Oberfläche eines Prismas ist.

9. Vorrichtung nach Anspruch 4 oder 6, die ein mikrobearbeitetes elektro-mechanisches System aufweist, das mit dem Spiegel (16) gekoppelt ist, um den Spiegel (16) zu drehen.

10. Vorrichtung nach Anspruch 5 oder 6, mit einem mikrobearbeiteten elektromechanischen System, um das optische Quellenmittel, das Fokussiermittel (14) und den Spiegel (16) linear anzutreiben.

11. Vorrichtung nach Anspruch 2 oder 4, die ferner eine Mehrzahl von optischen Kopplern (54) zwischen der primären optischen Quelle (50) und den Lichtleitfasern (10) aufweist, einen optischen Verzögerungsgenerator (64), der mit den optischen Kopplern und einem Detektormittel (58) gekoppelt ist, das mit den optischen Kopplern (54) gekoppelt ist, wobei die optischen Koppler (54) einen Teil der Strahlung von der primären optischen Quelle (50) entlang des ersten optischen Weges (20) übertragen und einen Teil der Strahlung von der primären optischen Quelle (50) zu dem optischen Verzögerungsgenerator (64) übertragen, wobei der optische Verzögerungsgenerator (64) einen zweiten optischen Weg bereitstellt, und wobei zwischen der entlang des ersten (20) und des zweiten optischen Weges zu den optischen Kopplern (54) zurückgeführten Strahlung ein Interferenzeffekt auftritt, und wobei die optischen Koppler (54) die entlang des ersten (20) und des zweiten optischen Weges zurückgeführte Strahlung zu dem Detektormittel (58) übertragen.

12. Vorrichtung nach Anspruch 11, die ferner eine Mehrzahl von primären optischen Quellen (50) und eine Mehrzahl von Baum-Kopplern (52) aufweist, wobei jeder Baum-Koppler (52) mit einer primären optischen Quelle (50) zusammenhängt und die eine primäre optische Quelle (50) mit wenigstens einem der optischen Koppler (54) koppelt.

13. Vorrichtung nach Anspruch 12, die eine Mehrzahl von optischen Zirkulatoren aufweist, die zwischen den optischen Kopplern (54) und den Detektoren (58) angeordnet sind, um wiedergewonnene optische Strahlung für die Detektoren (58) bereitzustellen.

14. Vorrichtung nach Anspruch 11, bei der eine Mehrzahl der Lichtleitfasern die optischen Koppler (54) mit dem optischen Verzögerungsgenerator (64) koppeln, wobei der optische Verzögerungsgenerator (64) ein Gitter und einen Scanner-Spiegel hat, wobei der Scanner-Spiegel eine Achse aufweist, und wobei das Gitter optische Strahlung von jeder Lichtleitfaser in spektrale Komponenten aufteilt, die auf dem Scanner-Spiegel linear orientiert sind, wobei der Mittelpunkt der spektralen Komponenten von der Achse des Scanner-Spiegels um einen Abstand (X_d) entfernt ist, um die spektralen Komponentenphasen zu modulieren.

15. Vorrichtung nach Anspruch 11, die eine Mehrzahl von Lichtleitfasern zum Koppeln jedes optischen Kopplers (54) mit einem Phasenmodulator und eine zweite Mehrzahl von Lichtleitfasern zum Koppeln jedes Phasenmodulators mit dem optischen Verzögerungsgenerator (64) aufweist, wobei der optische Verzögerungsgenerator (64) ein Gitter und einen Scanner-Spiegel aufweist, wobei der Scanner-Spiegel eine Achse aufweist, wobei der Phasenmodulator die optische Strahlung für jede Lichtleitfaser phasenmoduliert und das Gitter die phasenmodulierte optische Strahlung in spektrale Komponenten aufteilt, die auf dem Scanner-Spiegel linear orientiert sind, wobei der Mittelpunkt der spektralen Komponenten auf der Achse des Scanner-Spiegels zentriert ist, und wobei die spektralen Komponenten von jeder Lichtleitfaser von den spektralen Komponenten der optischen Strahlung von den anderen Lichtleitfasern beabstandet sind.

16. Vorrichtung nach Anspruch 11, die eine Mehrzahl von Lichtleitfasern aufweist, die jeden optischen Koppler (54) mit einem Baum-Koppler (52) koppeln, um optische Strahlung von jeder der Lichtleitfasern in eine erste Lichtleitfaser zu kombinieren, wobei die erste Lichtleitfaser mit einem Phasenmodulator verbunden ist, um die kombinierte optische Strahlung phasen zu modulieren, und wobei eine zweite Lichtleitfaser vorgesehen ist, um den Phasenmodulator und den optischen Verzögerungsgenerator (64) zu koppeln.

17. Vorrichtung nach Anspruch 4, 5 oder 6, bei der die Vorrichtung als ein Endoskop für die innere Untersuchung eines Körpers ausgebildet ist, wobei der erste optische Weg (20), das Fokussiermittel (14) und der Spiegel (16) in dem

Endoskop vorgesehen sind, und wobei das Endoskop wenigstens eines von Folgendem einschließt: wenigstens einen Kanal für Beleuchtung mit weißem Licht; einen Kanal zur Vorwärtsbetrachtung mit weißem Endoskop-Licht; einen Kanal für entweder ein Luftventil oder ein Wasserventil und einen Saugkanal/Biopsiekanal.

18. Vorrichtung nach Anspruch 17, bei der das Endoskop zur Durchführung von radialem, geradlinigem oder schraubenförmigem Scannen ausgebildet ist.

19. Vorrichtung nach Anspruch 18, bei der das Endoskop ferner ein mikrobearbeitetes elektro-mechanisches System als einen Antriebsmechanismus aufweist.

20. Verfahren zur optischen Untersuchung einer Probe (S, 65), wobei das Verfahren Folgendes aufweist:

(a) Bereitstellen einer Strahlung aus einer Mehrzahl von separaten optischen Strahlenquellen entlang eines ersten optischen Weges (20);
(b) Bereitstellen eines Fokussiermittels (14) in dem ersten optischen Weg (20);
(c) Fokussieren der optischen Strahlung von den optischen Quellen auf eine Mehrzahl von betreffenden Brennpunkten (21a, 21b, 22a, 22b, 23a, 23b) entlang einer Oberfläche (18) innerhalb des ersten optischen Weges (20), um im Wesentlichen eine kontinuierliche Abdeckung eines ausgewählten Bereiches des ersten optischen Weges (20) zu liefern; und
(d) Bereitstellen einer Probe (S, 65), die wenigstens teilweise innerhalb des ersten optischen Weges (20) liegt, und
(e) gleichzeitiges Scannen einer Mehrzahl von Punkten innerhalb der Probe (S, 65),

dadurch gekennzeichnet, dass das Verfahren ferner Folgendes aufweist:

Bereitstellen von optischen Kopplungsmitteln für die Mehrzahl von separaten optischen Strahlenquellen, wobei die optischen Kopplungsmittel eines von einer Mehrzahl von Lichtleitfasern (10) oder eine Mehrzahl von optischen Wellenleiter-Wafern aufweisen, wobei das Verfahren ferner das Abstufen der Enden der Mehrzahl von Lichtleitfasern (10) oder der Mehrzahl der optischen Wellenleiter-Wafer in Bezug auf einander in einer gemeinsamen Ebene entlang des ersten optischen Weges (20) aufweist, um optische Strahlung von jeder Lichtleitfaser (10) oder von jedem optischen Wellenleiter-Wafer durch eine gemeinsame Linse (14) auf einen unterschiedlichen Brennpunkt (21a, 21b, 22a, 22b, 23a, 23b) auf der Oberfläche (18) des ersten optischen Weges (20) zu fokussieren.

21. Verfahren nach Anspruch 20, das das Bereitstellen einer Strahlung von einer primären optischen Quelle und das Übertragen der Strahlung entlang der Mehrzahl von Lichtleitfasern (10) oder der Mehrzahl von optischen Wellenleiter-Wafern zu der Mehrzahl von getrennten optischen Strahlenquellen aufweist.

22. Verfahren nach Anspruch 20, bei dem das Verfahren ferner das Bereitstellen einer Mehrzahl von optischen Quellen (50) aufweist, das Verbinden der Mehrzahl von optischen Quellen (50) mit den optischen Strahlenquellen und das Verwenden einer Mehrzahl von optischen Kopplern (54), um die Intensität der optischen Strahlung einzustellen, die von jeder der Mehrzahl von Lichtleitfasern (10) oder von jedem der Mehrzahl von optischen Wellenleiter-Wafern geliefert wird, um ein tiefes oder ein flaches Scannen zu erleichtern.

23. Vorrichtung nach irgendeinem der Ansprüche 20 bis 22, das Folgendes aufweist:

(a) Bereitstellen eines drehbaren Spiegels (16) in dem ersten optischen Weg (20);
(b) Ablenken des ersten optischen Weges (20);
(c) Bewirken, dass die Mehrzahl von Brennpunkten (21a, 21b, 22a, 22b, 23a, 23b) auf einer Oberfläche (18) liegt;
(d) Durchführen eines axialen Scannens;
(e) Drehen des Spiegels (16), um die Oberfläche (18) zu bewegen, und
(f) Wiederholen des Schrittes (d) wenigstens zweimal und Durchführen des Schrittes (e) während jeder Wiederholung.

24. Verfahren nach irgendeinem der Ansprüche 20 bis 22, das Folgendes aufweist:

(a) Bereitstellen eines Spiegels (16) in dem ersten optischen Weg (20);
(b) Ablenken des ersten optischen Weges (20);

(c) Bewirken, dass die Mehrzahl von Brennpunkten (21, 21b, 22a, 22b, 23a, 23b) auf einer Oberfläche (18) liegt;
(d) Durchführen eines axialen Scannens;
(e) lineares Bewegen des Fokussiermittels (14), der Mehrzahl von optischen Strahlenquellen und des Spiegels (16) in Kombination, um die Oberfläche (18) zu bewegen; und
(f) Wiederholen des Schrittes (d) wenigstens zweimal und Durchführen des Schrittes (e) während jeder Wiederholung.

25. Verfahren nach irgendeinem der Ansprüche 20 bis 22, das Folgendes aufweist:

(a) Bereitstellen eines Spiegels (16) in dem ersten optischen Weg (18);
(b) Ablenken des ersten optischen Weges (20);
(c) Bewirken, dass die Mehrzahl von Brennpunkten (21a, 21b, 22a, 22b, 23a, 23b) auf einer Oberfläche (18) liegt;
(d) Durchführen eines axialen Scannens;
(e) gleichzeitiges Drehen des Spiegels (16) und lineares Bewegen des Fokussiermittels (14), der Mehrzahl von optischen Strahlenquellen und des Spiegels (16) in Kombination, um die Oberfläche (18) zu bewegen, und
(f) Wiederholen des Schrittes (d) wenigstens zweimal und Durchführen des Schrittes (e) während jeder Wiederholung.

26. Verfahren nach Anspruch 23, 24 oder 25, das das Bereitstellen einer Oberfläche eines Prismas als den Spiegel (16) umfasst.

27. Verfahren nach irgendeinem der Ansprüche 23, 24 oder 25, soweit abhängig von Anspruch 21, das das Bereitstellen von Strahlung von der primären optischen Quelle (50) durch eine Mehrzahl von Kopplern (54) für die Lichtleitfasern (10) umfasst, das Bereitstellen eines optischen Verzögerungsgenerators (64), der mit den optischen Kopplern (54) gekoppelt ist, und das Bereitstellen eines zweiten optischen Weges, der es erlaubt, dass Strahlung entlang des ersten (20) und des zweiten optischen Weges zu den Kopplern (54) zurückübertragen wird, um Interferenz zu erzeugen, und um Strahlung, die von dem ersten (20) und dem zweiten optischen Weg von den optischen Kopplern (54) erhalten wird, zu einem Detektionsmittel (58) zu übertragen, um das Interferenzmuster zu detektieren.

28. Verfahren nach Anspruch 27, das das Bereitstellen einer Mehrzahl von primären optischen Quellen (50) umfasst, und für jede optische Quelle (50) einen zugeordneten Baum-Koppler (52), und das Koppeln jeder primären optischen Quelle (50) über den betreffenden Baum-Koppler (52) mit jedem der optischen Koppler (54).

29. Verfahren nach Anspruch 27, das das Bereitstellen eines optischen Zirkulator-Mittels zwischen den optischen Kopplern (54) und dem Detektionsmittel (58) aufweist, um wiedererhaltene optische Strahlung an das Detektionsmittel (58) zu liefern.

30. Verfahren nach Anspruch 28, bei dem die primären optischen Quellen (50), die Baum-Koppler (52) und die optischen Koppler (54) als ein Endoskop konfiguriert sind, das dazu geeignet ist, einen internen Hohlraum des Körpers zu untersuchen, wozu wenigstens eines von Folgendem gehört: wenigstens ein Kanal für Beleuchtung mit weißem Licht, ein Kanal zur Vorwärtsbetrachtung mit einem Weißlichtendoskop, ein Saugkanal/Biopsiekanal, und ein Kanal für eines von einem Luftventil und einem Wasserventil.

31. Verfahren nach Anspruch 25, 26 oder 27, bei dem es eine Veränderung im Brechungsindex gibt zwischen einem Medium, das die optischen Strahlenquellen und die Probe (S, 65) enthält, und für jeden Brennpunkt eine Abstandsfehlabstimmung gibt, die infolge der Veränderung des Brechungsindex zwischen der Kohärenzschranke und jeder optischen Strahlenquelle und dem Brennpunkt in der Probe (S, 65) gemäß der folgenden Schritte erhalten wird:

(a) Scannen der optischen Strahlung von der Mehrzahl von optischen Strahlenquellen in den ersten optischen Weg (20), derart, dass die Brennpunkte (21a, 21b, 22a, 22b, 23a, 23b) der optischen Strahlenquellen entlang eines Weges ausgerichtet sind, der sich von dem Medium, das die optischen Strahlenquellen enthält, zu der Probe (S, 65) erstreckt;
(b) Detektieren der reflektierten optischen Strahlung für jeden Brennpunkt (21a, 21b, 22a, 22b, 23a, 23b) und
(c) Feststellen des Brennpunktes (21a, 21b, 22a, 22b, 23a, 23b), für den es eine große Veränderung der reflektierten optischen Strahlung gibt im Vergleich zu benachbarten Brennpunkten (21a, 21b, 22a, 22b, 23a, 23b), wobei deren Schritt (c) bestimmte Brennpunkte (21a, 21b, 22a, 22b, 23a, 23b) die Lage der Grenzfläche zwischen der Probe (S, 65) und dem Medium anzeigt, das die optischen Strahlenquellen enthält.

32. Verfahren nach Anspruch 31, bei dem das Verfahren ferner die Schritte Wiederholen der Schritte (a) bis (c) für jedes axiale Scannen aufweist, um eine gute Raumauflösung für die ausgewählte Scan-Zone zu erhalten.

Revendications

1. Dispositif pour l'examen optique d'un échantillon (S, 65), l'appareil comprenant :

Une source optique pour fournir une pluralité de sources de radiation optique séparée ;
Un premier chemin optique (20) s'étendant à partir de la source optique ;
Un moyen de focalisation (14) dans le premier chemin optique (20) pour focaliser la radiation optique de la source de radiation optique dans une pluralité de points focaux respectifs (21a, 21b, 22a, 22b, 23a, 23b) disposés sur une surface (18) avec dans le premier chemin optique (20) pour réaliser une couverture sensiblement continue d'une partie choisie du premier chemin optique (20), tandis qu'en cours d'utilisation un échantillon (S, 65) peut être disposé au moins partiellement dans ladite portion choisie, permettant ainsi un balayage simultané d'une pluralité de points dans l'échantillon (S, 65) ; **caractérisé en ce que** :

La source optique comporte des moyens de couplage optique présentant une pluralité de fibres (10) optiques ou une pluralité de tranches de guides d'ondes optiques tandis que les extrémités de la pluralité des fibres optiques (10) ou la pluralité des tranches d'ondes optiques sont échelonnées les uns par rapport aux autres, le long du premier chemin optique (20), et tandis que la radiation optique de chaque fibre optique (10) ou chaque tranche guide d'onde optique est focalisée sur un poids focal différent (21a, 21b, 22a, 22b, 23a, 23b) sur la surface (18) du premier chemin optique (20).

2. Appareil selon la revendication 1, **caractérisé en ce que** la source optique comporte en outre une source optique primaire et tandis que les moyens de couplage connectent la source optique primaire aux sources de radiation optique.

3. Appareil selon la revendication 1, **caractérisé en ce que** la source optique comporte en outre une pluralité de sources optiques (50), tandis que les moyens de couplage optique connectent la pluralité de sources optiques (50) aux sources de radiation optique et inclut en outre une pluralité de coupleurs optiques (54) apte à ajuster l'intensité de la radiation optique fournie par chacune de la pluralité des fibres optiques (10), ou chacune de la pluralité des tranches de guides d'ondes optiques, pour faciliter le balayage profond ou en surface.

4. Appareil selon l'une des revendications 1, 2 ou 3, qui inclut un miroir (16) rotatif dans le premier chemin optique (20), pour réfléchir l'irradiation des sources de radiation optique afin de permettre le mouvement en rotation de la surface (18).

5. Appareil selon l'une des revendications 1, 2 ou 3, qui inclut un miroir (16) rotatif dans le premier chemin optique (20), et tandis que la source optique, les moyens de focalisation (14) et le miroir (16), en combinaison, peuvent être translatés de manière linéaire pour permettre le mouvement linéaire de la surface (18).

6. Appareil selon l'une des revendications 1, 2 ou 3, **caractérisé en ce qu'**il inclut un miroir (16) rotatif dans le premier chemin optique (20), et **en ce que** la source optique, les moyens de focalisation (14) et le miroir rotatif (16), en combinaison, peuvent être translatés de manière linéaire pour permettre un mouvement hélicoïdal de la surface (18).

7. Appareil selon l'une des revendications 4, 5 ou 6, **caractérisé en ce que** la surface (18) est une surface complexe.

8. Appareil selon l'une des revendications 4, 5 ou 6, **caractérisé en ce que** le miroir (16) est une surface d'un prisme.

9. Appareil selon l'une des revendications 4 ou 6, **caractérisé en ce qu'**il inclut un système électromécanique micro-usiné, couplé au miroir (16), pour entraîner en rotation le miroir (16).

10. Appareil selon l'une des revendications 5 ou 6, incluant un système électromécanique micro-usiné, pour translater linéairement la source optique, les moyens de focalisation (14) et le miroir (16).

11. Appareil selon l'une des revendications 2 ou 4, **caractérisé en ce qu'**il comporte en outre une pluralité de coupleurs (54) optiques entre la source optique primaire (50) et les fibres optiques (10), un générateur de retard optique (64)

couplé aux coupleurs (54) optiques, et des moyens de détection couplés aux coupleurs (54) optiques, **caractérisé en ce que** les coupleurs optiques (54) transmettent une partie de la radiation à partir de la source optique primaire (50) le long du premier chemin optique (20) et une partie de la radiation à partir de la source optique primaire (50), vers le générateur (64) de retard optique, ce dernier procurant un second chemin optique, et **en ce qu'**un effet d'interférence apparaît entre la radiation retournée le long du premier (20) et second chemins optiques, vers les coupleurs (54) optiques, et ces derniers transmettent la radiation retournée le long du premier (20) et second chemins optiques, vers le moyen de détection (58).

12. Appareil selon la revendication 11, **caractérisé en ce qu'**il incorpore une pluralité de sources optiques primaires et une pluralité de coupleurs en arborescence (52), chaque coupleur en arborescence (52) étant associé à une source optique primaire (50) et couplant ladite source optique primaire (50) à au moins l'un des coupleurs optiques (54).

13. Appareil selon la revendication 12, **caractérisé en ce qu'**il comporte une pluralité de circulateurs optiques, placés entre les coupleurs optiques (54) et les détecteurs (58) pour réaliser une radiation optique sauvegardée vers les détecteurs (58).

14. Appareil selon la revendication 11, **caractérisé en ce qu'**il comporte une pluralité de fibres optiques couplant les coupleurs optiques (54) au générateur (64) de retard optique, le générateur (64) de retard optique présentant une grille et un miroir de balayage, le miroir de balayage ayant un axe, et **en ce que** la grille sépare la radiation optique de chaque fibre optique en des composants spectraux orientés linéairement sur le miroir de balayage, et **en ce que** le point milieu desdits composants spectraux est décalé par rapport à l'axe du miroir de balayage d'une distance x_d pour moduler en phase lesdits composants spectraux.

15. Appareil selon la revendication 11, **caractérisé en ce qu'**il incorpore une première pluralité de fibres optiques pour le couplage de chaque coupleur optique (54) à un modulateur de phase et une seconde pluralité de fibres optiques pour le couplage de chaque modulateur de phase au générateur (64) de retard optique, ce dernier présentant une grille et un miroir de balayage, le miroir de balayage présentant un axe, et **en ce que** pour chaque fibre optique, le modulateur de phase module en phase la radiation optique et ladite grille sépare ladite radiation optique modulée en phase, en composants spectraux qui sont linéairement orientés sur ledit miroir de balayage, le point milieu desdits composants spectraux étant centré sur l'axe dudit miroir de balayage, et **en ce que** les composants spectraux de chaque fibre optique sont espacés des composants spectraux, de la radiation optique, des autres fibres optiques.

16. Appareil selon la revendication 11, **caractérisé en ce qu'**il inclut une pluralité de fibres optiques couplant chaque coupleur optique (54) à un coupleur en arborescence (52), pour combiner la radiation optique de chacune des fibres optiques en une première fibre optique, ladite première fibre optique reliée à un modulateur de phase pour la modulation en phase de ladite radiation optique combinée et incluant une seconde fibre optique pour le couplage dudit modulateur de phase et dudit générateur (64) de retard optique.

17. Appareil selon l'une des revendications 4, 5 ou 6, **caractérisé en ce qu'**il est configuré sous la forme d'un endoscope pour un examen interne d'un corps et **en ce que** le premier chemin optique (20), les moyens de focalisation (14) et le miroir (16) sont prévus dans l'endoscope, et **en ce que** l'endoscope inclut au moins l'un des éléments suivants : au moins un canal pour l'illumination de lumière blanche ; un canal pour une vision vers l'avant d'endoscope en lumière blanche ; un canal pour l'un de buse d'air et de buse d'eau ; et un canal de succion /biopsie.

18. Appareil selon la revendication 17, **caractérisé en ce que** l'endoscope est adapté à réaliser des balayages radiaux, translationnels ou hélicoïdaux.

19. Appareil selon la revendication 18, **caractérisé en ce que** l'endoscope inclut en outre un système électromécanique micro-usiné en tant que mécanisme d'entraînement.

20. Procédé pour l'examen optique d'un échantillon (S, 65), le procédé comprenant :

(a) pourvoir une radiation à partir d'une pluralité de sources de radiation optique séparées, le long d'un premier chemin optique (20) ;
(b) fournir des moyens de focalisation (14) dans le premier chemin optique (20) ;
(c) focaliser la radiation optique à partir des sources optiques en une pluralité de points focaux respectifs (21a, 21b, 22a, 22b, 23a, 23b) le long d'une surface (18) sur le premier chemin optique (20) pour réaliser une couverture

sensiblement continue d'une partie choisie du premier chemin optique (20) ; et
(d) fournir un échantillon (S, 65) localisé au moins partiellement sur le premier chemin optique (20) ; et,
(e) balayer simultanément une pluralité de points dans l'échantillon (S, 65) ;

Caractérisé en ce que le procédé comporte en outre :

Prévoir un moyen de couplage optique pour la pluralité de sources de radiation optique séparées et **en ce que** les moyens de couplage optique présentent une pluralité de fibres optiques (10), ou une pluralité de tranches de guides d'ondes optiques, et **en ce qu'**il comporte en outre l'étape de décaler les extrémités d'une pluralité de fibres optiques (10) ou la pluralité de tranches de guides d'ondes optiques l'un par rapport aux autres, dans un plan commun le long du premier chemin optique (20) pour focaliser la radiation optique à partir de chaque fibre optique (10) ou chaque tranche de guide d'onde optique au travers d'une lentille commune (14), en un point focal différent (21a, 21b, 22a, 22b, 23a, 23b) sur la surface (18) du premier chemin optique (20).

21. Procédé selon la revendication 20, **caractérisé en ce qu'**il inclut l'étape de fournir une radiation à partir d'une source optique primaire et transmettre la radiation le long d'une pluralité de fibres optiques (10), ou la pluralité de tranches de guides d'ondes optiques vers la pluralité de sources de radiation séparées.

22. Procédé selon la revendication 20, **caractérisé en ce qu'**il inclut en outre l'étape de fournir une pluralité de sources optiques (50), relier la pluralité de sources optiques (50) aux sources de radiation optique et utiliser une pluralité de coupleurs optiques (54) pour ajuster l'intensité de la radiation optique fournie par chacune de la pluralité des fibres optiques (10), ou chacune de la pluralité de tranches de guides d'ondes optiques pour faciliter le balayage profond ou peu profond.

23. Procédé selon l'une des revendications 20 à 22, **caractérisé en ce qu'**il inclut :

(a) fournir un miroir rotatif (16) dans le premier chemin optique (20) ;
(b) dévier le premier chemin optique (20);
(c) faire en sorte que la pluralité de points focaux (21a, 21b, 22a, 22b, 23a, 23b) est disposée sur une surface (18) ;
(d) réaliser un balayage axial ;
(e) mettre en rotation le miroir (16) pour déplacer la surface (18) ; et
(f) répéter l'étape (d) au moins deux fois et réaliser l'étape (e) entre chaque répétition.

24. Procédé selon l'une des revendications 20 à 22, **caractérisé en ce qu'**il inclut :

(a) fournir un miroir rotatif (16) dans le premier chemin optique (20) ;
(b) dévier le premier chemin optique (20) ;
(c) faire en sorte que la pluralité de points focaux (21a, 21b, 22a, 22b, 23a, 23b) est disposée sur une surface (18) ;
(d) réaliser un balayage axial ;
(e) translater de manière linéaire en combinaison les moyens de focalisation (14), la pluralité des sources de radiation optique et le miroir (16) pour déplacer la surface (18) ; et
(f) répéter l'étape (d) au moins deux fois et réaliser l'étape (e) entre chaque répétition.

25. Procédé selon l'une des revendications 20 à 22, **caractérisé en ce qu'**il inclut :

(a) fournir un miroir (16) dans le premier chemin optique (18) ;
(b) dévier le premier chemin optique (20) ;
(c) faire en sorte que la pluralité de points focaux (21a, 21b, 22a, 22b, 23a, 23b) est disposée sur une surface (18) ;
(d) réaliser un balayage axial ;
(e) simultanément mettre en rotation le miroir (16) et en translation linéaire, en combinaison, les moyens de focalisation (14), la pluralité de sources optiques de radiation et le miroir (16) pour déplacer la surface (18) ; et
(f) répéter l'étape (d) au moins deux fois et réaliser l'étape (e) entre chaque répétition.

26. Procédé selon l'une des revendications 23, 24 ou 25, qui inclut la fourniture d'une surface d'un prisme en tant que miroir (16).

27. Procédé selon l'une des revendications 23, 24 ou 25 dépendantes de la revendication 21, **caractérisé en ce qu'**il inclut la fourniture d'une radiation à partir de la source optique primaire (50) au travers d'une pluralité de coupleurs

(54) vers les fibres optiques (10), fournir un générateur (64) de retard optique connecté aux coupleurs optiques (54) et fournir un second chemin optique, permettant à la radiation d'être transmise en retour le long du premier (20) et second chemins optiques vers les coupleurs (54), pour former des interférences, et transmettre la radiation reçue des premier (20) et second chemins optiques, aux coupleurs optiques (54), vers lesdits moyens de détection (58) pour la détection du motif d'interférence.

28. Procédé selon la revendication 27, **caractérisé en ce qu'**il inclut en outre l'étape de fournir une pluralité de sources optiques primaires (50) et pour chaque source primaire optique (50) un coupleur en arborescence (52) respectif, et coupler chaque source primaire optique (50) au travers dudit coupleur en arborescence respectif (52) à chaque coupleur optique (54).

29. Procédé selon la revendication 27, **caractérisé en ce qu'**il inclut : fournir un moyen de circulation optique entre les coupleurs optiques (54) et les moyens de détection (58) pour réaliser une radiation optique sauvegardée vers les moyens de détection (58).

30. Procédé selon la revendication 28, **caractérisé en ce que** les sources optiques primaires (50), les coupleurs en arborescence (52) et les coupleurs (54) optiques sont configurés en tant que endoscope apte à l'examen d'une cavité interne d'un corps, incluant au moins l'un de : au moins un canal pour l'illumination en lumière blanche, un canal de vision vers l'avant endoscope à lumière blanche, un canal de succion/biopsie et un canal pour l'utilisation d'une puce d'air et d'une puce d'eau.

31. Procédé selon l'une des revendications 25, 26 ou 27, **caractérisé en ce qu'**il est prévu un changement d'index de réfraction entre un milieu contenant les sources de radiation optiques et l'échantillon (S, 65) et pour chaque point focal, un décalage de distance dû aux changements d'indice de réfraction entre la perte de cohérence de chaque source de radiation optique et le point focal dans l'échantillon (S, 65) est obtenu selon les étapes de :

(a) balayer la radiation optique à partir de la pluralité de sources de radiation optique dans ledit premier chemin optique (20) de façon que les point focaux (21a, 21b, 22a, 22b, 23a, 23b) des sources de radiation optique sont alignés le long d'un chemin s'étendant à partir du milieu contenant les sources de radiation optique dans l'échantillon (S, 65) ;
(b) détecter la radiation optique réfléchie pour chaque point focal (21a, 21b, 22a, 22b, 23a, 23b) ; et,
(c) localiser le point focal (21a, 21b, 22a, 22b, 23a, 23b) pour lesquels il y a un changement important de radiation optique réfléchie comparée aux points focaux avoisinants (21a, 21b, 22a, 22b, 23a, 23b), tandis que le point focal (21a, 21b, 22a, 22b, 23a, 23b) posé dans l'étape (c) indique l'endroit de l'interférence entre l'échantillon (S, 65) et le milieu contenant les sources de radiation optiques.

32. Procédé selon la revendication 31, **caractérisé en ce qu'**il comporte en outre la répétition des étapes (a) à (c) pour chaque balayage axial pour obtenir une résolution spaciale adaptée pour la zone de balayage choisie.

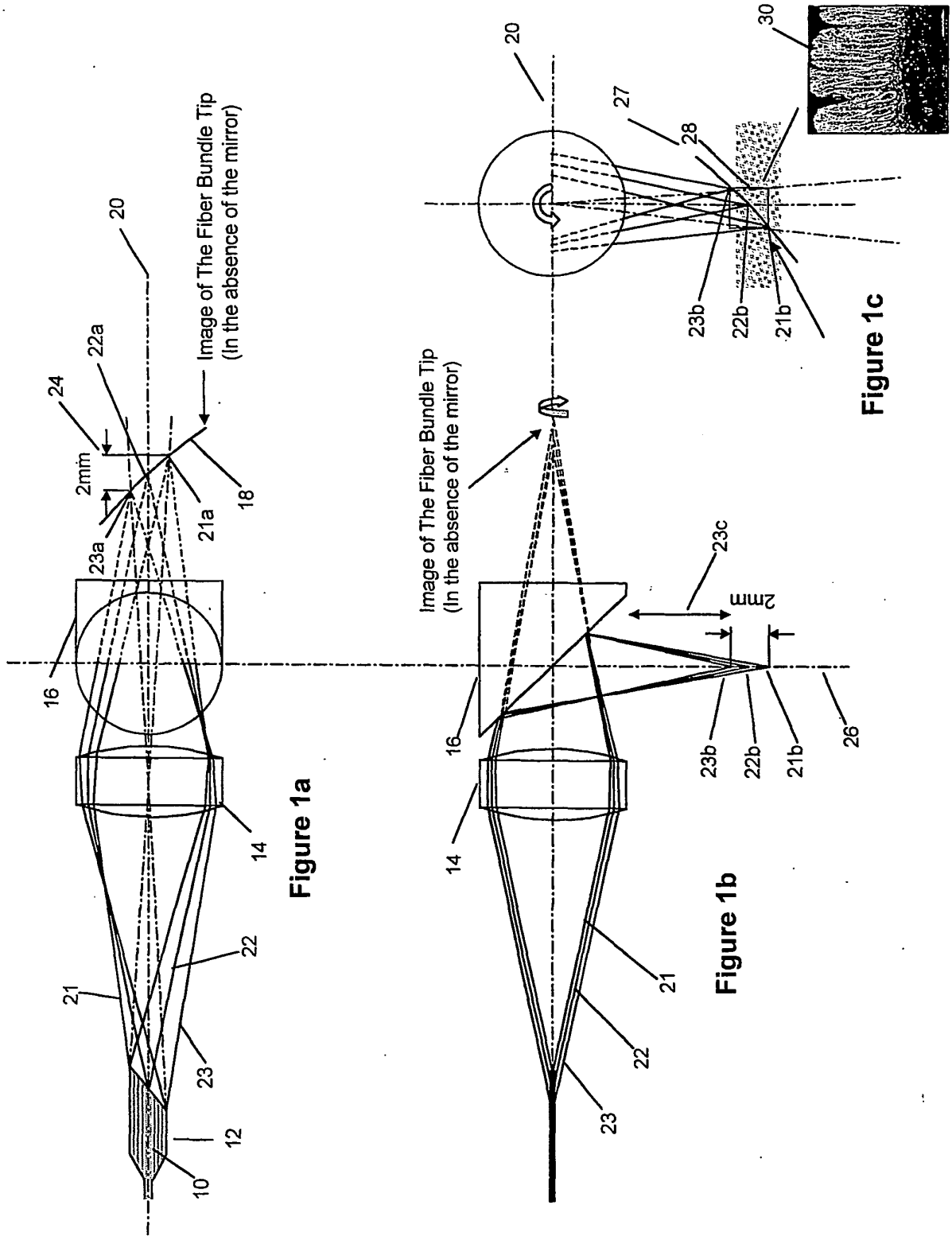
Image of The Fiber Bundle Tip
(In the absence of the mirror)
20
22a
24
2mm
23a
21a
18
16
14
22
21
23
12
10
Figure 1a
20
Image of The Fiber Bundle Tip
(In the absence of the mirror)
23c
2mm
16
14
23b
22b
21b
26
21
22
23
Figure 1b
30
27
28
23b
22b
21b
Figure 1c

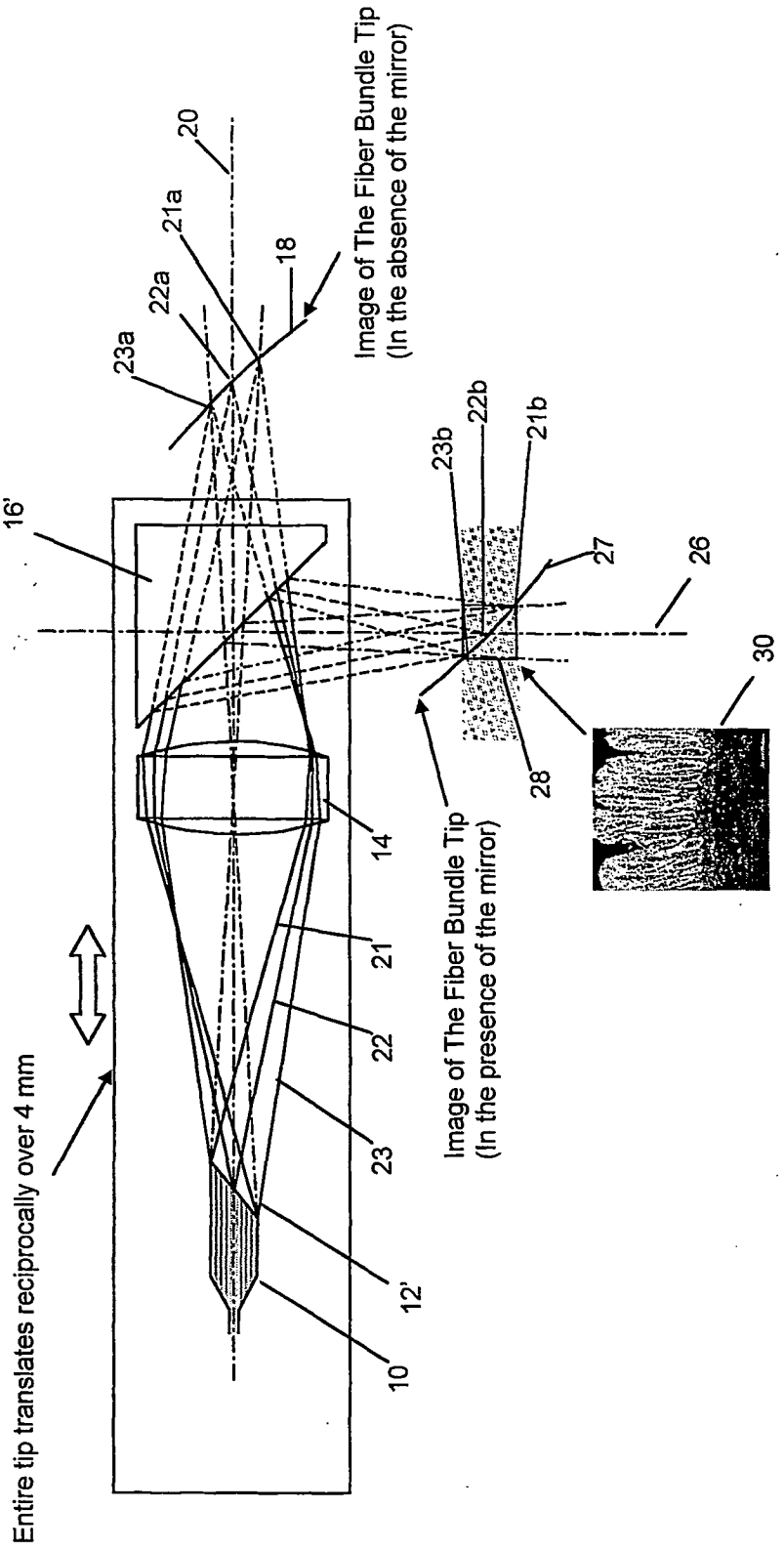
Image of The Fiber Bundle Tip
(In the absence of the mirror)
20
21a
22a
23a
18
16'
23b
22b
21b
27
26
30
28
14
21
22
23
12'
10
Image of The Fiber Bundle Tip
(In the presence of the mirror)
Entire tip translates reciprocally over 4 mm

Figure 1d

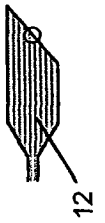

Figure 2a

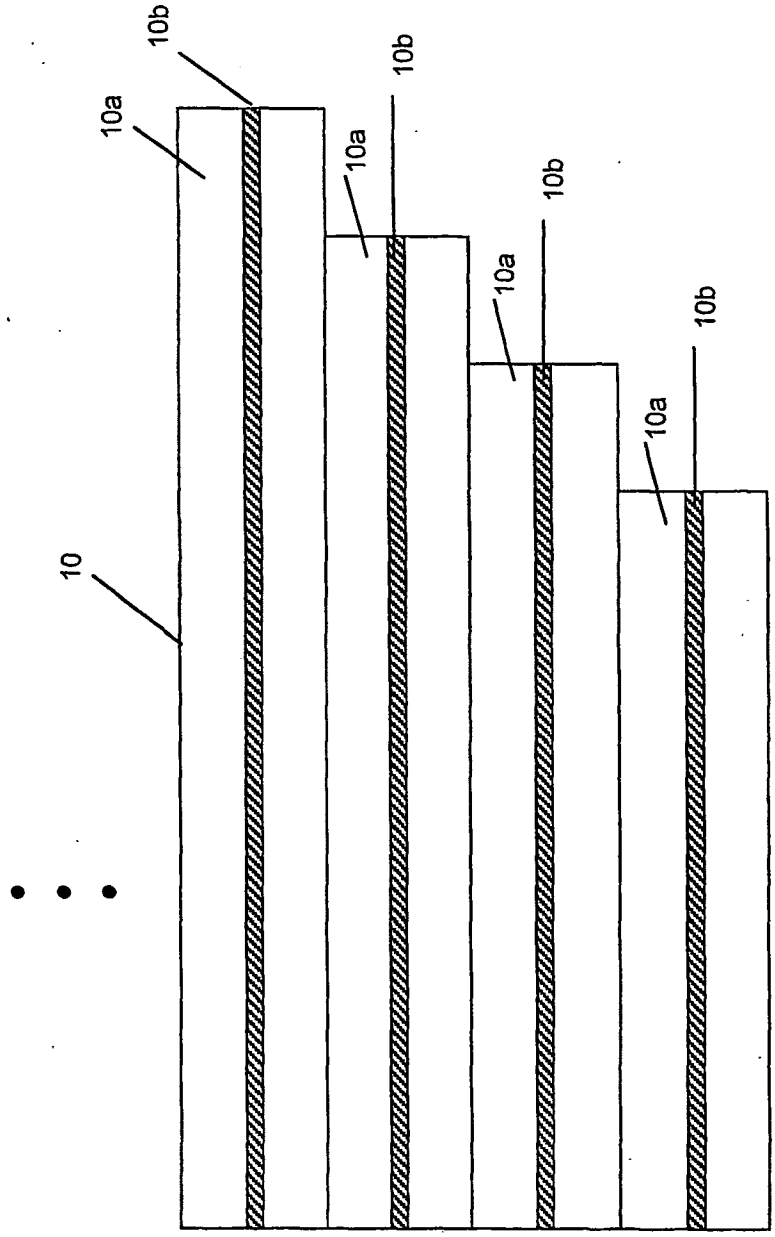

Figure 2b

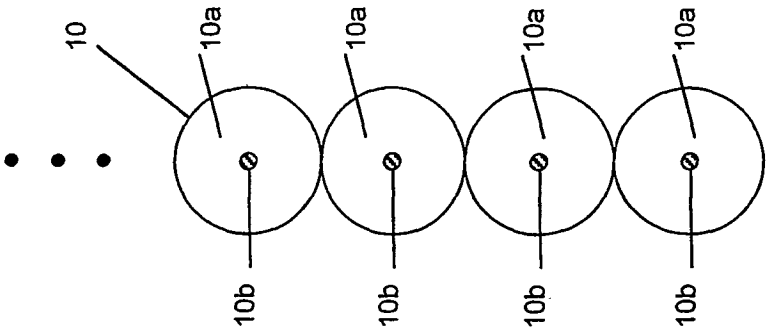

Figure 2c

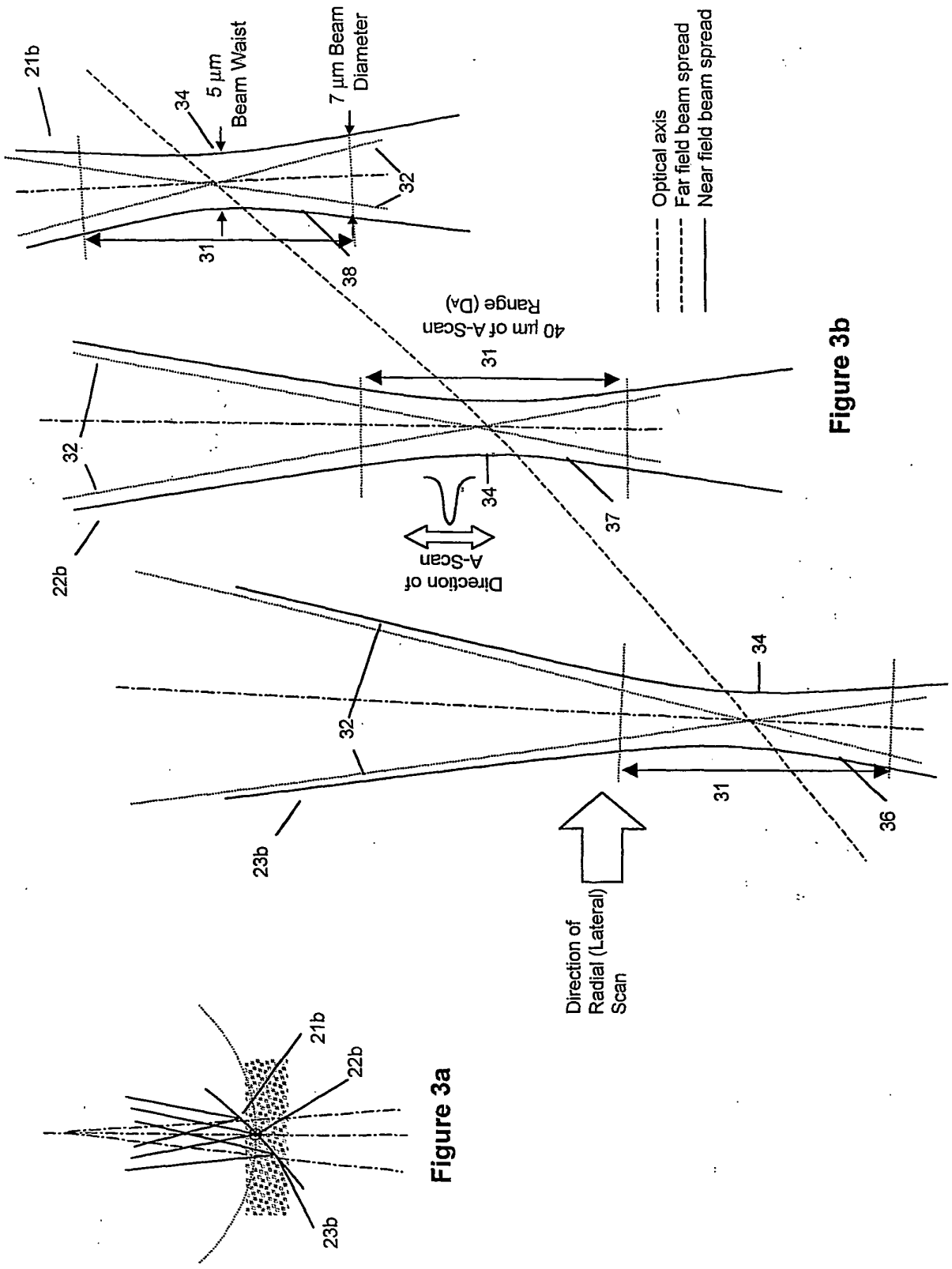

Figure 3b

Figure 3a

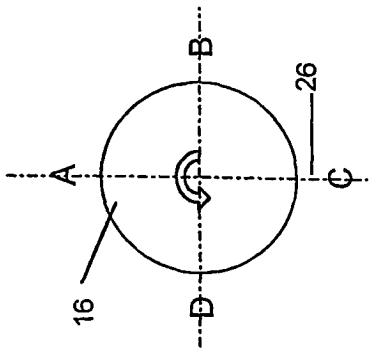

Figure 4a

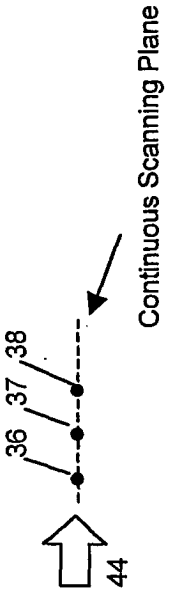

Figure 4b

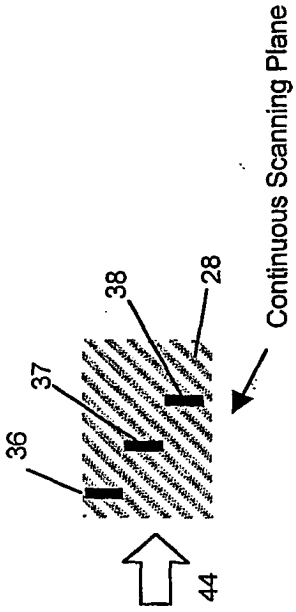

Figure 4c

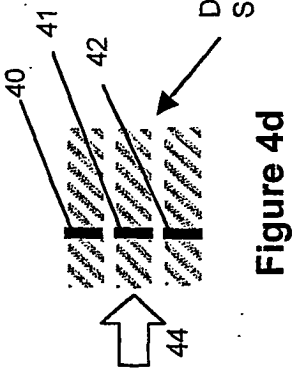

Figure 4d

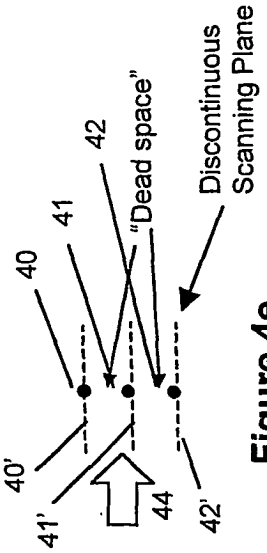

Figure 4e

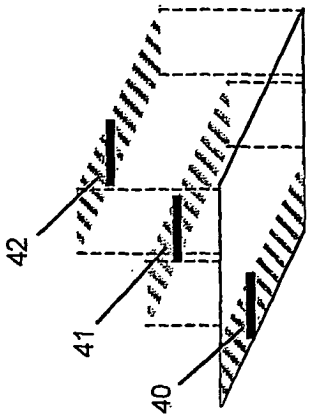

Figure 4f

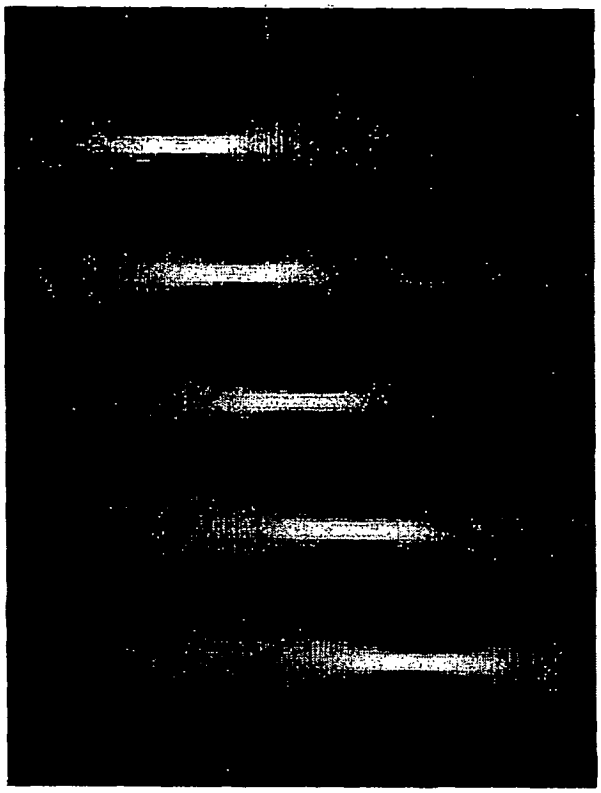

Figure 5b

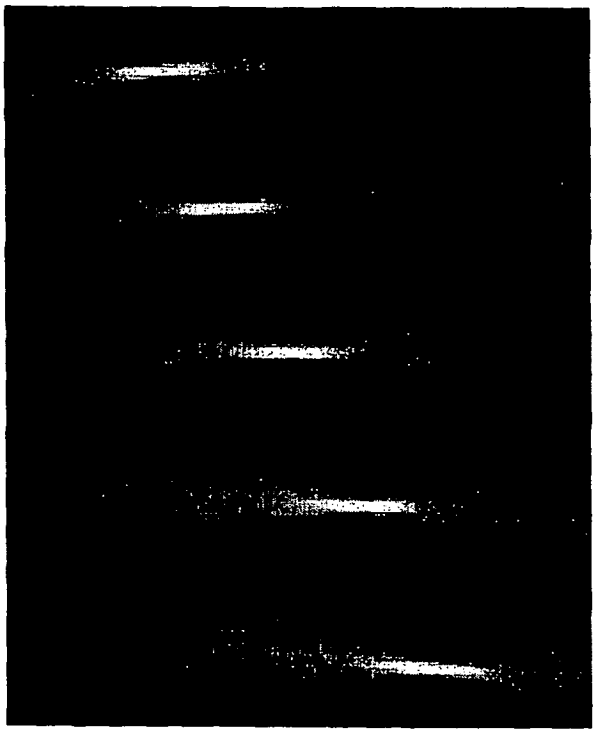

Figure 5a

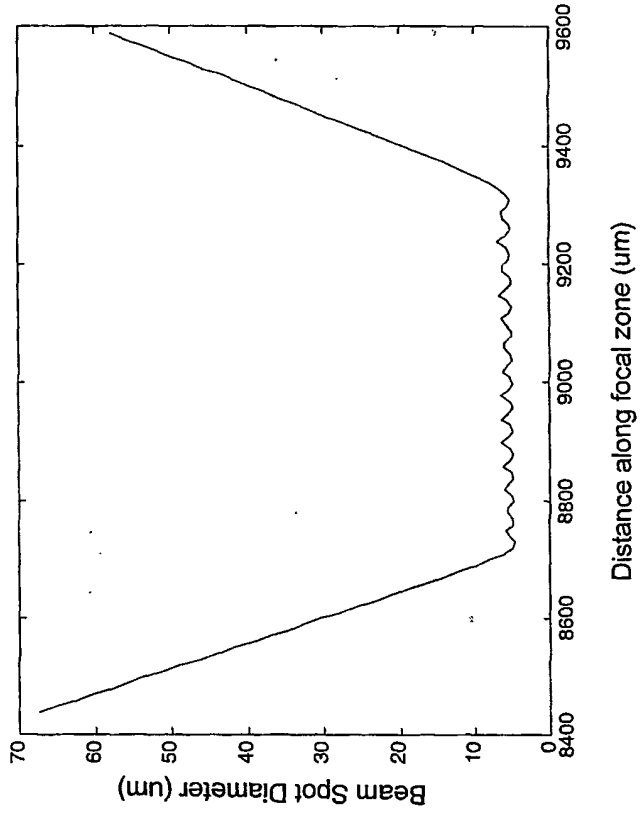

Figure 5d

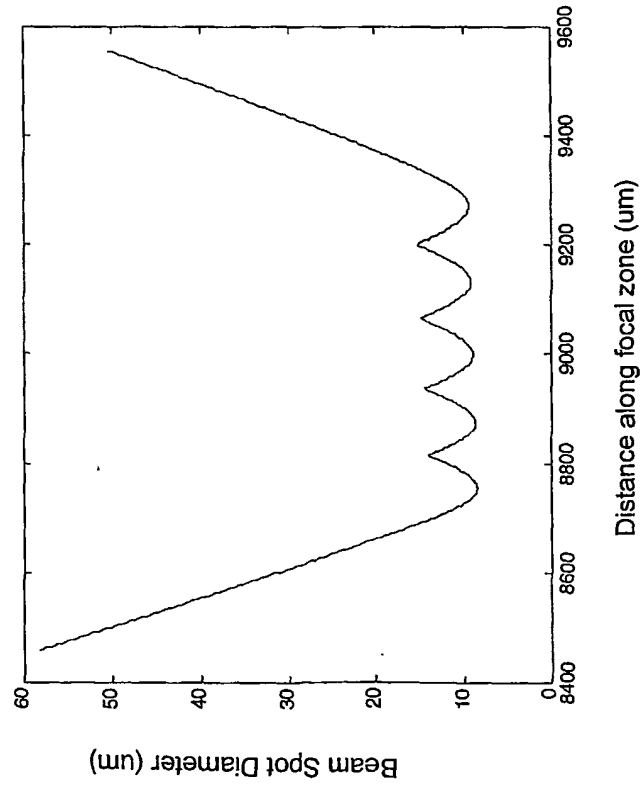

Figure 5c

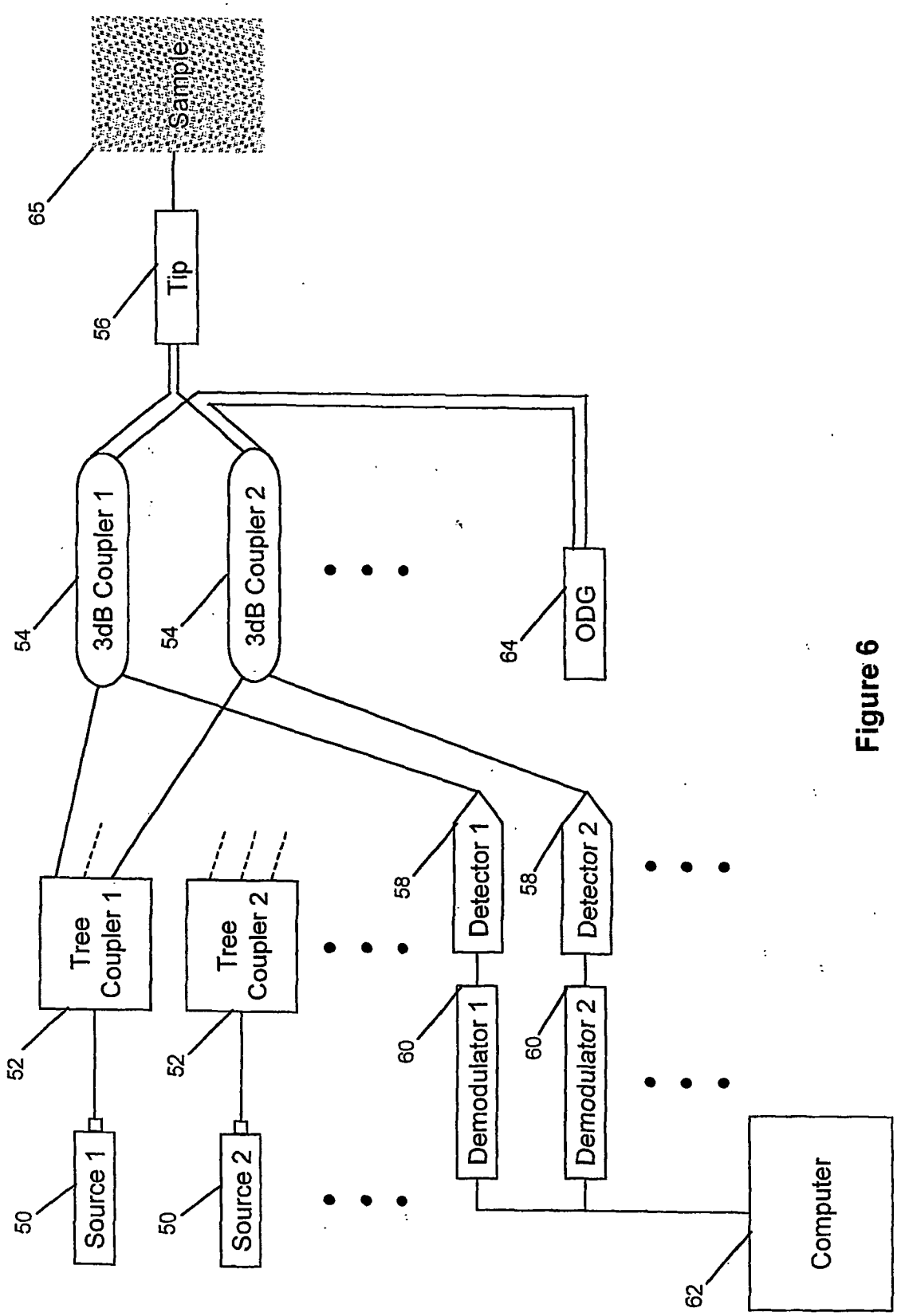
Sample
65
Tip
56
3dB Coupler 1
54
3dB Coupler 2
54
ODG
64
Tree Coupler 1
52
Tree Coupler 2
52
Source 1
50
Source 2
50
Detector 1
58
Detector 2
58
Demodulator 1
60
Demodulator 2
60
Computer
62

Figure 6

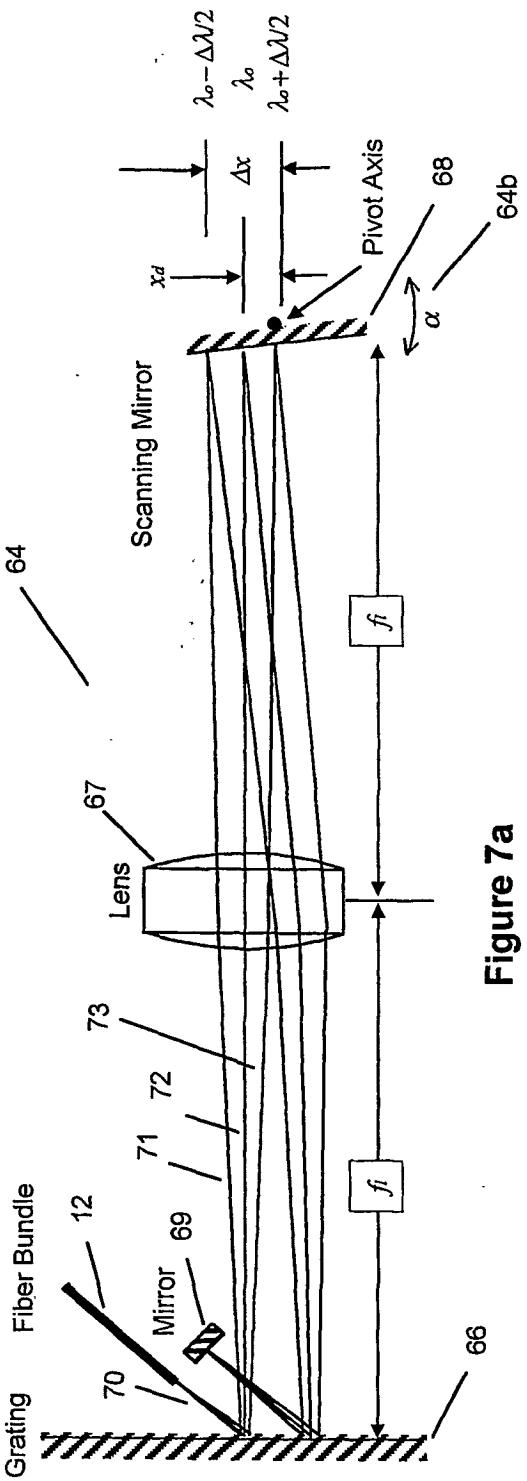

Figure 7a

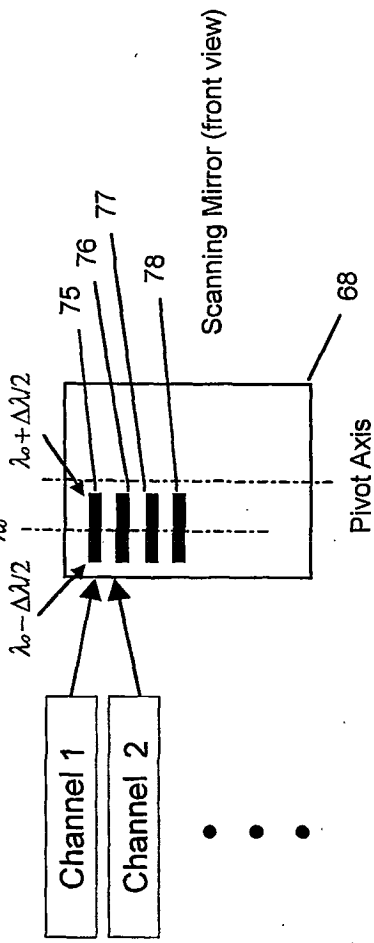

Figure 7b

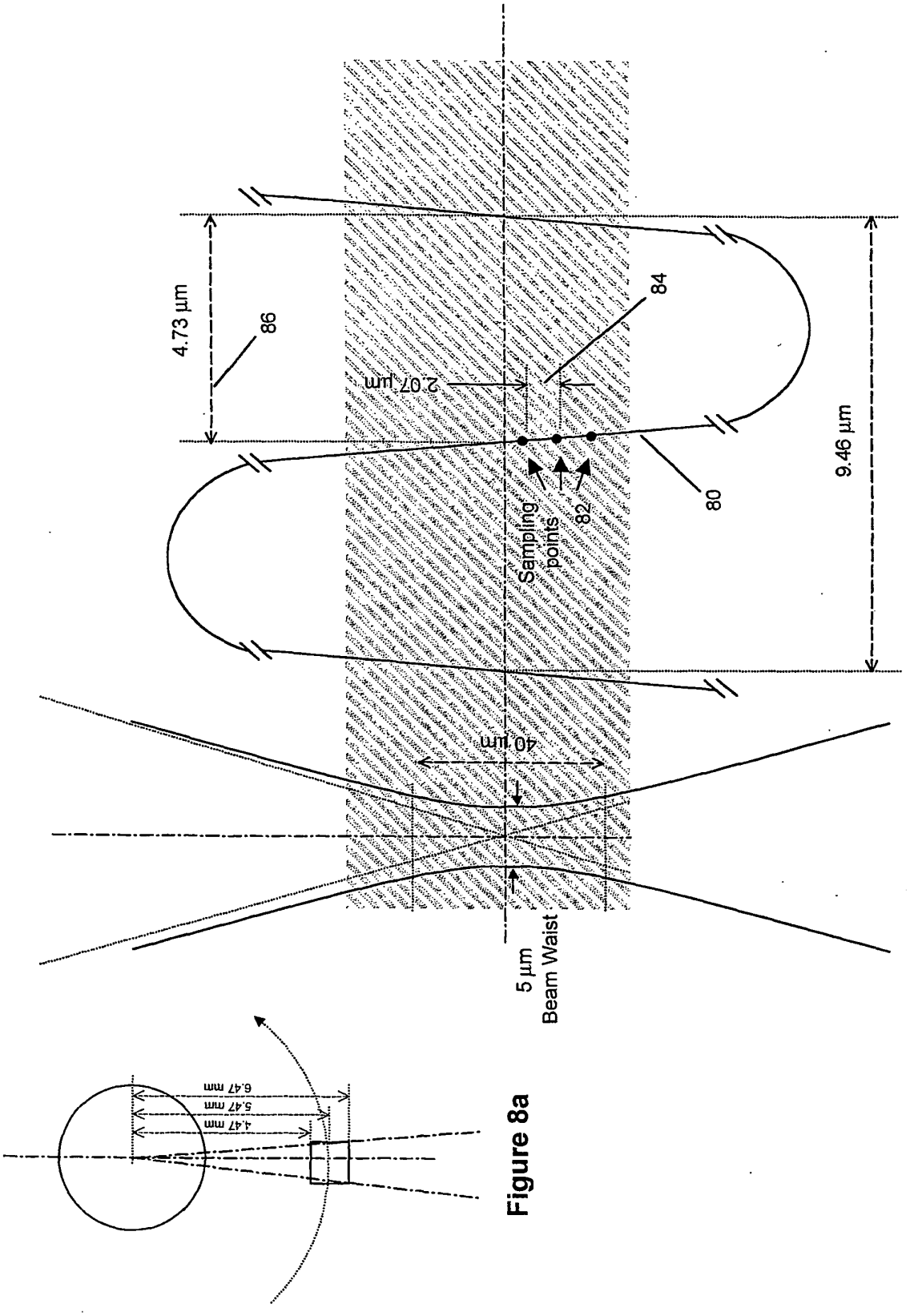

Figure 8a

Figure 8b

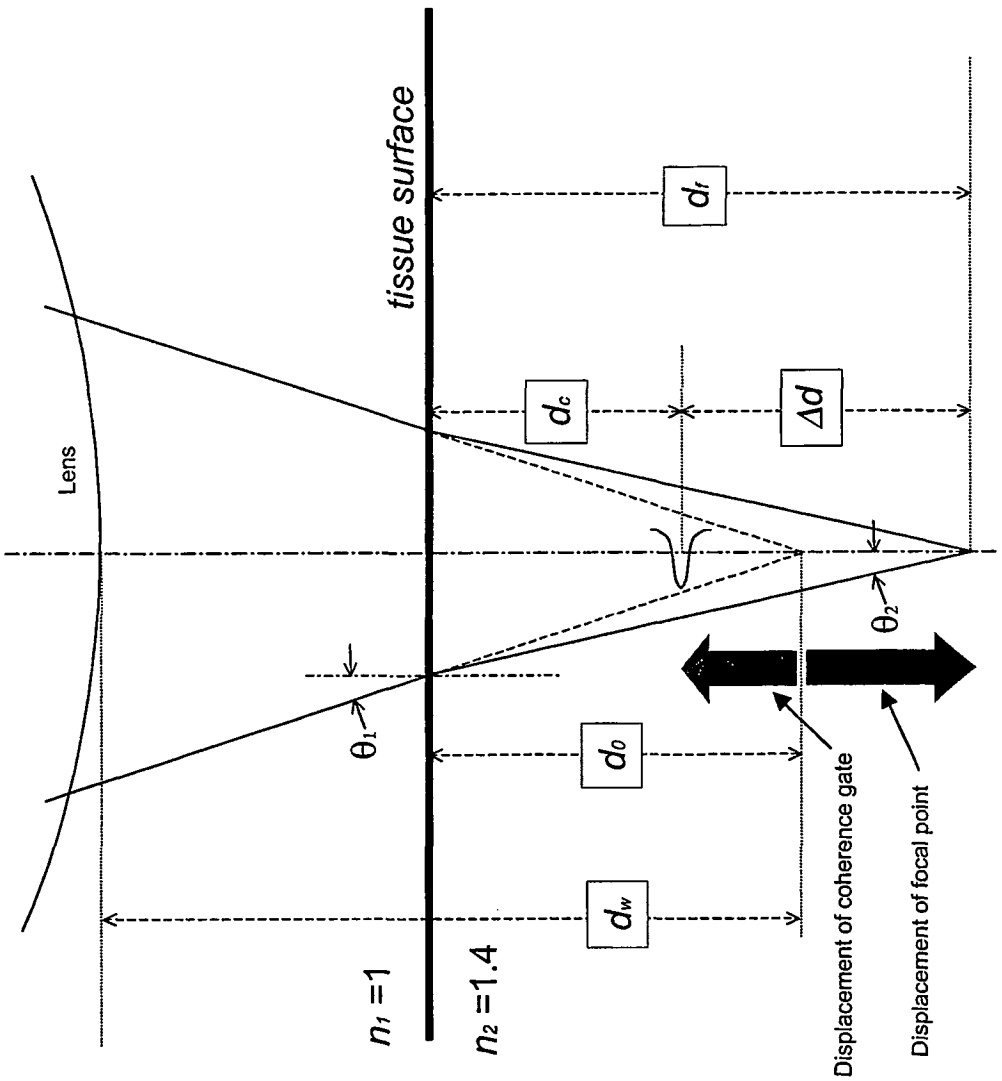
tissue surface
Lens
d_f
d_c
Δd
θ_1
θ_2
d_o
d_w
$n_1 = 1$
$n_2 = 1.4$
Displacement of coherence gate
Displacement of focal point

Figure 9

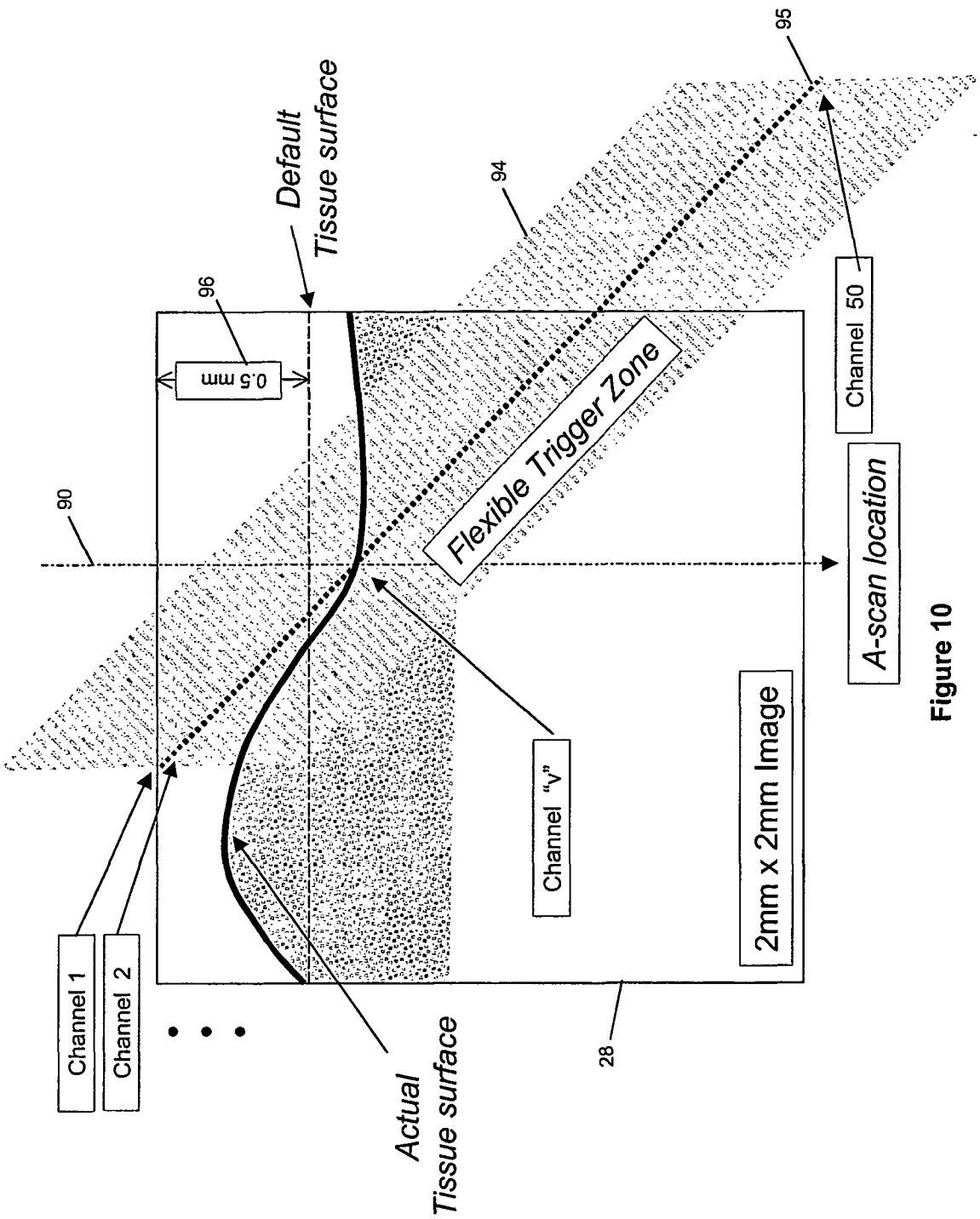
Default
Tissue surface
96
0.5 mm
94
95
Channel 50
90
Flexible Trigger Zone
A-scan location
Channel 1
Channel 2
Channel "v"
2mm x 2mm Image
Actual
Tissue surface
28

Figure 10

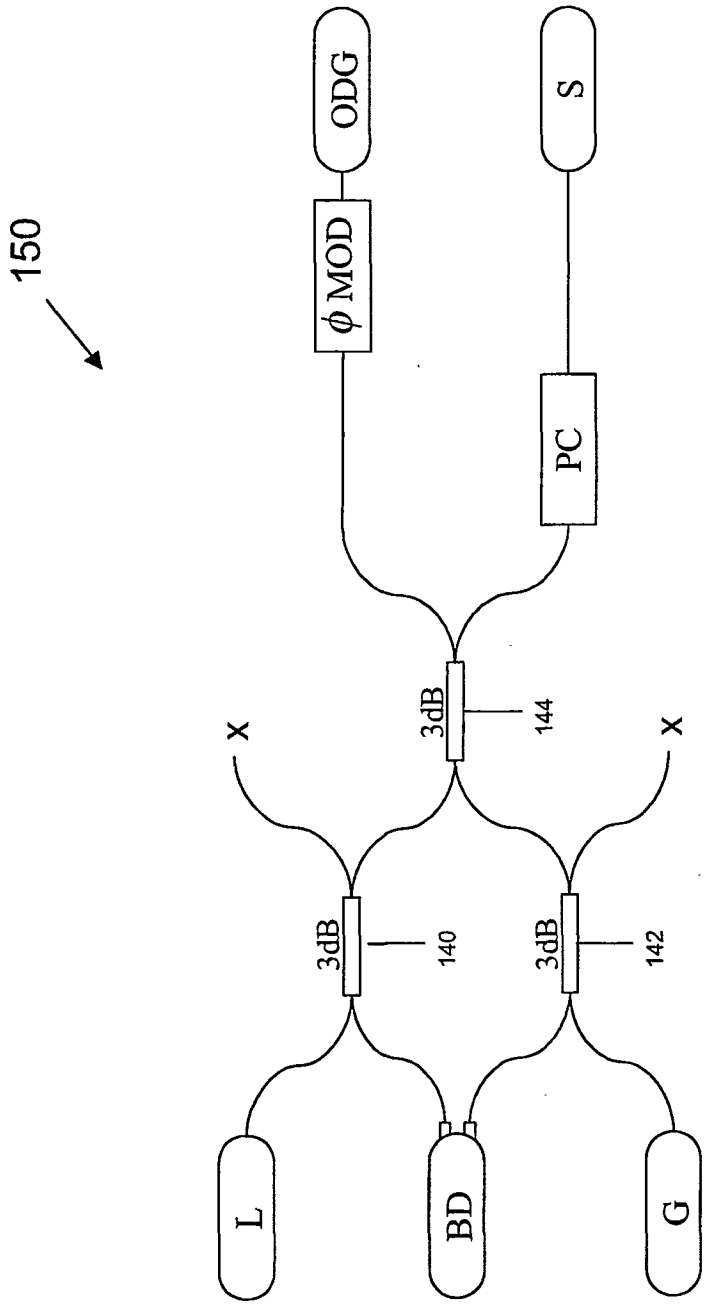

"Prior Art"

Figure 11a

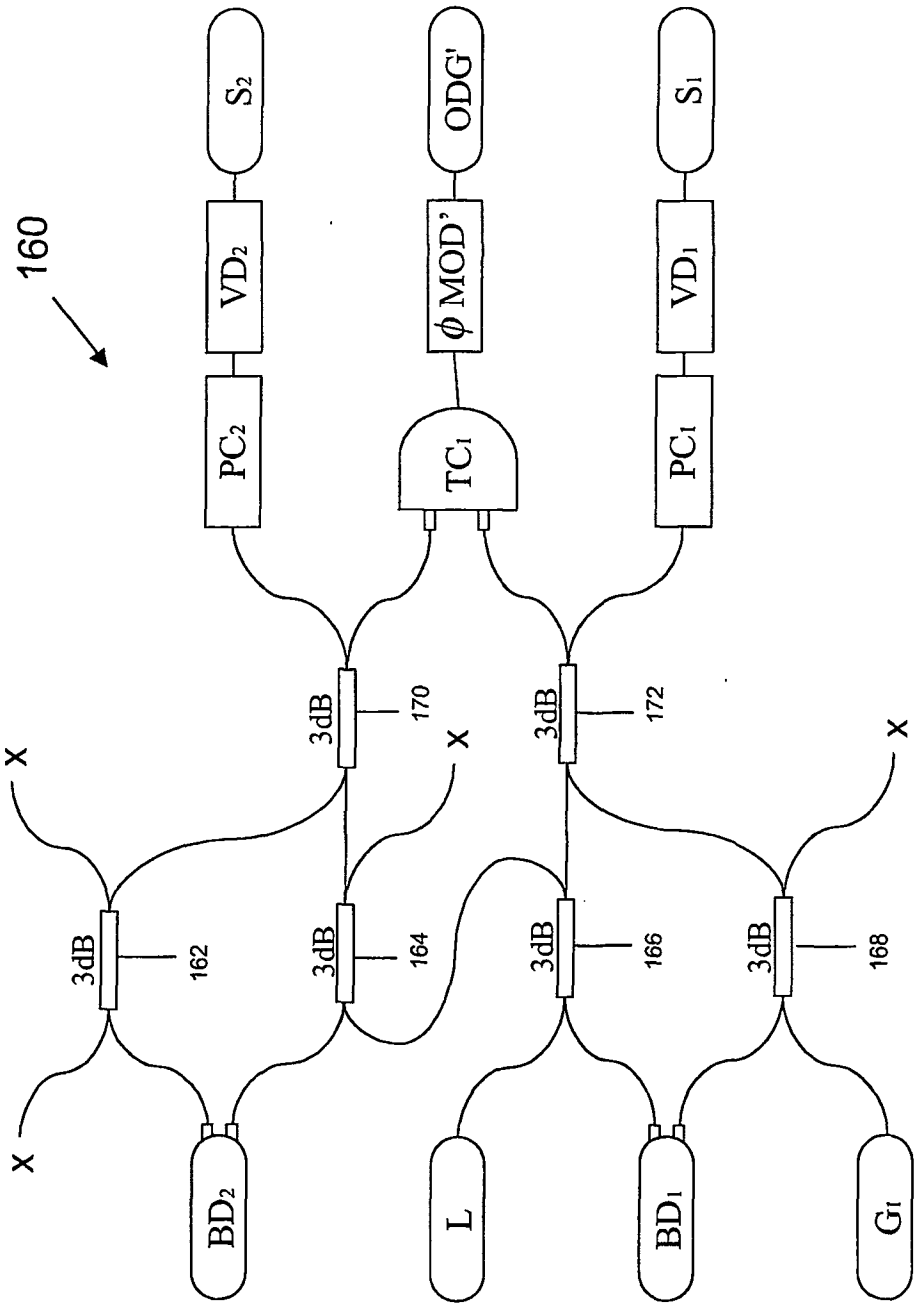
160
S2
VD2
PC2
ODG'
φ MOD'
TC1
S1
VD1
PC1
3dB
170
3dB
172
3dB
162
3dB
164
3dB
166
3dB
168
X
X
X
X
BD2
L
BD1
G1

Figure 11b

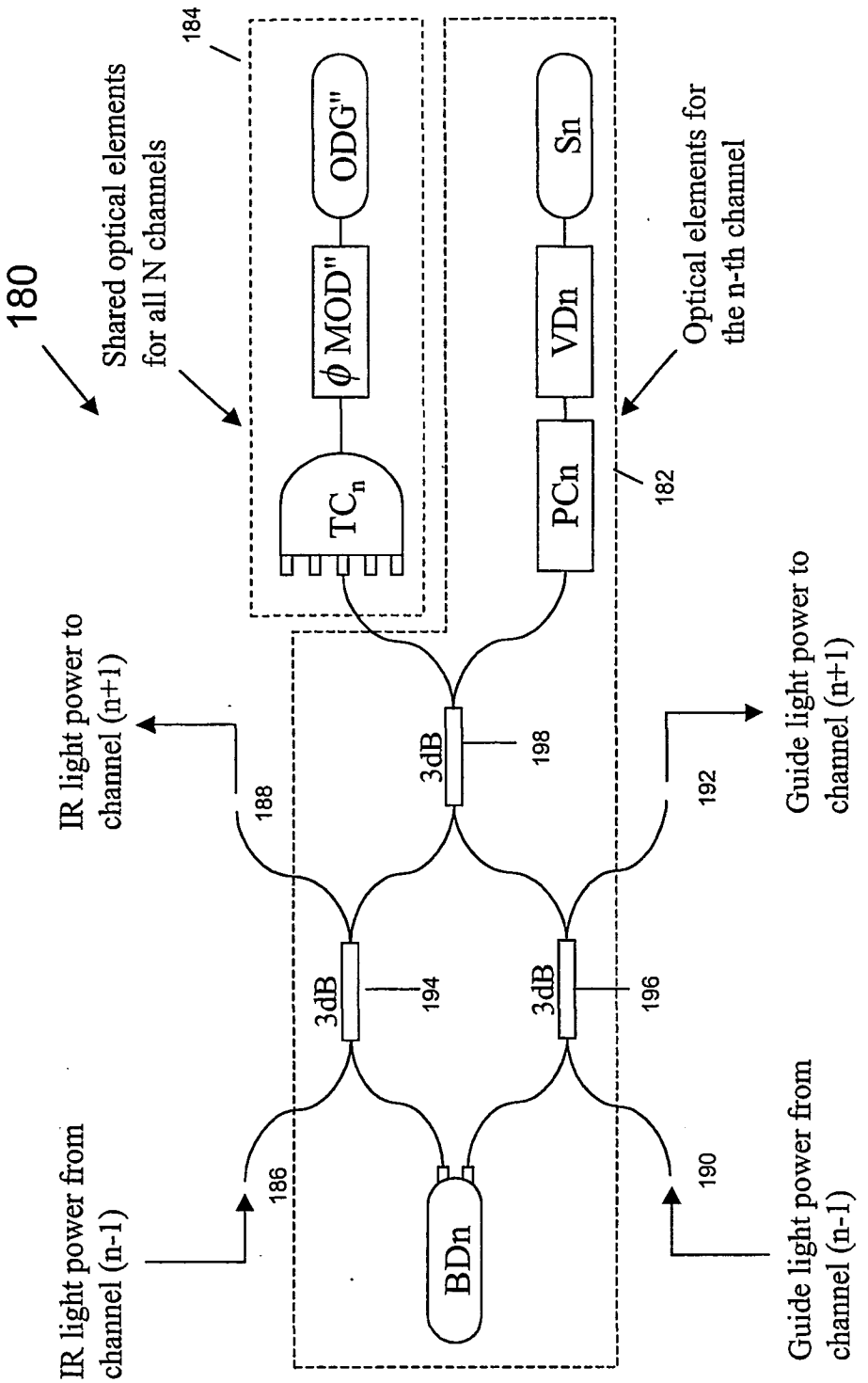
180
Shared optical elements for all N channels
184
ODG"
ϕ MOD"
TC_n
Sn
VDn
PCn
Optical elements for the n-th channel
182
IR light power to channel (n+1)
188
3dB
198
192
Guide light power to channel (n+1)
3dB
194
3dB
196
IR light power from channel (n-1)
186
BDn
190
Guide light power from channel (n-1)

Figure 11c

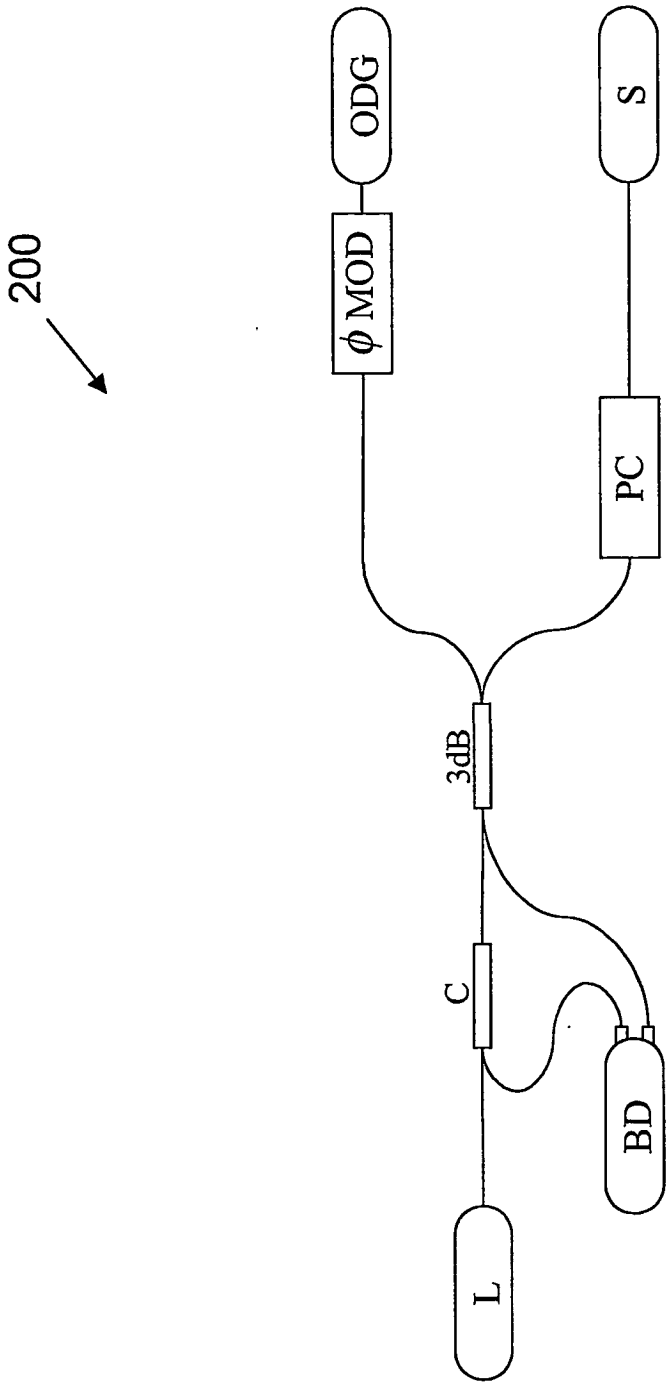

"Prior Art"

Figure 12a

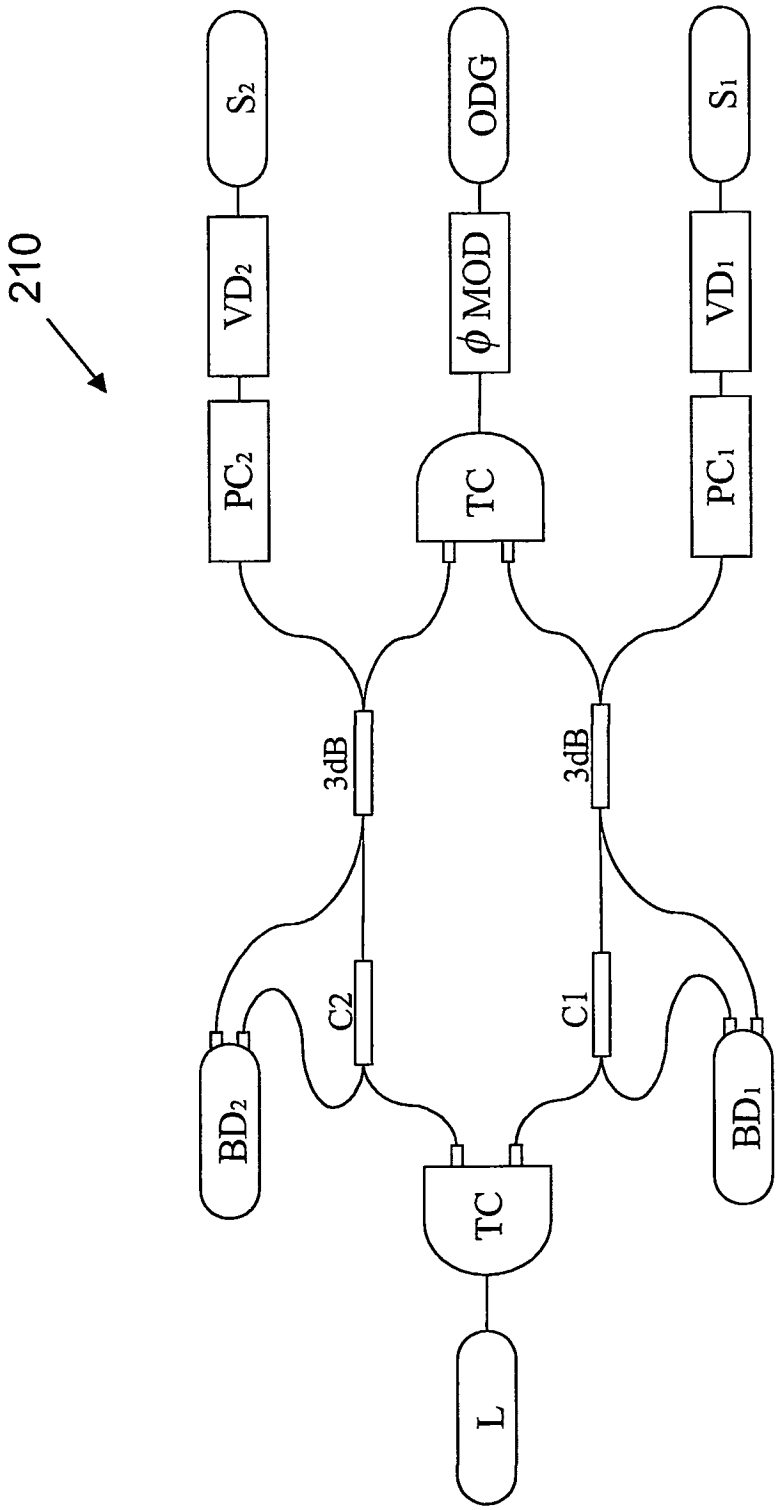

Figure 12b

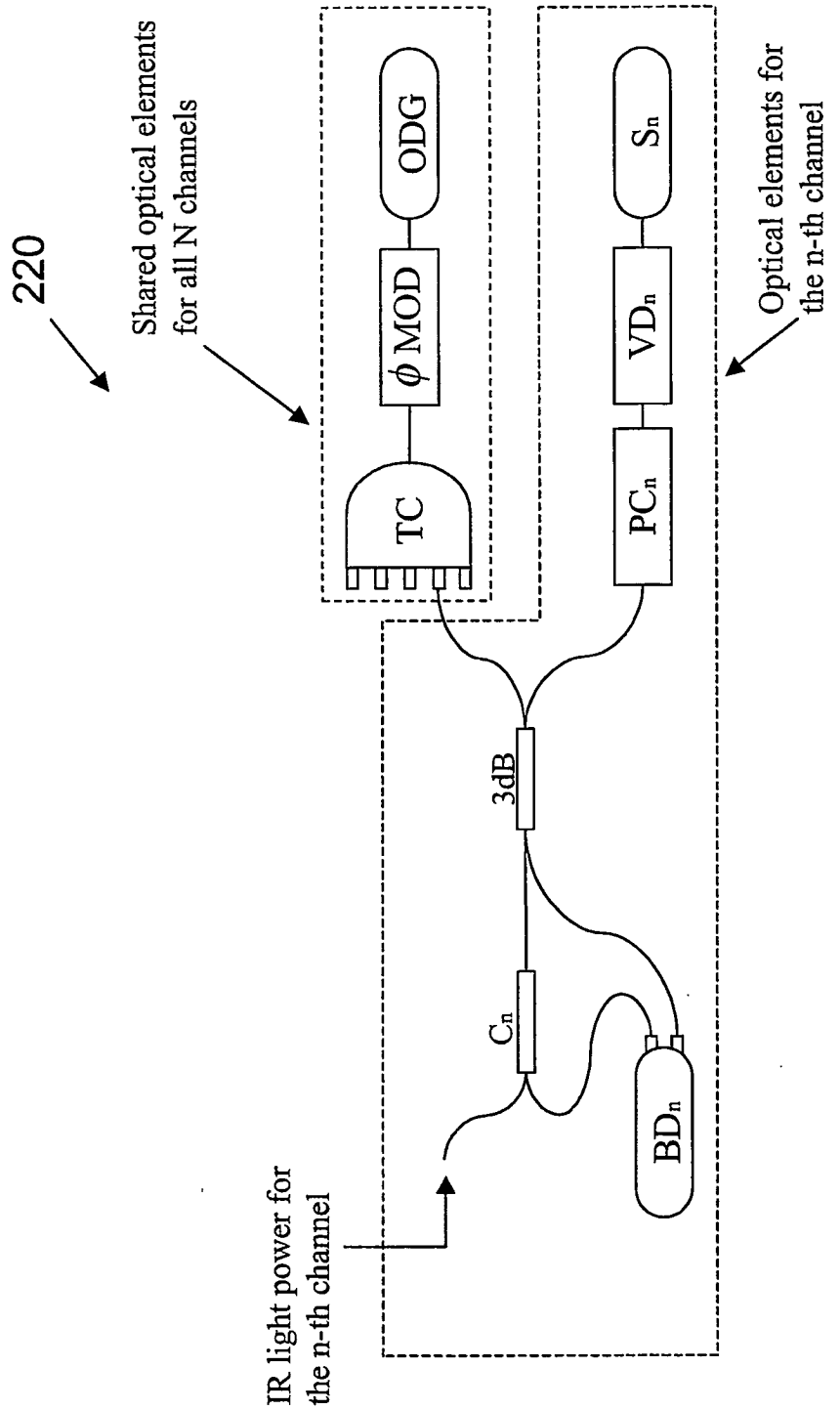
220
Shared optical elements for all N channels
ODG
φ MOD
TC
Optical elements for the n-th channel
Sn
VDn
PCn
3dB
Cn
BDn
IR light power for the n-th channel

Figure 12c

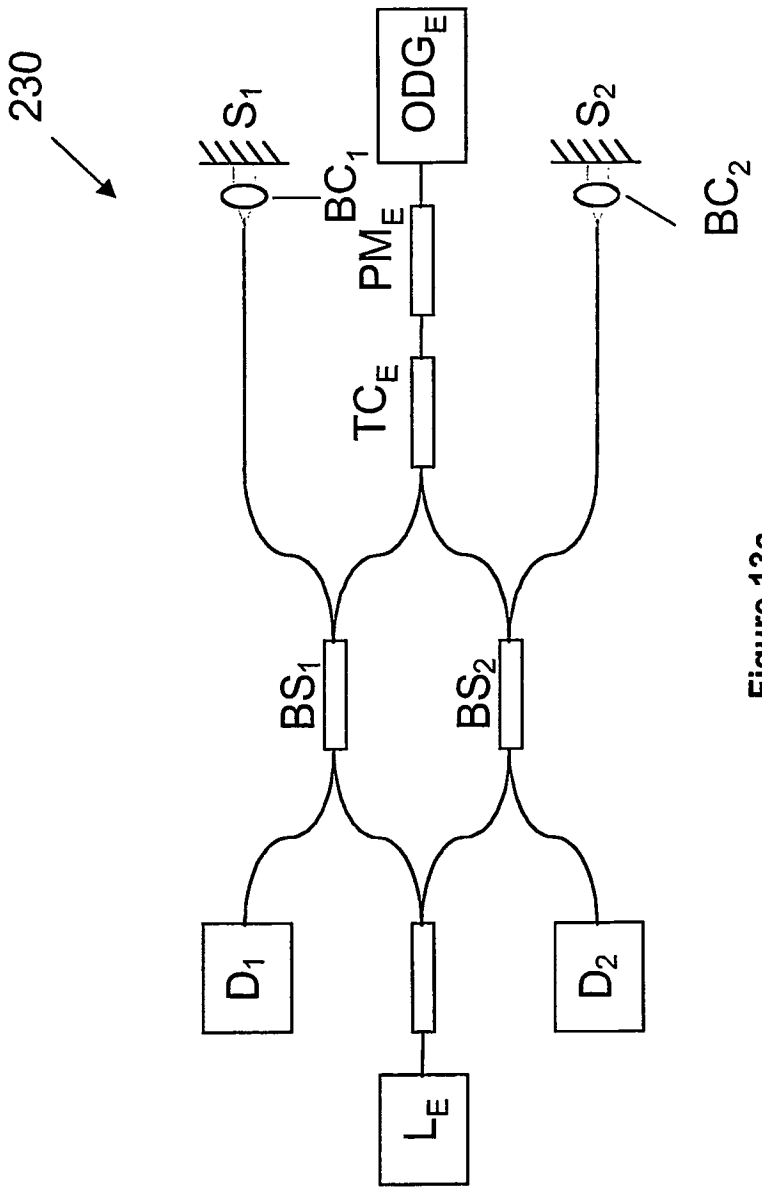

Figure 13a

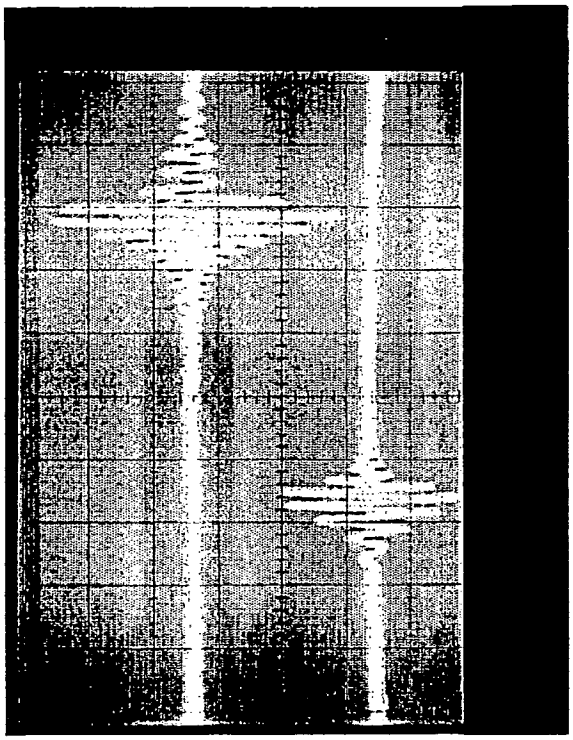

Figure 13c

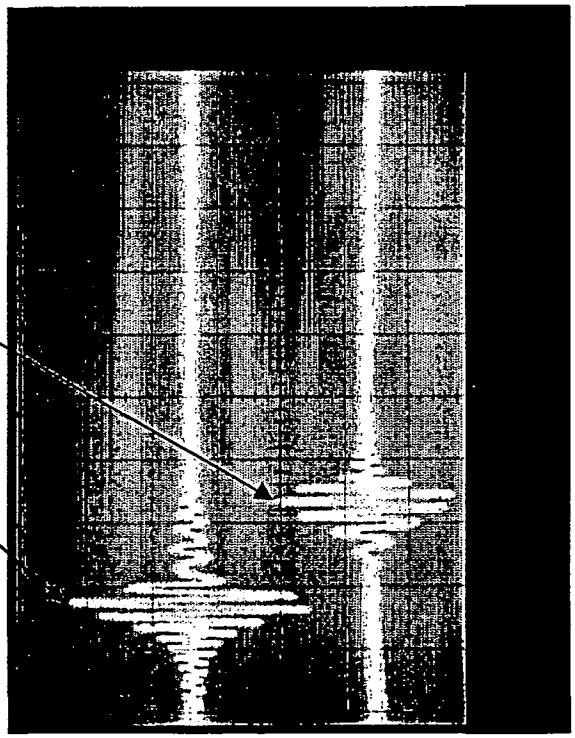

Figure 13b

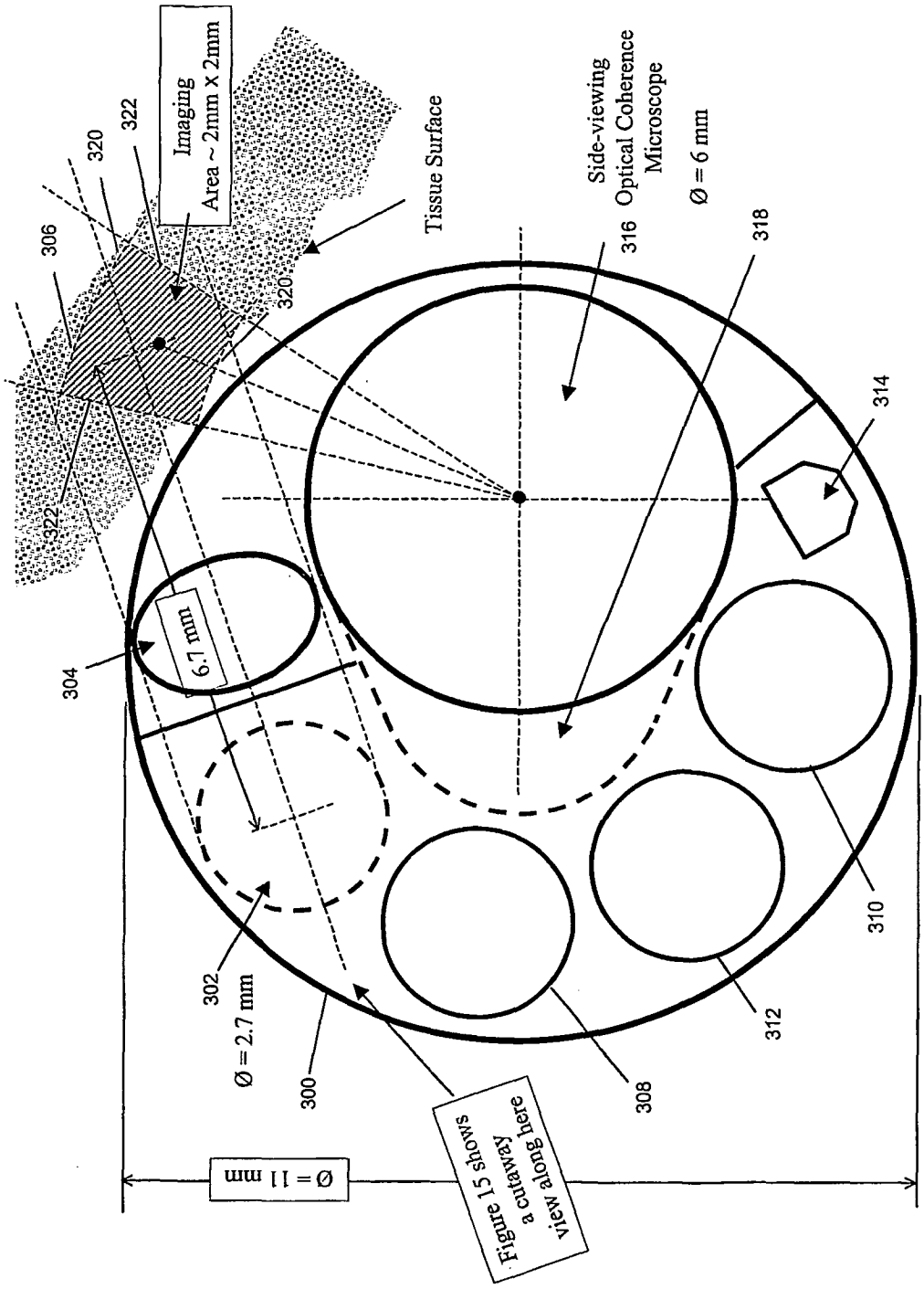
Imaging
Area ~ 2mm x 2mm
322
320
306
Tissue Surface
320
Side-viewing
Optical Coherence
Microscope
Ø = 6 mm
316
318
314
322
304
6.7 mm
302
Ø = 2.7 mm
300
308
312
310
Ø = 11 mm
Figure 15 shows
a cutaway
view along here

Figure 14

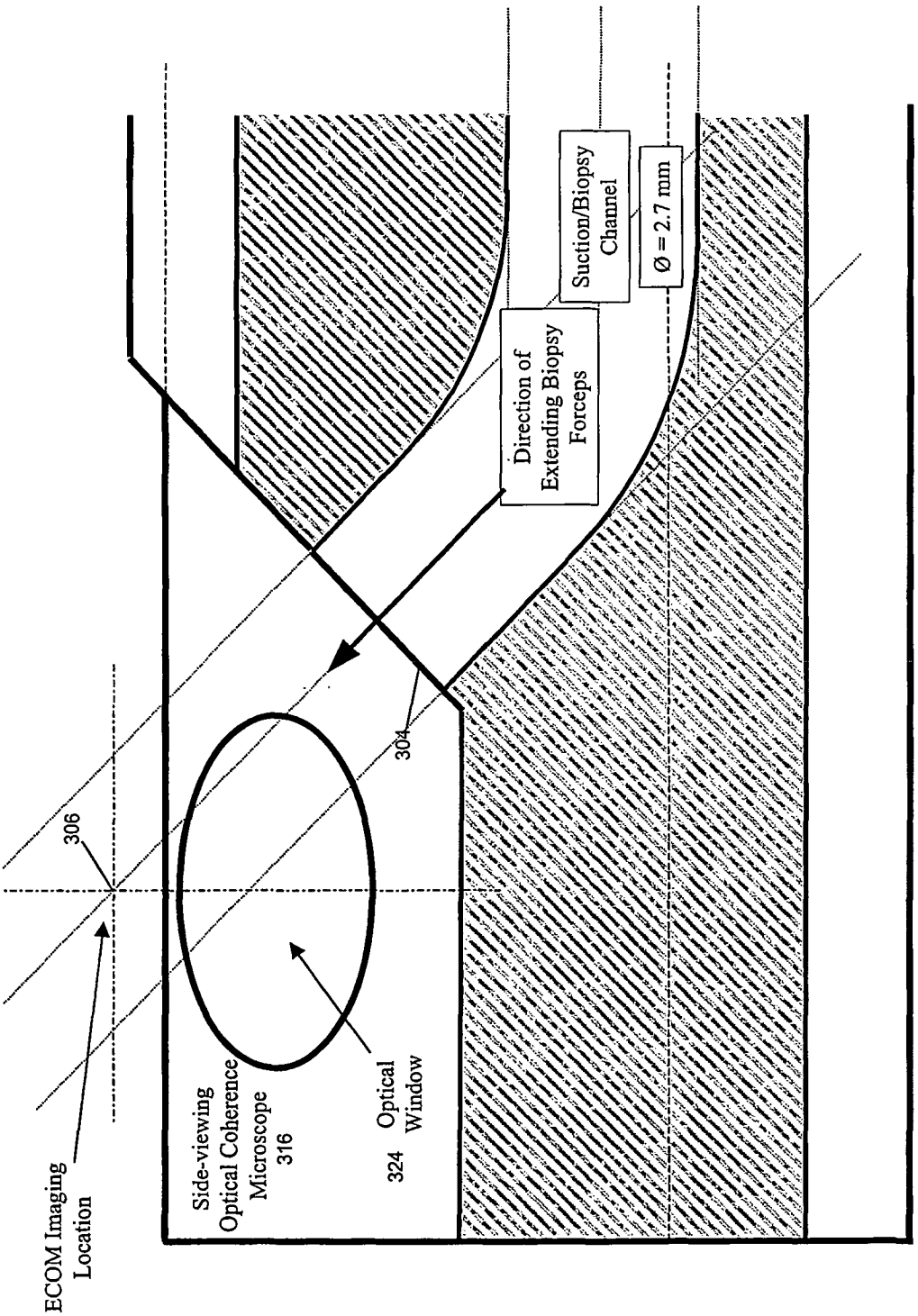
ECOM Imaging Location
306
Side-viewing Optical Coherence Microscope 316
Optical Window
324
304
Direction of Extending Biopsy Forceps
Suction/Biopsy Channel
Ø = 2.7 mm

Figure 15

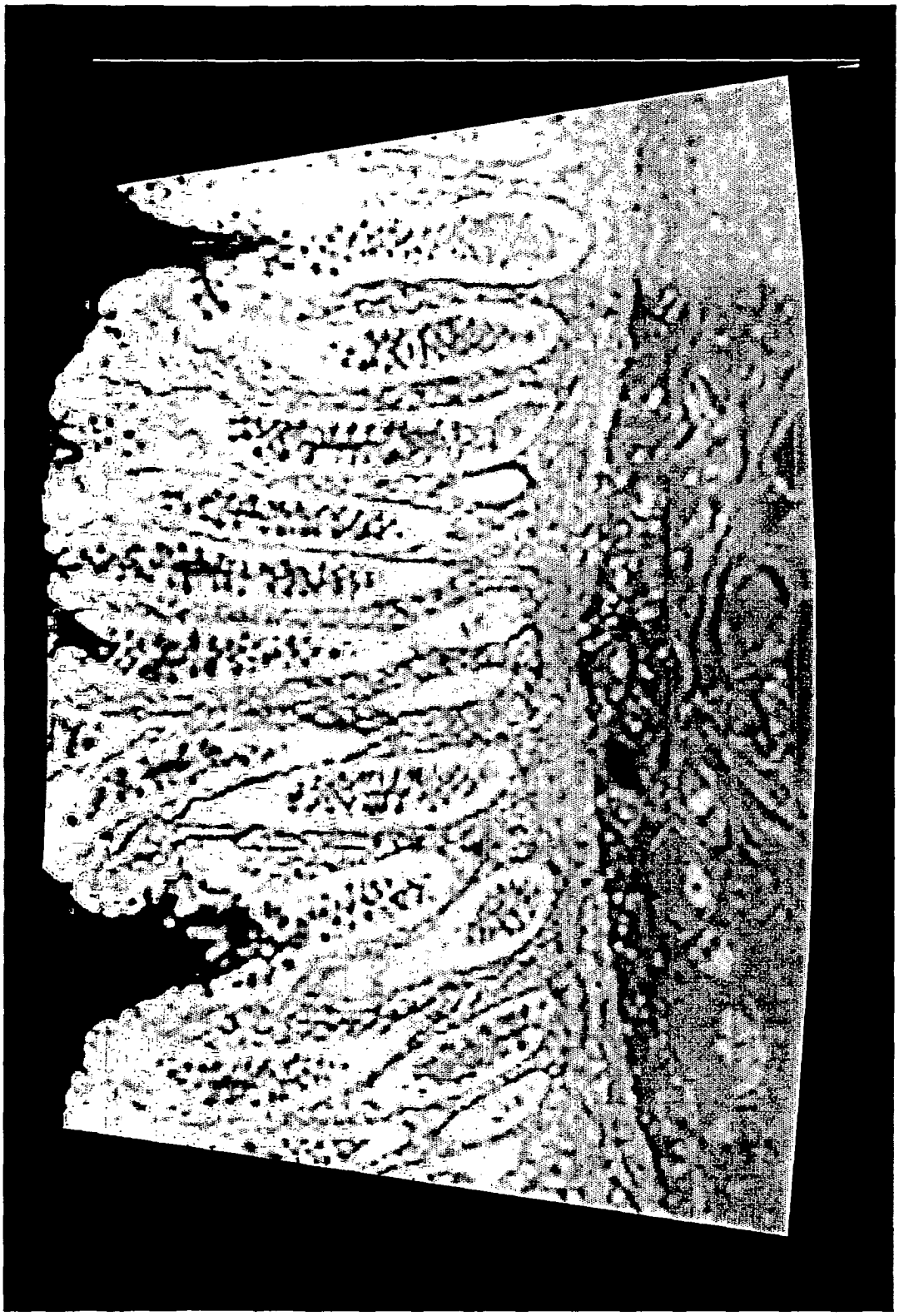

Figure 16

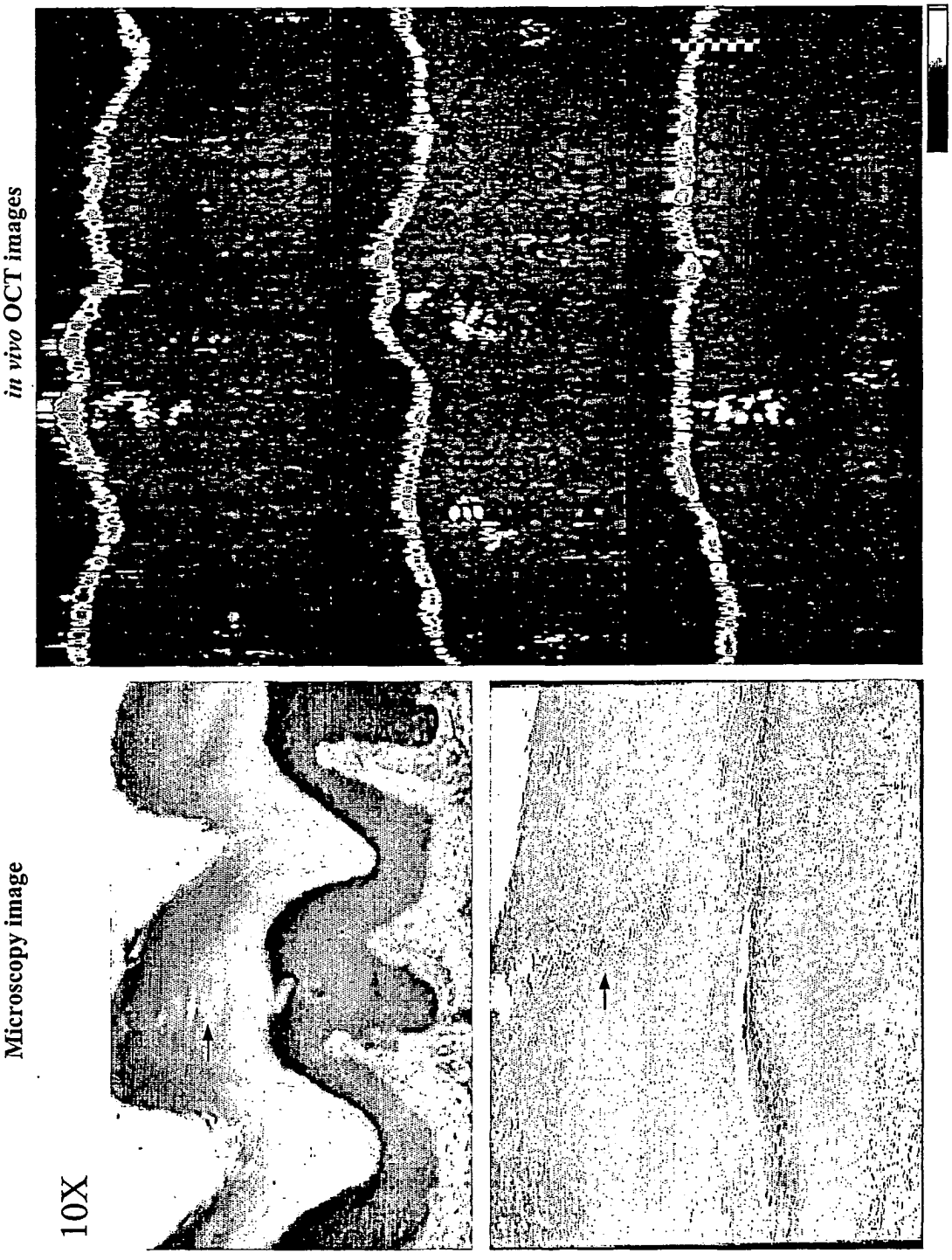

Figure 17b

Figure 17a

专利名称(译)	用于高分辨率相干光学成像的方法和设备		
公开(公告)号	EP1299711B1	公开(公告)日	2006-05-24
申请号	EP2001951277	申请日	2001-07-10
[标]申请(专利权)人(译)	大学健康网络		
申请(专利权)人(译)	大学健康网络		
当前申请(专利权)人(译)	大学健康网络		
[标]发明人	YANG VICTOR XIAO DONG VITKIN I ALEX WONGKEESONG LOUIE KATZ SHARON GORDON MARGARET LESLIE WILSON BRIAN C MOK ALVIN HO KWAN		
发明人	YANG, VICTOR, XIAO, DONG VITKIN, I., ALEX WONGKEESONG, LOUIE KATZ, SHARON GORDON, MARGARET, LESLIE WILSON, BRIAN, C. MOK, ALVIN, HO, KWAN		
IPC分类号	G01N21/47 G01N21/17 A61B1/00 A61B1/05 A61B5/00 G02B6/04 G02B23/26		
CPC分类号	A61B5/6852 A61B1/00096 A61B1/00172 A61B1/05 A61B5/0066 G01N21/4795		
代理机构(译)	HARRISON GODDARD FOOTE		
优先权	60/217090 2000-07-10 US		
其他公开文献	EP1299711A2		
外部链接	Espacenet		

摘要(译)

提供了一种用于检查样品的亚表面微结构的方法和设备。来自多个光学辐射源的辐射沿第一光学路径行进。在第一光路中，装置将来自每个光源的光辐射聚焦成沿第一光路的多个相应焦点，以提供第一光路的选定部分的基本上连续的覆盖。然后，沿着第一光路的所选部分扫描在延伸到样品中的所选长度内的第一光路上的样品。